

# NAVAL POSTGRADUATE SCHOOL

## Monterey, California



## THESIS

### **CODING-SPREADING TRADEOFF IN CDMA SYSTEMS**

by

Eduardo J. Bolas

September 2002

Thesis Advisor:

Thesis Co-Advisor:

Second Reader:

Tri T. Ha

Jan E. Tighe

Jovan Lebaric

**Approved for public release; distribution is unlimited**

THIS PAGE INTENTIONALLY LEFT BLANK

<b>REPORT DOCUMENTATION PAGE</b>			Form Approved OMB No. 0704-0188	
Public reporting burden for this collection of information is estimated to average 1 hour per response, including the time for reviewing instruction, searching existing data sources, gathering and maintaining the data needed and completing and reviewing the collection of information. Send comments regarding this burden estimate or any other aspect of this collection of information, including suggestions for reducing this burden, to Washington headquarters Services, Directorate for Information Operations and Reports, 1215 Jefferson Davis Highway, Suite 1204, Arlington, VA 22202-4302 and to the Office of Management and Budget, Paperwork Reduction Project (0704-0188) Washington DC 20503.				
<b>1. AGENCY USE ONLY (Leave blank)</b>		<b>2. REPORT DATE</b> September 2002	<b>3. REPORT TYPE AND DATES COVERED</b> Master's Thesis	
<b>4. TITLE AND SUBTITLE:</b> Coding-Spreading Tradeoff in CDMA Systems			<b>5. FUNDING NUMBERS</b>	
<b>6. AUTHOR(S)</b> Eduardo Bolas				
<b>7. PERFORMING ORGANIZATION NAME(S) AND ADDRESS(ES)</b> Naval Postgraduate School Monterey, CA 93943-5000			<b>8. PERFORMING ORGANIZATION REPORT NUMBER</b>	
<b>9. SPONSORING /MONITORING AGENCY NAME(S) AND ADDRESS(ES)</b> N/A			<b>10. SPONSORING/MONITORING AGENCY REPORT NUMBER</b>	
<b>11. SUPPLEMENTARY NOTES</b> The views expressed in this thesis are those of the author and do not reflect the official policy or position of the Department of Defense or the U.S. Government.				
<b>12a. DISTRIBUTION / AVAILABILITY STATEMENT</b> Approved for public release; distribution is unlimited.			<b>12b. DISTRIBUTION CODE</b>	
<b>13. ABSTRACT (maximum 200 words)</b> <p>In this thesis we investigate the use of low rate codes primarily to provide the total bandwidth expansion required for a CDMA system. Comparing different combinations of coding and spreading with a traditional DS-CDMA, as defined in the IS-95 standard, allows the criteria to be defined for the best coding-spreading tradeoff in CDMA systems. The analysis of the coding-spreading tradeoff is divided into two parts. The first part is dedicated to the study of the deterministic components of the problem. This includes the different factors with non-random behavior that the system's designer can determine. The processing gain, the code characteristics and the number of users are well-defined variables that can determine the overall performance and can consequently affect the tradeoff. The second part of the study is dedicated to analyzing different combinations of coding and spreading with no ideal channel estimation and interference reduction techniques. Small-scale fading channel conditions are emulated through Nakagami-<math>m</math> distribution. Large-scale path loss was incorporated through the extended Hata model while Lognormal shadowing considered the fluctuations on the received power at points with the same distance to the transmitter. We assessed the performance of different combinations of coding and spreading considered in two cases: a worst-case scenario in which the mobile user was located at the corner of a hexagon cell in a seven-cell cluster and a more realistic scenario in which the user could be physically located anywhere in the cell, following a uniform probability distribution function. Furthermore, we investigated the improvement in performance generated by interference reduction techniques, such as sectoring and power control.</p>				
<b>14. SUBJECT TERMS</b> Coding, Spreading, Low Rate Codes, Code-Spreading, Nakagami Fading, Lognormal Shadowing, CDMA, Wireless, Performance Analysis, Antenna Sectoring, Power Control.			<b>15. NUMBER OF PAGES</b> 111	
			<b>16. PRICE CODE</b>	
<b>17. SECURITY CLASSIFICATION OF REPORT</b> Unclassified	<b>18. SECURITY CLASSIFICATION OF THIS PAGE</b> Unclassified	<b>17. SECURITY CLASSIFICATION OF REPORT</b> Unclassified	<b>18. SECURITY CLASSIFICATION OF THIS PAGE</b> Unclassified	

THIS PAGE INTENTIONALLY LEFT BLANK

**Approved for public release; distribution is unlimited**

**CODING-SPREADING TRADEOFF IN CDMA SYSTEMS**

Eduardo J. Bolas  
Lieutenant, Portuguese Navy  
B.S., Portuguese Naval Academy, 1994

Submitted in partial fulfillment of the  
requirements for the degree of

**MASTER OF SCIENCE IN ELECTRICAL ENGINEERING**

from the

**NAVAL POSTGRADUATE SCHOOL  
September 2002**

Author: Eduardo J. Bolas

Approved by: Tri T. Ha  
Thesis Advisor

Jan E. Tighe  
Thesis Co-Advisor

Jovan E. Lebaric  
Second Reader

John Powers  
Chairman  
Electrical and Computer Engineering Department

THIS PAGE INTENTIONALLY LEFT BLANK

## ABSTRACT

In this thesis we investigate the usage of low rate codes primarily to provide the total bandwidth expansion required for a CDMA system. Comparing different combinations of coding and spreading with a traditional DS-CDMA, as defined in the IS-95 standard, allows the criteria to be defined for the best coding-spreading tradeoff in CDMA systems. The analysis of the coding-spreading tradeoff is divided into two parts. The first part is dedicated to the study of the deterministic components of the problem. This includes the different factors with non-random behavior that the system's designer can determine. The processing gain, the code characteristics and the number of users are well-defined variables that can determine the overall performance and can consequently affect the tradeoff. The second part of the study is dedicated to analyzing different combinations of coding and spreading with no ideal channel estimation and interference reduction techniques. Small-scale fading channel conditions are emulated through Nakagami- $m$  distribution. Large-scale path loss was incorporated through the extended Hata model while Lognormal shadowing considered the fluctuations on the received power at points with the same distance to the transmitter. We assessed the performance of different combinations of coding and spreading considering in two cases: a worst-case scenario in which the mobile user was located at the corner of a hexagon cell in a seven-cell cluster and a more realistic scenario in which the user could be physically located anywhere in the cell, following a uniform probability distribution function. Furthermore, we investigated the improvement in performance generated by interference reduction techniques, such as sectoring and power control.

THIS PAGE INTENTIONALLY LEFT BLANK



# TABLE OF CONTENTS

I.	INTRODUCTION .....	1
A.	BACKGROUND .....	1
B.	OBJECTIVE .....	1
C.	RELATED WORK .....	2
D.	THESIS OUTLINE .....	3
II.	CODING AND SPREADING FUNDAMENTALS .....	5
A.	SPREADING SEQUENCES .....	5
B.	CONVOLUTIONAL CODES .....	7
C.	DIRECT SEQUENCE VERS US CODE-SPREADING.....	9
D.	SUMMARY.....	12
III.	DETERMINISTIC TRADEOFF FACTORS .....	13
A.	PERFORMANCE ANALYSIS .....	13
B.	ASYMPTOTIC CODING GAIN .....	15
C.	CODE DISTANCE SPECTRUM.....	19
	21	
D.	NUMBER OF USERS .....	24
E.	SUMMARY.....	25
IV.	RANDOM TRADEOFF FACTORS .....	27
A.	PERFORMANCE IN FADING-SHADOWING CHANNELS .....	27
1.	Worst-case .....	30
a.	<i>Fading Variations</i> .....	32
b.	<i>Shadowing Variations</i> .....	35
c.	<i>Variations in the Number of Users</i> .....	37
2.	Uniform User Distribution.....	41
a.	<i>Fading Variations</i> .....	44
b.	<i>Shadowing Variations</i> .....	46
d.	<i>Variations in the Number of Users</i> .....	48
B.	PERFORMANCE WITH INTERFERENCE REDUCTION TECHNIQUES .....	52
1.	Sectoring .....	53
a.	<i>Fading Variations</i> .....	53
b.	<i>Shadowing Variations</i> .....	56
c.	<i>Variations in the Number of Users</i> .....	58
2.	Power Control.....	60
a.	<i>Fading Variations</i> .....	61
b.	<i>Variations in the Number of Users</i> .....	63
C.	SUMMARY.....	72
V.	CONCLUSIONS AND FUTURE WORK .....	75

A.	CONCLUSIONS .....	75
B.	FUTURE WORK.....	77
APPENDIX A. NESTED MAXIMUM FREE DISTANCE CODES .....		79
LIST OF REFERENCES .....		81
BIBLIOGRAPHY .....		85
INITIAL DISTRIBUTION LIST .....		87

## LIST OF FIGURES

Figure 1.	Asymptotic coding gain for codes of $K=9$ . $R=1/2$ is presented in [24] and all the others in Table 1. ....	17
Figure 2.	Performance of $R=1/2$ , some samples of code group A and $R=1/20$ for $K=9$ , $N=128$ and 10 users.....	18
Figure 3.	Asymptotic Coding Gain for maximum free distance codes of $K=9$ .....	20
Figure 4.	Performance for codes of Table 2, for 40 users, in a Rayleigh fading channel, for $N=128$ . ....	20
Figure 5.	Probability of bit error as a function of the system normalized load, for codes of Table 2 and $E_b/N_0=10$ dB, in a Rayleigh fading channel .....	21
Figure 6.	Distance spectrum of nested codes as a function of the distance for $K=9$ .....	22
Figure 7	Slopes of the Distance Spectrum Lines of selected codes. ....	23
Figure 8.	Average SNIR per coded bit for a $E_b/N_0$ of 12 dB, as a function of the system's normalized load. ....	25
Figure 9.	Mobile in the worst-case position on a seven (hexagon) cell cluster. ....	30
Figure 10.	Probability of bit error for different code rates with the total bandwidth expansion $N=128$ in a Nakagami Fading ( $m=0.5$ ) and Lognormal Shadowing ( $s_{dB}=4$ ) channel, for 10 users per cell – Worst-case. ....	33
Figure 11.	Probability of bit error for different code rates with the total bandwidth expansion $N=128$ in a Nakagami Fading ( $m=1$ ) and Lognormal Shadowing ( $s_{dB}=4$ ) channel, for 10 users per cell – Worst-case. ....	34
Figure 12.	Probability of bit error for different code rates with the total bandwidth expansion $N=128$ in a Nakagami Fading ( $m=2$ ) and Lognormal Shadowing ( $s_{dB}=4$ ) channel, for 10 users per cell – Worst-case. ....	34
Figure 13.	Probability of bit error for different code rates with the total bandwidth expansion $N=128$ in a Nakagami Fading ( $m=0.5$ ) and Lognormal Shadowing ( $s_{dB}=7$ ) channel, for 10 users per cell – Worst-case. ....	36
Figure 14.	Probability of bit error for different code rates with the total bandwidth expansion $N=128$ in a Nakagami Fading ( $m=1$ ) and Lognormal Shadowing ( $s_{dB}=7$ ) channel, for 10 users per cell – Worst-case. ....	36
Figure 15.	Probability of bit error for different code rates with the total bandwidth expansion $N=128$ in a Nakagami Fading ( $m=2$ ) and Lognormal Shadowing ( $s_{dB}=7$ ) channel, for 10 users per cell – Worst-case. ....	37
Figure 16.	Probability of bit error for different code rates with the total bandwidth expansion $N=128$ in a Nakagami Fading ( $m=0.5$ ) and Lognormal Shadowing ( $s_{dB}=7$ ) channel, for 20 users per cell – Worst-case. ....	38
Figure 17.	Probability of bit error for different code rates with the total bandwidth expansion $N=128$ in a Nakagami Fading ( $m=0.5$ ) and Lognormal Shadowing ( $s_{dB}=7$ ) channel, for 40 users per cell – Worst-case. ....	39

Figure 18.	Probability of bit error for different code rates with the total bandwidth expansion $N=128$ in a Nakagami Fading ( $m=1$ ) and Lognormal Shadowing ( $s_{dB}=7$ ) channel, for 20 users per cell – Worst-case. ....	39
Figure 19.	Probability of bit error for different code rates with the total bandwidth expansion $N=128$ in a Nakagami Fading ( $m=1$ ) and Lognormal Shadowing ( $s_{dB}=7$ ) channel, for 40 users per cell – Worst-case. ....	40
Figure 20.	Probability of bit error for different code rates with the total bandwidth expansion $N=128$ in a Nakagami Fading ( $m=2$ ) and Lognormal Shadowing ( $s_{dB}=7$ ) channel, for 20 users per cell – Worst-case. ....	40
Figure 21.	Probability of bit error for different code rates with the total bandwidth expansion $N=128$ in a Nakagami Fading ( $m=2$ ) and Lognormal Shadowing ( $s_{dB}=7$ ) channel, for 40 users per cell – Worst-case. ....	41
Figure 22.	Mobile in a Seven (Circular) Cell Cluster. ....	42
Figure 23.	Probability of bit error for different code rates with the total bandwidth expansion $N=128$ in a Nakagami Fading ( $m=0.5$ ) and Lognormal Shadowing ( $s_{dB}=4$ ) channel, for 10 users per adjacent cell – Uniform User Distribution. ....	45
Figure 24.	Probability of bit error for different code rates with the total bandwidth expansion $N=128$ in a Nakagami Fading ( $m=1$ ) and Lognormal Shadowing ( $s_{dB}=4$ ) channel, for 10 users per adjacent cell – Uniform User Distribution. ....	45
Figure 25.	Probability of bit error for different code rates with the total bandwidth expansion $N=128$ in a Nakagami Fading ( $m=2$ ) and Lognormal Shadowing ( $s_{dB}=4$ ) channel, for 10 users per adjacent cell – Uniform User Distribution. ....	46
Figure 26.	Probability of bit error for different code rates with the total bandwidth expansion $N=128$ in a Nakagami Fading ( $m=0.5$ ) and Lognormal Shadowing ( $s_{dB}=7$ ) channel, for 10 users per adjacent cell – Uniform User Distribution. ....	47
Figure 27.	Probability of bit error for different code rates with the total bandwidth expansion $N=128$ in a Nakagami Fading ( $m = 1$ ) and Lognormal Shadowing ( $s_{dB}=7$ ) channel, for 10 users per adjacent cell – Uniform User Distribution. ....	47
Figure 28.	Probability of bit error for different code rates with the total bandwidth expansion $N=128$ in a Nakagami Fading ( $m=2$ ) and Lognormal Shadowing ( $s_{dB}=7$ ) channel, for 10 users per adjacent cell – Uniform User Distribution. ....	48
Figure 29.	Probability of bit error for different code rates with the total bandwidth expansion $N=128$ in a Nakagami Fading ( $m = 0.5$ ) and Lognormal Shadowing ( $s_{dB}=7$ ) channel, for 20 users per adjacent cell – Uniform User Distribution. ....	49

Figure 30.	Probability of bit error for different code rates with the total bandwidth expansion $N=128$ in a Nakagami Fading ( $m=0.5$ ) and Lognormal Shadowing ( $s_{dB}=7$ ) channel, for 40 users per adjacent cell – Uniform User Distribution. ....	50
Figure 31.	Probability of bit error for different code rates with the total bandwidth expansion $N=128$ in a Nakagami Fading ( $m=1$ ) and Lognormal Shadowing ( $s_{dB}=7$ ) channel, for 20 users per adjacent cell – Uniform User Distribution. ....	50
Figure 32.	Probability of bit error for different code rates with the total bandwidth expansion $N=128$ in a Nakagami Fading ( $m=1$ ) and Lognormal Shadowing ( $s_{dB}=7$ ) channel, for 40 users per adjacent cell – Uniform User Distribution. ....	51
Figure 33.	Probability of bit error for different code rates with the total bandwidth expansion $N=128$ in a Nakagami Fading ( $m=2$ ) and Lognormal Shadowing ( $s_{dB}=7$ ) channel, for 20 users per adjacent cell – Uniform User Distribution. ....	51
Figure 34.	Probability of bit error for different code rates with the total bandwidth expansion $N=128$ in a Nakagami Fading ( $m=2$ ) and Lognormal Shadowing ( $s_{dB}=7$ ) channel, for 40 users per adjacent cell – Uniform User Distribution. ....	52
Figure 35.	Probability of bit error for different code rates with the total bandwidth expansion $N=128$ in a Nakagami Fading ( $m=0.5$ ) and Lognormal Shadowing ( $s_{dB}=4$ ) for 10 users per adjacent cell – Uniform User Distribution with Six Sectors. ....	54
Figure 36.	Probability of bit error for different code rates with the total bandwidth expansion $N=128$ in a Nakagami Fading ( $m=1$ ) and Lognormal Shadowing ( $s_{dB}=4$ ) for 10 users per adjacent cell – Uniform User Distribution with Six Sectors. ....	55
Figure 37.	Probability of bit error for different code rates with the total bandwidth expansion $N=128$ in a Nakagami Fading ( $m=2$ ) and Lognormal Shadowing ( $s_{dB}=4$ ) for 10 users per adjacent cell – Uniform User Distribution with Six Sectors. ....	55
Figure 38.	Probability of bit error for different code rates with the total bandwidth expansion $N=128$ in a Nakagami Fading ( $m=0.5$ ) and Lognormal Shadowing ( $s_{dB}=7$ ) channel, for 10 users per adjacent cell – Uniform User Distribution with Six Sectors. ....	56
Figure 39.	Probability of bit error for different code rates with the total bandwidth expansion $N=128$ in a Nakagami Fading ( $m=1$ ) and Lognormal Shadowing ( $s_{dB}=7$ ) channel, for 10 users per adjacent cell – Uniform User Distribution with Six Sectors. ....	57

Figure 40.	Probability of bit error for different code rates with the total bandwidth expansion $N=128$ in a Nakagami Fading ( $m=2$ ) and Lognormal Shadowing ( $s_{dB}=7$ ) channel, for 10 users per adjacent cell – Uniform User Distribution with Six Sectors. ....	57
Figure 41.	Probability of bit error for different code rates with the total bandwidth expansion $N=128$ in a Nakagami Fading ( $m=0.5$ ) and Lognormal Shadowing ( $s_{dB}=7$ ) channel, for 20 users per adjacent cell – Uniform User Distribution with Six Sectors. ....	58
Figure 42.	Probability of bit error for different code rates with the total bandwidth expansion $N=128$ in a Nakagami Fading ( $m=1$ ) and Lognormal Shadowing ( $s_{dB}=7$ ) channel, for 20 users per adjacent cell – Uniform User Distribution with Six Sectors. ....	59
Figure 43.	Probability of bit error for different code rates with the total bandwidth expansion $N=128$ in a Nakagami Fading ( $m=2$ ) and Lognormal Shadowing ( $s_{dB}=7$ ) channel, for 20 users per adjacent cell – Uniform User Distribution with Six Sectors. ....	59
Figure 44.	Probability of bit error for different code rates with the total bandwidth expansion $N=128$ in a Nakagami Fading ( $m=0.5$ ) for 10 users per adjacent cell – Uniform User Distribution with Six Sectors and Power Control. ....	61
Figure 45.	Probability of bit error for different code rates with the total bandwidth expansion $N=128$ in a Nakagami Fading ( $m=1$ ) channel, for 10 users per adjacent cell – Uniform User Distribution with Six Sectors and Power Control. ....	62
Figure 46.	Probability of bit error for different code rates with the total bandwidth expansion $N=128$ in a Nakagami Fading ( $m=2$ ) channel, for 10 users per adjacent cell – Uniform User Distribution with Six Sectors and Power Control. ....	62
Figure 47.	Probability of bit error for different code rates with the total bandwidth expansion $N=128$ in a Nakagami Fading ( $m=0.5$ ) for 40 users per adjacent cell – Uniform User Distribution with Six Sectors and Power Control. ....	64
Figure 48.	Probability of bit error for different code rates with the total bandwidth expansion $N=128$ in a Nakagami Fading ( $m=0.5$ ) for 80 users per adjacent cell – Uniform User Distribution with Six Sectors and Power Control. ....	65
Figure 49.	Probability of bit error for different code rates with the total bandwidth expansion $N=128$ in a Nakagami Fading ( $m=0.5$ ) for 120 users per adjacent cell – Uniform User Distribution with Six Sectors and Power Control. ....	65
Figure 50.	Probability of bit error for different code rates with the total bandwidth expansion $N=128$ in a Nakagami Fading ( $m=0.5$ ) for 160 users per adjacent cell – Uniform User Distribution with Six Sectors and Power Control. ....	66

Figure 51.	Probability of bit error for different code rates with the total bandwidth expansion $N=128$ in a Nakagami Fading ( $m=0.5$ ) for 200 users per adjacent cell – Uniform User Distribution with Six Sectors and Power Control. ....	66
Figure 52.	Probability of bit error for different code rates with the total bandwidth expansion $N=128$ in a Nakagami Fading ( $m=1$ ) for 40 users per adjacent cell – Uniform User Distribution with Six Sectors and Power Control. ....	67
Figure 53.	Probability of bit error for different code rates with the total bandwidth expansion $N=128$ in a Nakagami Fading ( $m=1$ ) for 80 users per adjacent cell – Uniform User Distribution with Six Sectors and Power Control. ....	67
Figure 54.	Probability of bit error for different code rates with the total bandwidth expansion $N=128$ in a Nakagami Fading ( $m=1$ ) for 120 users per adjacent cell – Uniform User Distribution with Six Sectors and Power Control. ....	68
Figure 55.	Probability of bit error for different code rates with the total bandwidth expansion $N=128$ in a Nakagami Fading ( $m=1$ ) for 160 users per adjacent cell – Uniform User Distribution with Six Sectors and Power Control. ....	68
Figure 56.	Probability of bit error for different code rates with the total bandwidth expansion $N=128$ in a Nakagami Fading ( $m=1$ ) for 200 users per adjacent cell – Uniform User Distribution with Six Sectors and Power Control. ....	69
Figure 57.	Probability of bit error for different code rates with the total bandwidth expansion $N=128$ in a Nakagami Fading ( $m=2$ ) for 40 users per adjacent cell – Uniform User Distribution with Six Sectors and Power Control. ....	69
Figure 58.	Probability of bit error for different code rates with the total bandwidth expansion $N=128$ in a Nakagami Fading ( $m=2$ ) channel, for 80 users per adjacent cell – Uniform User Distribution with Six Sectors and Power Control. ....	70
Figure 59.	Probability of bit error for different code rates with the total bandwidth expansion $N=128$ in a Nakagami Fading ( $m=2$ ) channel, for 120 users per adjacent cell – Uniform User Distribution with Six Sectors and Power Control. ....	70
Figure 60.	Probability of bit error for different code rates with the total bandwidth expansion $N=128$ in a Nakagami Fading ( $m=2$ ) channel, for 160 users per adjacent cell – Uniform User Distribution with Six Sectors and Power Control. ....	71
Figure 61.	Probability of bit error for different code rates with the total bandwidth expansion $N=128$ in a Nakagami Fading ( $m=2$ ) channel, for 200 users per adjacent cell – Uniform User Distribution with Six Sectors and Power Control. ....	71

THIS PAGE INTENTIONALLY LEFT BLANK



## LIST OF TABLES

Table 1.	Convolutional Codes with Maximum Free Distance.....	16
Table 2.	Low-rate Codes with Maximum Asymptotic Coding Gain.....	19

THIS PAGE INTENTIONALLY LEFT BLANK

## **ACKNOWLEDGMENTS**

This thesis is dedicated to the memory of my beloved father, Eduardo dos Santos Paredes Bolas. I am eternally grateful to him and my mother for the support and love they gave me throughout my life. His strength taught me the importance of diligence and responsibility. I could not have completed this thesis without his exemplary constitution always serving as my model. I also must express my appreciation and my adoration of my wife, Rita, who patiently and lovingly stood by me through the rigors of my research here at the Naval Postgraduate School. Words cannot express my love and gratitude for all she has done. More than a remarkable wife, she is a remarkable human being. Finally, I would like to thank my editor, Ron Russell, for his attentive assistance and I finally must say thanks to all of the dedicated professors who sacrificed their time and energy to further my education.

THIS PAGE INTENTIONALLY LEFT BLANK

## EXECUTIVE SUMMARY

In future personal communications systems, speech is expected to be the main service, but with a much higher quality than in today's systems. Other services like video and image or data transmission and wireless computing are also expected to become popular ways to communicate. Therefore, mobile communications systems will have many different services to support, each one with its own requirements on data rate and quality of service. Typical transmission rates will vary from 10 Kbps to 2 Mbps, while the acceptable bit error rates will go from  $10^{-2}$  for speech and images to  $10^{-6}$  or lower for data transmission. So supporting variable bit rates and providing reliable communications are two highly important features of tomorrow's wireless communications systems.

Spread spectrum techniques became popular in wireless communication systems because of their superiority in combating fading due to multipath propagation and because of their suitability for being applied to multiple access techniques, like Direct Sequence Code Division Multiple Access (DS-CDMA). Introducing bandwidth redundancy into the signal to occupy the entire spectral bandwidth, which allows the multiple access, involves the spreading of bandwidth required to transmit information. Bandwidth redundancy is generated from a data modulated carrier that is phase modulated a second time by using a wideband spreading signal. Those types of signals are characterized by their bandwidth—which is much greater than the information rate. The spreading is designated to have properties to facilitate demodulation of the transmitted signal by the intended receiver and to make demodulation by an unintended receiver as difficult as possible. DS-CDMA systems can extraordinarily increase capacity because they can efficiently assign bandwidth to accommodate many users simultaneously. This is one of the reasons that determined the selection of CDMA to be the multiple access technique of the third generation of wireless communications.

This thesis addresses the CDMA systems in a different perspective. We investigate the usage of low rate codes primarily to provide the total bandwidth expansion re-

quired for a CDMA system. These systems, further designated as Code Spreading (CS) CDMA, are compared with a traditional DS-SS-CDMA, as defined in the IS-95 standard [1], in which a code rate of  $1/2$  is used in conjunction with a spreading sequence with a processing gain of 64. Comparing different combinations of coding and spreading allows the criteria to be defined for the best coding-spreading tradeoff in CDMA systems.

The analysis of the coding-spreading tradeoff is divided into two parts. The first one is dedicated to the study of the deterministic components of the problem. This includes the different factors with non-random behavior that the system's designer can determine. This can potentially influence the performance. The processing gain, the code characteristics and the number of users are well defined variables that can determine the overall performance and can consequently affect the tradeoff. Understanding the deterministic part of the problem can better interpret the randomness introduced by the communication channel.

The second part of the study is dedicated to analyzing different combinations of coding and spreading with no ideal channel estimation and interference reduction techniques. The statistical model chosen to emulate the small-scale fading channel conditions was the Nakagami- $m$  distribution. Large-scale path loss was incorporated through the extended Hata model while Lognormal shadowing considered the fluctuations on the received power at points with the same distance to the transmitter. We assessed the performance of different combinations of coding and spreading considering in two cases. First, a worst-case scenario in which the mobile user was located at the corner of a hexagon cell in a seven cell cluster. In this case, the mobile received the signal of three base stations, with each approximately possessing the same energy. Secondly, we considered a more realistic scenario in which the user could be physically located anywhere in the cell, following a uniform probability distribution function.

Furthermore, we investigated the improvement in performance generated by interference reduction techniques, such as sectoring and power control. The sectoring reduced the effect of the co-channel interference. The interference received in each antenna of a cell was only a fraction of the co-channel interference, which allowed an increase in the

system's capacity that was proportional to the number of sectors. On the other hand, the power control eliminated the effect of Lognormal Shadowing and reduced the co-channel interference. The base station transmitted power was adjusted in a way that each user received the same power independently of its position in the cell, so the effects of shadowing were eliminated and the transmitted power was reduced to the minimum value required for a given probability of bit error.

The analysis presented in this thesis has major applications in commercial systems. However, there is always potential military interest in all the studies related with spread spectrum communications. Future battlefield communications systems will demand variable bit rates and low bit error rates, which makes them similar to commercial systems.

THIS PAGE INTENTIONALLY LEFT BLANK



# **I. INTRODUCTION**

## **A. BACKGROUND**

Future personal communications systems will have many services to support, from high quality speech to data transmission, each one with its own requirements on data rate and quality of service. The third generation of mobile communications will need to support transmission rates that can vary from 10 Kbps to 2 Mbps and bit error rates that can go from  $10^{-2}$  for speech and images to  $10^{-6}$  or lower for data transmission. The support of such demanding features requires the use of a multiple access technique that not only can increase the present systems' capacity, but also can efficiently assign bandwidth to accommodate many users simultaneously. Therefore, the selected multiple access technique for the third generation of wireless communications was Code Division Multiple Access.

On the other hand, military communications systems, which use spread spectrum techniques for different purposes, are as demanding as commercial systems. In fact, future battlefield communications systems will demand variable bit rates and low bit error rates, which make them similar to commercial systems. Therefore, most of the features used in personal communications systems unquestioningly have applications in military systems.

## **B. OBJECTIVE**

The major drawback of CDMA systems is their interference limited characteristic. In CDMA systems all traffic channels share the same radio carrier channel. As described by Lee in [2], CDMA is analogous to a cocktail party where everybody needs to talk in a "civilized" manner to allow for the different conversations between the guests. "Uncivilized" conversations will result in interference that simply block all communication.

Therefore, any efforts spent on interference reduction in a CDMA system are amply compensated for improved system performance.

This thesis addresses the CDMA systems in a different perspective. We investigate the usage of low rate codes to mainly provide the total bandwidth expansion required for a CDMA system. These systems, further designated as Code Spreading (CS) CDMA, are compared with a traditional DS-SS-CDMA, as defined in the IS-95 standard [1], in which a code rate of  $1/2$  is used in conjunction with a spreading sequence with a processing gain of 64. The comparison between different combinations of coding and spreading allow the definition of criteria for the best coding-spreading tradeoff in CDMA systems.

The analysis of the coding-spreading tradeoff is divided into two parts. The first one is dedicated to the study of the deterministic components of the problem. This includes the different factors with non-random behavior that the system's designer can determine. This can potentially influence the performance. The processing gain, the code characteristics and the number of users are well defined variables that can determine the overall performance and consequently affect the tradeoff. The second part of the study is dedicated to the analysis of different combinations of coding and spreading with no ideal channel estimation and interference reduction techniques. The statistical model chosen to emulate the small-scale fading channel conditions was the Nakagami- $m$  distribution. Large-scale path loss was incorporated through the extended Hata model while Log-normal shadowing considered the fluctuations on the received power at points with the same distance to the transmitter. Furthermore, we investigate improved performance resulting from interference reduction techniques like sectoring and power control.

## **C. RELATED WORK**

The idea of employing low rate codes alone for bandwidth expansion is not new. In fact, [3] has demonstrated that it allows great improvements in efficiency and [4] showed its benefits in capacity maximization. However, the limiting factor has been the lack of good low rate codes. Several authors had studied the use of orthogonal convolutional codes [3] and [5], bi-orthogonal codes [6] and trellis codes and a variation of or-

thogonal codes called super-orthogonal convolutional codes [7], but the best results have been achieved by [8] with a proposed low rate convolutional codes with maximum free distance (MFD). It was showed that MFD codes not only out-perform the other types of codes, but also allow simple encoder and decoder implementations.

Other authors studied the coding-spreading tradeoff in a generic way, giving special emphasis to the detector influence on the performance. The analysis in [9] presented a discussion regarding the usage of different receivers, minimum mean-square error and matched filters and how the systems spectral efficiency affects the performance of the codes. In [10] the study involved linear minimum mean-square error detectors and the matched filters. Single and multi-user decoders were also addressed. The conclusions of both of these works indicated that the coding-spreading tradeoff is a function of the type of receiver used.

None of the mentioned studies included any analysis regarding practical systems using low rate codes nor considered the tradeoff problem with imperfect channel estimation and power control over more realistic channel models. Actually, some of these studies mentioned the subject presented in this thesis as an interesting topic of future research.

## **D. THESIS OUTLINE**

Chapter II briefly introduces spreading sequences and convolutional codes. The low-rate convolutional codes used in the analysis of the tradeoff problem are presented and the fundamental differences between bandwidth expansion component due to spreading sequences and due to coding are discussed.

Chapter III is dedicated to analyzing deterministic components of the coding-spreading problem. Factors with non-random behavior, such as the processing gain, the code characteristics and the number of users that can be determined by the system's designer, which can potentially influence the performance, are investigated.

Chapter IV addresses the randomness introduced by a non-ideal channel and investigates how it influences the performance of the different combinations of coding-spreading once again. The point of departure is the IS-95 standard and the benchmark is the performance of a system that uses a total bandwidth expansion,  $N=128$ , an encoder with a code rate,  $R=1/2$  and a constraint length,  $K=9$ . This system is compared to systems of different combinations of coding and spreading with the same processing gain. This is done for a different number of users, channel fading and shadowing and using different techniques for interference reduction.

Finally, in Chapter V the conclusions are summarized and areas for further research are discussed.

## II. CODING AND SPREADING FUNDAMENTALS

Before starting the analysis of coding-spreading tradeoff, we introduce the basic concepts behind the problem. This chapter presents a brief introduction to spreading sequences and convolutional codes, which have comprehensive explanations in references [11-14] and also presents the low-rate convolutional codes that are used in the analysis of the tradeoff problem. Furthermore, we discuss the fundamental differences between bandwidth expansion component, due to spreading sequences and due to coding. Again, this is another well documented topic and further information can be obtained in articles like [9] or [10]. Finally, we discuss some advantages and disadvantages of these two methods for achieving bandwidth redundancy.

### A. SPREADING SEQUENCES

The Direct Sequence is the most popular means of spreading the data signal in spread spectrum communications. The concept is quite simple; a data modulated signal is modulated a second time using a sequence of bits, which has a bandwidth that is considerably greater than the original signal. The result is a signal with the same information but which occupies a larger bandwidth that can appear random to anyone but the intended receiver. This capacity of a receiver to separate a user sharing the same spectrum, based on its spreading sequence, is the key point of multiple-access techniques.

The DS-CDMA spreading is achieved by multiplying the information data by a spreading sequence having a bit rate, normally designated “chip rate,” much higher than the data bit rate. This procedure not only increases the data rate and consequently the bandwidth, but also introduces redundancy to the system, which thereby improves the overall system performance. The quantification of this improvement or gain—also an approximate measure of the interference rejection capability—can be determined by the ratio between the spreading sequence chip rate  $R_{chip}$  and the coded data rate  $R_c$ . This is usually called “processing gain” and is defined as

$$N_c = \frac{R_{chip}}{R_c} = \frac{R_{chip}}{\frac{R_b}{R}} = \frac{RR_{chip}}{R_b} \quad (2.1)$$

where  $R$  represents the code rate and  $R_b$  the uncoded bit rate.

Ideal spreading sequences would be infinite random sequences of equally likely binary bits, although these infinite sequences would make them impossible to use in real systems. An infinite sequence requires an infinite storage capacity in both transmitter and receiver and a random sequence would make demodulation impossible, since the receiver must reproduce the modulated sequence in order to demodulate the data signal. The solution is to create a quasi-ideal spreading sequence, known as pseudo-random (PN) sequence.

A PN sequence is a deterministic binary sequence, known to both transmitter and receiver, which appears to have the statistical properties of a random sequence to an unauthorized user. PN sequences are used in CDMA systems for data scrambling and for spread-spectrum modulation. The data scrambling process consists of changing the data sequence in a nearly random way in order to have the information signal appear like noise. However, if the generated sequence were completely random, the receiver could not recover the information. On the other hand, if the generated sequence is “too” deterministic, it does not look like noise. The compromise is a code generated by mathematically precise rules that nearly satisfy the requirements of a truly random sequence, such as having nearly an equal number of zeros and ones, a very low correlation between shifted versions of the sequence (autocorrelation), or a very low cross-correlation between any two sequences.

The autocorrelation property of PN sequences is what makes implementing DS-SS systems possible. The “two-level autocorrelation function” of PN sequences allows, under perfect synchronization, a peak in the receiver for the desired signal and a low value for all of the unsynchronized interferers. A two-level autocorrelation function provides a mechanism for achieving a processing gain, but more importantly it allows the information signal from the multiple access interference environment to be extracted. This autocorrelation function is also responsible for the capacity to combat multipath

fading because delayed versions of the transmitted PN signal have poor correlation with the original PN sequence.

In systems like DS-CDMA, where each user is assigned a PN generator whose polynomial is distinct from all the other users, the cross-correlation between two distinct PN sequences is a highly important issue. The signals are demodulated at the receiver through cross-correlation with a locally generated version of the pseudo-random carrier. Therefore, the cross-correlation from an undesired user creates a minute amount of wide-band noise at the receiver output. Low cross-correlation between user signatures (spreading sequences) is translated in detections that are more reliable.

Additionally, spreading sequences can provide other features to the spreading signals. A DS-CDMA system, using a combination of spreading sequences with different characteristics, allows multiple users in the same bandwidth and assigns them to a particular base station. Spreading orthogonal sequences, like the Walsh functions, are used to separate signals from the same base station, while spreading sequences with good autocorrelation properties, like the PN sequences, are used for multiple-access purposes [12].

## **B. CONVOLUTIONAL CODES**

Although the theory of block codes is much richer than the theory of convolutional codes and although block codes are particularly powerful when the channel errors occur in clusters, the convolutional codes are the most popular error correction codes used in wireless communications. This is true because employing soft-decision information in block codes fully is difficult. Furthermore, code synchronization is generally much simpler for convolutional codes [14]. Thus, to implement the Forward Error Correction (FEC) coding scheme in CDMA systems, while maintaining the same ability to deal with burst errors, a convolutional encoder followed by an interleaver is often used.

The basic building blocks of a convolutional encoder are shift register and modulo 2 adders (XOR gates). The data bits are convolutionally encoded by introducing depend-

ence between the symbols and by performing more than one modulo-2 addition operation for each input (convolution). This procedure provides information redundancy and gives the code its error correcting capability.

A convolutional code is basically described by two numbers, code rate ( $R$ ) and constraint length ( $K$ ). The code rate represents the information per coded bit. In other words, it represents the ratio between the information bits and the coded bits that are actually being sent. Therefore, the error correction capability of a convolution coding scheme increases as the code rate decreases. This is a consequence of the amount of redundancy introduced by the code. The constraint length corresponds to the number of memory elements required for the convolutional encoder and this constraint length represents the number of stages in the shift register. The error correction capacity of the code increases as the constraint length increases because the dependency between symbols increases. However, the number of code states and consequently the complexity of the encoder increases exponentially with the constraint length. A maximum likelihood decoder requires approximately  $2^K$  computations to decode an information bit [15]. Additionally, increasing the constraint length will increase the fractional rate loss, due to the addition of extra bits that allow the content of the memory cells in the convolutional encoder to be exhausted. This reduces the effective rate of the code [16].

The bandwidth of a coded transmitted signal is greater than the original data stream, due to the redundant bits introduced by the convolutional code. In the limit, when very low-rate codes are used, a spread spectrum signal can be obtained simply by the bandwidth expansion provided by the code. This is the idea behind the code spreading signals. As mentioned previously, Hui [4] and Viterbi [3] demonstrated that using low-rate convolutional codes alone for bandwidth expansion greatly improves efficiency and capacity maximization. However the limiting factor has been the lack of good low-rate codes.

There are no general algebraic methods for designing good convolutional codes. Computer searches, based on criterion, which depends on code application or decoding methods or simply random choices, are common ways to define the codes. The first attempts to find good “all purpose” codes were restricted to finding maximum free distance



(MFD) codes. Bit error rates of coded systems are not only determined by the free distance of the codes, but also—and particularly in fading environments—by the information error weight on each error path ( $\mathbf{b}_d$ ). As a result, subsequent design criteria included maximizing the free distance and low information error weight on each error path, such as the case of [8], in which they define this maximization as the *optimum distance spectrum* criterion.

Basically, two methods exist to obtain low-rate codes, by simply repeating the code symbol of a higher rate code or, more general, by nesting, which is the generation of the extra redundant symbol through a new generator polynomial. Lee [17] used nesting of convolutional codes to reduce the burden of the code searching. Later Lefrancois and Haccoun [18] and [19] reinvented these nesting convolutional codes to find very low-rate convolutional codes. In this method a generator polynomial of a higher rate code is used and the new polynomial is selected from an existing one.

The codes used in our analysis of coding-spreading tradeoff, presented in Appendix A, were found by nested code search and have an *optimum distance spectrum*. They are part of a family of low-rate convolutional codes, for different constraint lengths, presented in [8]. The structure of this family of codes leads to simple encoder and decoder implementations.

### C. DIRECT SEQUENCE VERSUS CODE-SPREADING

In DS-CDMA systems, like IS-95, the objective of bandwidth expansion is achieved by using error correction codes and pseudo-random spreading sequences that together provide the desired bandwidth redundancy. So, we define  $N$  as the total bandwidth expansion,

$$N = \frac{R_{chip}}{R_b} \quad (2.2)$$

and, consequently, the processing gain  $N_c$  defined in (2.1) is given by

$$N_c = RN \quad (2.3)$$

which means that different combinations of coding and spreading exist to achieve the same bandwidth expansion. However, there are fundamental differences between the bandwidth expansion due to the spreading sequence and the bandwidth expansion due to the coding. This makes them contribute to the system's performance differently.

The spreading sequences have two major purposes, one is to spread the information signal and the other is to perform interference rejection. As mentioned previously, the re-modulation of the data modulated signal through a sequence of bits with a larger bandwidth will result in a spread spectrum transmitted signal. Additionally, the spreading sequences are used for interference rejection. Due to the low cross-correlation property of the PN sequences, it is possible to isolate different signals, using the same bandwidth, by assigning different sequences to each one. Therefore, when a information bit stream is modulated with this unique PN sequence, it will increase its bandwidth and simultaneously be isolated from the other signals that share the same frequency band. Therefore, CDMA systems in which spreading sequences mainly provide bandwidth expansion, have their interference suppression capability provided by the isolation ability of the PN sequences. These systems are further designated as DS-CDMA systems. The error correction code used has a relatively high code rate, which normally is not as powerful as the low-rate codes, so the capacity of these systems depends on the cross-correlation properties of the set of sequences used. There are different methods for improving this isolation between the signals, such as using Gold sequences or orthogonal sequences like Walsh sequences. These methods, however, are outside the scope of this thesis and can be found in different sources such as [12] or [20].

Eventually, such systems are limited due to their own mechanism of interference rejection. The capacity of reducing the effect of interference is based on the fact that spreading sequences make any interference appear to be noise. So, spreading sequences do not reduce the energy of the interference. This simply changes its form. The result is a significant reduction in the capacity of interference cancellation when the number of interferers increases drastically. On the other hand, the systems that use spreading sequences have an extraordinary property, namely the facility of synchronization.

The code spreading is the process of achieving bandwidth expansion mainly through the use of error correction coding. As we have seen, introducing dependence between the symbols provides information redundancy and gives the code its error correcting capability. This redundancy is translated in bandwidth expansion and, in an optimal case, it can be sufficient to obtain a spread spectrum signal.

CDMA systems with bandwidth expansion mainly obtained by using coding are designated as Code Spreading (CS) CDMA. These systems rely on the code's capability to deliver the information without errors. So the encoder must add enough redundant information to the input data to be transmitted in order to provide a means of detecting and correcting the errors in the transmission. The detection of a user relies on the error correction properties of the code used since a significant cross-correlation between the different users' signals exists. Then, once this value is sufficiently low to compensate for the lack of spreading sequences, the coding gain becomes a major factor in lowering the signal-to-noise-plus-interference (SNIR) that is required to achieve the same performance.

Code spreading systems not only have a better capacity to deal with heavy loads, but they also can benefit from the possibility of coding to achieve diversity. In most cases this significantly improves performance. The major limitation to code-spreading systems is the difficulty of synchronization, which results in a loss of energy.

Therefore, a natural question arises from this discussion: for a given bandwidth expansion, how should the spreading be allocated between the CS and DS, or as commonly noted in literature, what is the coding-spreading tradeoff?

The coding-spreading tradeoff problem can easily be reduced to the search of the code rate that provides better system performance for a given bandwidth expansion. But since the features associated with the spreading sequences and the coding are so different, we should expect that the problem will have different variables. Therefore, the best code rate is a function of the system load, the required bit error rate, the error correction capability of the applied codes and the channel properties. Moreover, the best code rate is also closely related to the receiver structure, as mentioned in [10] and [21]. The analysis in [4] showed that low-rate codes can be employed to maximize the total throughput, which means that bandwidth expansion using CS-CDMA may lead to better performance over

DS-CDMA. However, results in [22] indicated that lowering the code rates does not necessarily improve system performance for certain types of modulation and channels. Consequently, different system requirements lead to different code rates.

Another factor that should be considered is the practical constraints of implementation, in which decoding complexity may limit the usefulness of very low-rate codes and in which using a significant fraction of the bandwidth expansion for DS may be justified. The difficulty of synchronization and the throughput are also variables of the problem.

## **D. SUMMARY**

Chapter II presented briefly introduced the concepts behind the coding-spreading tradeoff problem. We discussed the basic characteristics of PN sequences and concepts like autocorrelation and cross-correlation, associated with PN sequences and their importance in implementing DS-CDMA systems. Then the characteristics and design issues of convolutional codes and the low-rate convolutional codes that are used in analyzing the tradeoff problem were summarized. Finally, we discussed the fundamental differences between the bandwidth expansion component due to spreading sequences and due to coding. In the following chapter we analyze the deterministic components of the coding-spreading problem.

### III. DETERMINISTIC TRADEOFF FACTORS

This chapter presents the analysis of deterministic components of the coding-spreading problem. These components include the different factors with non-random behavior that can be determined by the system's designer, which can potentially influence the performance. We investigate how the processing gain, the code characteristics and the number of users determine the overall performance and consequently affect the tradeoff. Additionally, we present a comprehensive analysis of the cases that apparently do not follow the general rule.

Section A defines the model used in the performance comparison of this code. As mentioned previously, the benchmark is the IS-95 standard and, in this chapter, the channel is modeled, as a Rayleigh fading environment. Section B is dedicated to the study of asymptotic coding gain and how it affects performance. In addition we filter the proposed MFD codes to perform code spreading of the signals and discard the ones with the unquestionably worst performance. Section C analyzes the codes distance spectrum and studies the cases in which the difference in performance cannot be interpreted through the asymptotic coding gain analysis. Finally, section D investigates the influence of the load in the tradeoff problem.

#### A. PERFORMANCE ANALYSIS

In the performance analysis of the different coding-spreading systems we consider the case of a BPSK system in a Rayleigh fading environment. In the case of convolutional coded systems, the performance can be approximated by applying a union bound on the probability of bit error ( $P_b$ ) given by [11]

$$P_b \leq \sum_{d=d_{free}}^{\infty} b_d P_2(d) \quad (3.1)$$

where  $\mathbf{b}_d$  represents the sum of all possible bit errors that can occur when the all-zeros code word is transmitted and a path of weight  $d$  is selected;  $P_2(d)$  is the probability that an error path of distance  $d$  is chosen instead of the all-zeros code word and  $d_{free}$  is the free distance of the code. Equation (3.1) is a rather good estimate of the probability of bit error for the code at probability of bit errors below  $10^{-3}$  as long as sufficient terms in the  $\mathbf{b}_d$  spectrum are included, which accordingly with [8] should be a number greater or equal to 200. In our case, we use 300 terms for each code.

The first event error probability is the probability where at a node B in the trellis diagram, one of the paths that merges with the all-zero paths (correct path) for the first time and the merging path has a metric that exceeds the all-zero path metric. This probability of error in the pair-wise comparison of these two paths that differ in  $d$  bits, on an uncorrelated Rayleigh fading channel, with perfect phase estimates and soft decisions, is given by [11]:

$$P_2(d) = q^d \sum_{k=0}^{d-1} \binom{d-1+k}{k} (1-q)^k \quad (3.2)$$

where the probability of bit error for a binary symmetric channel  $q$  is given by

$$q = \frac{1}{2} \left( 1 - \sqrt{\frac{\bar{\mathbf{g}}_b}{1 + \bar{\mathbf{g}}_b}} \right) \quad (3.3)$$

and  $\bar{\mathbf{g}}_b$  represents the average effective SNIR per coded bit, which accounts for the interference caused by the different users [23]

$$\bar{\mathbf{g}}_b = \left( \left( R \frac{E_b}{N_0} \right)^{-1} + \frac{2(L-1)}{3N_c} \right)^{-1} = \frac{R}{\left( \frac{E_b}{N_0} \right)^{-1} + \frac{2(L-1)}{3N}} \quad (3.4)$$

or

$$\bar{\mathbf{g}}_b = \frac{R}{\left( \frac{E_b}{N_0} \right)^{-1} + \frac{2}{3} \Lambda} \quad (3.5)$$

where  $\Lambda = (L-1)/N$  is the system's normalized load.

In equation (3.4),  $R$  represents the code rate,  $E_b$  is the energy per information bit,  $N_0$  is the single-sided spectral density of thermal noise,  $L$  represents the number of users,  $N_c$  represents the processing gain (that is, the component of the spreading provided by the spreading sequence as defined in (2.1)) and  $N$  is the total bandwidth expansion as defined in (2.2).

## B. ASYMPTOTIC CODING GAIN

When the objective is to search for the code that can provide the best system performance, the quickest way to check the general improvement, associated with the usage of each code, is to compute the Asymptotic Coding Gain (ACG). It does not represent the true coding gain for a given  $E_b/N_0$ , but can roughly estimate the potential increase in performance due to coding.

The asymptotic coding gain, for soft decision decoding, defined as [11]

$$\mathbf{x} = 10\log(d_{free} R) \text{ [dB]} \quad (3.6)$$

is a function of the code rate  $R$  and the constraint length  $K$ , since  $d_{free}$  is determined by  $K$  and represents a very meaningful measure of performance, since it accounts for the rate loss. Therefore, in our search for the code that provides the optimum performance, the first step should be an analysis of the ACG of the available codes, keeping in mind that this is not the only variable of the problem. Obviously,  $1/R$  cannot exceed the total bandwidth expansion  $N$  in (2.2) so that  $N_c \geq 1$  always holds. Thus, we consider only the code groups from A to G of Table A.1, reproduced in Table 1.

From Table 1, we infer that the ACG, within a code group, decreases as the code rate decreases and since the ACG is related with the performance, it is expected that, within a code group, the performance favors the high rate codes. In Figure 1 we plot the ACG versus the inverse code rate for the codes considered in Table 1 and for the code rate  $1/2$  presented in [24], which has a  $d_{free}$  value of 12. We can observe that the ACG,

not only changes cyclically with the code rate, but also has a damped behavior with the decreasing code rate. Within a code group (same  $d_{free}$ ), the decreasing code rate has the same effect on the ACG. However, in the transition of the code group, a small decrease in the code rate is compensated by a huge increase in the free distance and this will amount to an increase in the gain.

<i>Code Group</i>	<i>Code Rate (R)</i>	<i>d<sub>free</sub> (K=9)</i>
A	$\frac{1}{4}, \frac{1}{5}, \frac{1}{6}, \dots, \frac{1}{19}$	24
B	$\frac{1}{20}, \frac{1}{21}, \frac{1}{22} \dots \frac{1}{39}$	125
C	$\frac{1}{40}, \frac{1}{41}, \frac{1}{42} \dots \frac{1}{59}$	251
D	$\frac{1}{60}, \frac{1}{61}, \frac{1}{62} \dots \frac{1}{79}$	376
E	$\frac{1}{80}, \frac{1}{81}, \frac{1}{82} \dots \frac{1}{99}$	502
F	$\frac{1}{100}, \frac{1}{101}, \frac{1}{102} \dots \frac{1}{119}$	628
G	$\frac{1}{120}, \frac{1}{121}, \frac{1}{122} \dots \frac{1}{139}$	754

Table 1. Convolutional Codes with Maximum Free Distance

As mentioned previously, the ACG merely estimates the potential increase in performance. The verification of the results must be done by analyzing the probability of bit error. Figure 2 presents the probability of bit error as a function of the  $E_b/N_0$ , in a Rayleigh fading environment, for  $R=1/2$ , some sample codes of Code Group A and the highest code rate from Code Group B.

The results obtained are very interesting. They basically confirm the importance of the ACG analysis to predict the performance of the system but, on the other hand, they show that for some particularly cases, the ACG analysis cannot help at all. The superior performance of  $R=1/20$  over the other code rates of Code Group A was predicted by the analysis of Figure 1, given that  $R=1/20$  has the highest ACG. Although, in the cases of  $R=1/2$  and  $1/4$ , their equal ACG values may provide the wrong impression that their performance, at least, would be similar, when in fact there is a huge difference in perform-



ance between  $R=1/2$  and  $R=1/4$ . In addition, there are other discrepancies regarding the information provided by the ACG and the actual performance of the systems. The difference in ACG for  $R=1/4$  and  $1/8$  of 3 dB in Figure 1 is about the same as the coding gain difference for  $P_b=10^{-4}$  between  $R=1/4$  and  $R=1/8$  in Figure 2, while a difference in ACG of less than 0.2 dB, for  $R=1/4$  and  $1/20$ , corresponds to a difference in performance, for the same probability of bit error, of over 1 dB. Finally we have the case of  $R=1/2$  and  $R=1/8$ , where a difference of 3 dB in ACG does not have any influence in performance below  $P_b=10^{-4}$  where the results are the same as seen in Figure 2. Thus, this combined evidence raises another question: What determines the increase in performance for code rates that have similar ACG? This issue will be addressed in the next section.

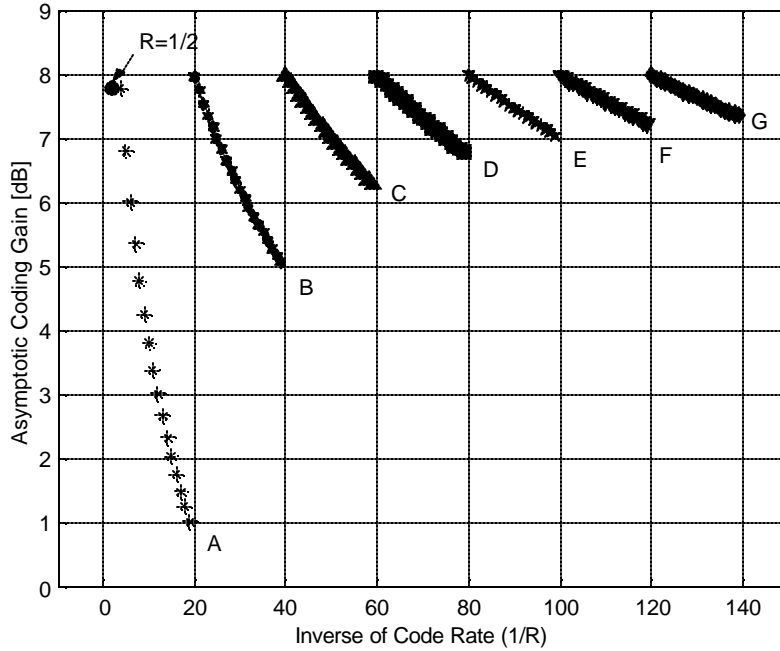


Figure 1. Asymptotic coding gain for codes of  $K=9$ .  $R=1/2$  is presented in [24] and all the others in Table 1.

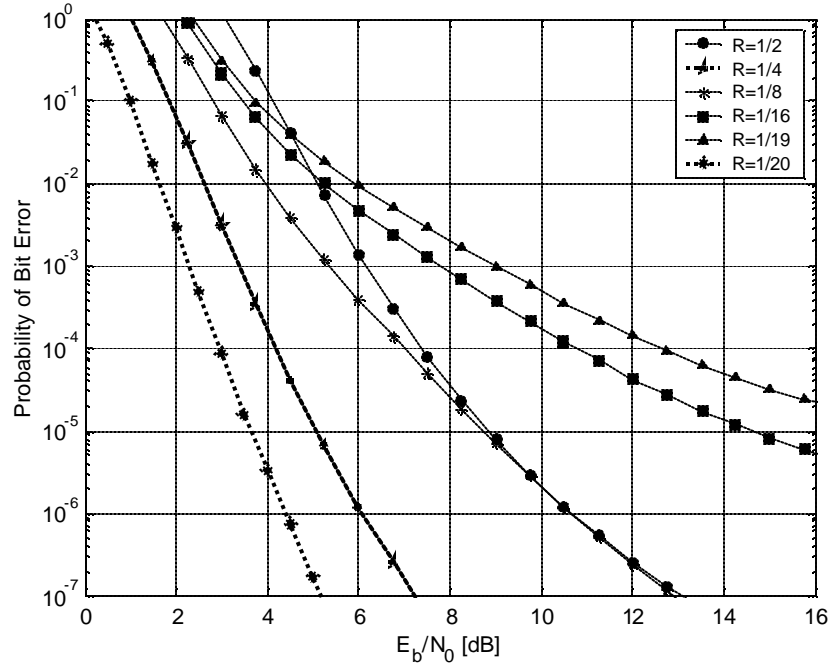


Figure 2. Performance of  $R=1/2$ , some samples of code group A and  $R=1/20$  for  $K=9$ ,  $N=128$  and 10 users.

In conclusion, the ACG is an easy and quick way to check the general improvement associated with the usage of a particular code, although its information may not be accurate in some particular cases, especially when the compared codes do not belong to the same family of codes. For the codes presented in Table 1, the information provided by the ACG allows us to evaluate the first filtering of the best codes to be used in a system with the characteristics of IS-95. Within a Code Group the best performance is clearly provided by the ones with the highest ACG, so the eligible codes to be used in CDMA systems, with the characteristics of IS-95, to code-spread the signal are reduced to the codes presented in Table 2.

<i>Code Group</i>	<i>Code Rate (R)</i>	<i>d<sub>free</sub> (K=9)</i>	<i>x (dB)</i>
A	$\frac{1}{4}$	24	7.782
B	$\frac{1}{20}$	125	7.959
C	$\frac{1}{40}$	251	7.976
D	$\frac{1}{60}$	376	7.970
E	$\frac{1}{80}$	502	7.976
F	$\frac{1}{100}$	628	7.980
G	$\frac{1}{120}$	754	7.982

Table 2. Low-rate Codes with Maximum Asymptotic Coding Gain.

### C. CODE DISTANCE SPECTRUM

The ACG represents a potential increase in performance due to coding; however, there are some cases in which the information provided by the ACG does not match the system's performance. For the code rates presented in Table 2, the values of ACG, plotted in Figure 3, may suggest that the performance would be similar for all of the codes.

In fact, the performance analysis reveals, not only that the codes have different results, but also that this result changes with the number of users. This can be confirmed in Figures 4 and 5, which suggest that sometimes other factors overcame the ACG.

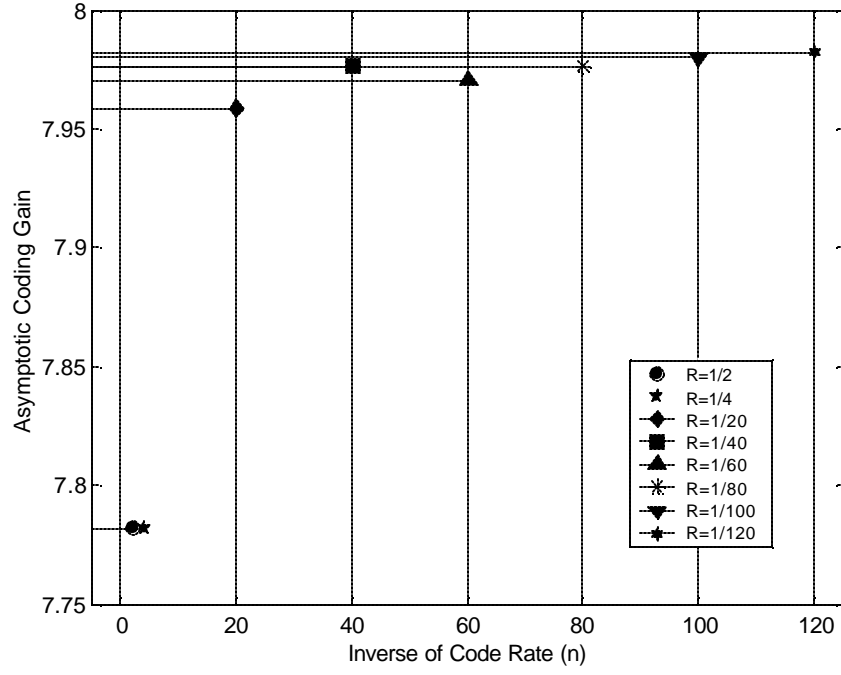


Figure 3. Asymptotic Coding Gain for maximum free distance codes of  $K=9$ .

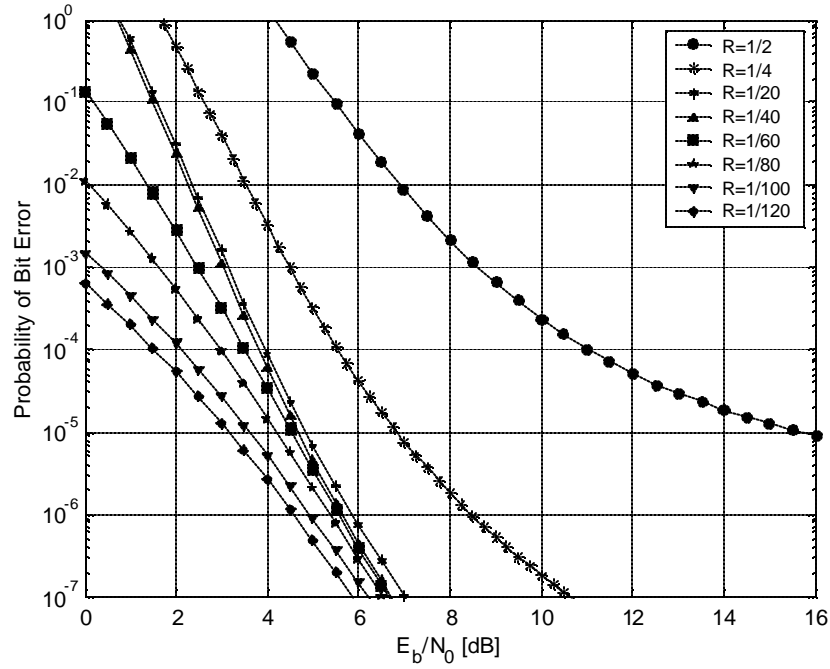


Figure 4. Performance for codes of Table 2, for 40 users, in a Rayleigh fading channel, for  $N=128$ .

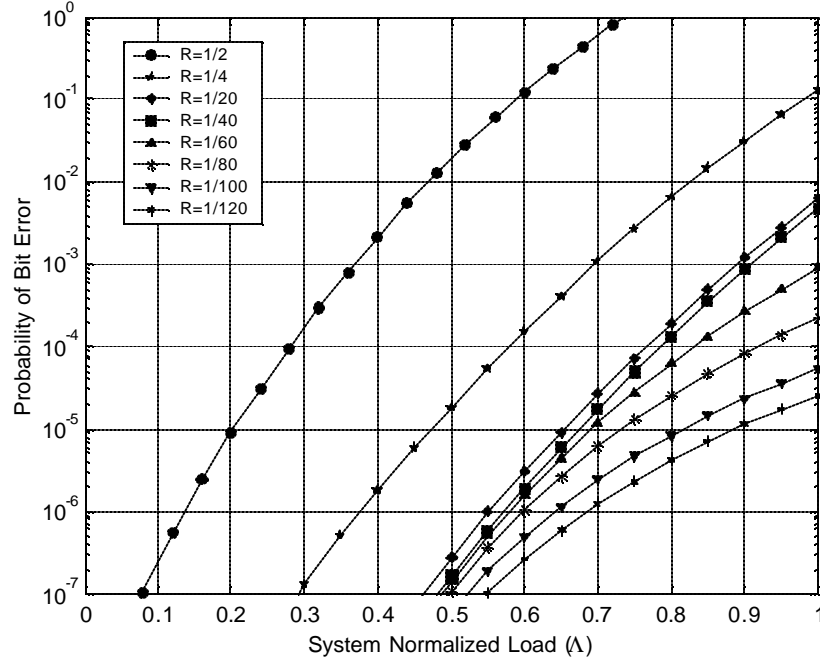


Figure 5. Probability of bit error as a function of the system normalized load, for codes of Table 2 and  $E_b/N_0=10$  dB, in a Rayleigh fading channel

This section presents the analysis of the distance spectrum and its influence in the system's performance. The distance spectrum is a characteristic of a code and represents the number of paths with a given distance  $d$  to the all-zero path. So it is intuitive that if the number of paths is small, for a given  $d$ , the probability of choosing a wrong path is low as well. Consequently, the error correction capacity of a code is directly related with the value of its information error weights  $\mathbf{b}_d$ . Small values of  $\mathbf{b}_d$  will correspond to better codes. In other words, the smaller the growing rate of the  $\mathbf{b}_d$  with the distance  $d$ , the better the code. Since the considered codes are obtained from feed-forward convolutional encoders, the information error weight,  $\mathbf{b}_d$ , is at a minimum, which means the codes are optimum-distance spectrum-convolutional codes [8]. That is, the slope of the lines of each code spectrum, represented in Figure 6, is at a minimum.

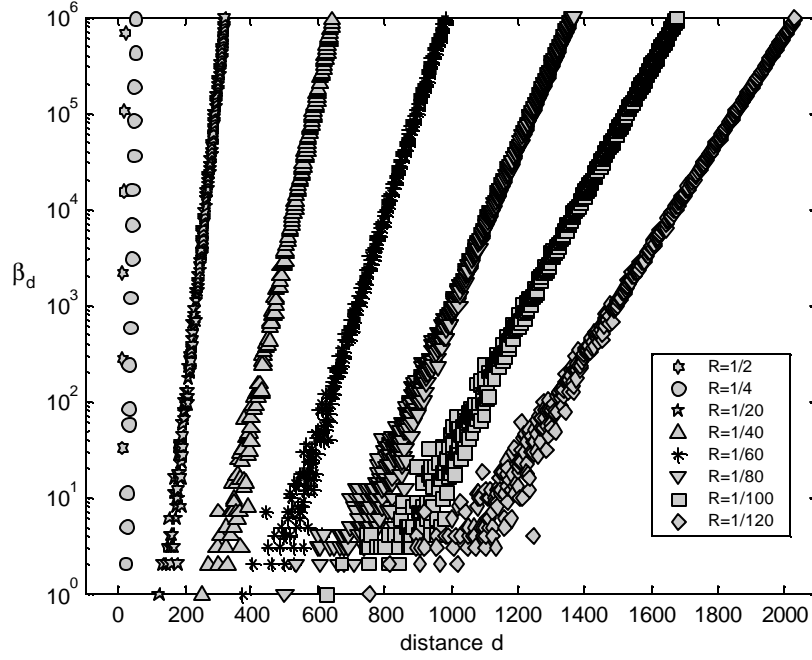


Figure 6. Distance spectrum of nested codes as a function of the distance for  $K=9$

Analyzing the rate of change of  $\mathbf{b}_d$  with the distance  $d$  of different codes requires a definition to represent the logarithmic variation of the Y-axis of Figure 6 by a unique number. This number, whose absolute value has no meaning, allows us to compare the different codes in terms of the variation of  $\mathbf{b}_d$  with  $d$ , by simply comparing its value. Therefore, the comparison criterion would be the slope of the logarithmic representation of the error weights approximated by a linear regression. Figure 7 represents a qualitative comparison between those slopes for the different considered codes.

Based on this criterion, we can easily identify the general behavior of the growing of  $\mathbf{b}_d$ , for each code. However, note that the error correction capacity of a code depends, not only on the rate of increase of the information error weight with the distance, but also on its  $d_{free}$  and consequently on the ACG. Therefore, the information provided in Figure 7 only directly influences performance results if the codes have the same ACG value. In other words, only when codes have the same ACG it is possible to conclude that smaller angles correspond to better performances.

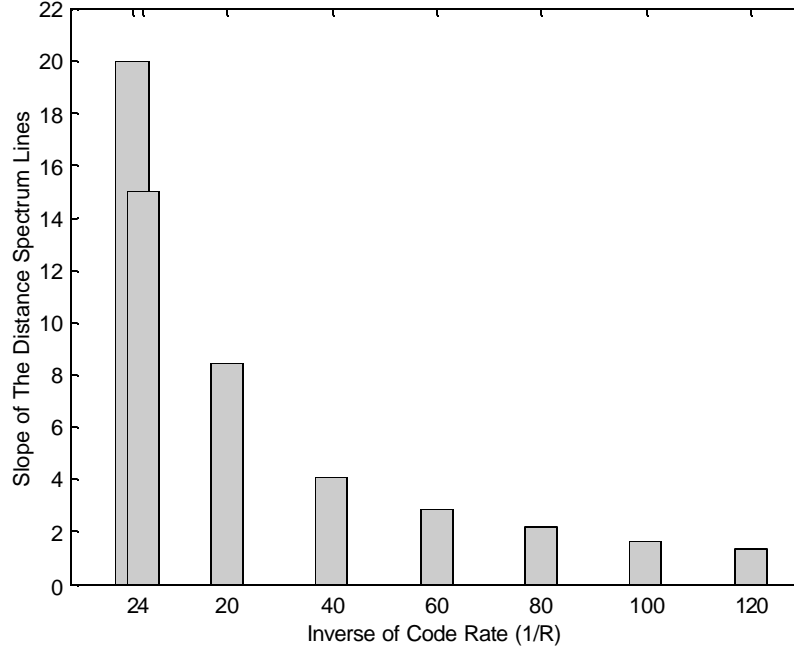


Figure 7 Slopes of the Distance Spectrum Lines of selected codes.

Subsequently, some of the results presented in Figure 5 can now be better interpreted.

In the cases of similar ACG's, like  $R=1/2$  and  $R=1/4$  or  $R=1/20$  to  $R=1/120$ , the best performance is achieved by the code with the smaller rate of increase of the information error weight. In relative terms, if the slope value of the distance spectrum lines is small, the rate of increase of the different terms in the summation of Equation (3.1) will be small and consequently the probability of bit error will be smaller as well. Additionally, Figure 7 provides information about the relationship between the performances of the different codes. Since the slope of the distance spectrum lines exponentially decreases with the inverse of the code rate, it is expected that the amount of increase in the system's performance would also decrease exponentially. So the separation between the curves of different codes in the performance plot would have the same behavior as the difference in slope. This can be confirmed in Figure 4.

#### D. NUMBER OF USERS

Since CDMA systems are especially sensitive to interference, it is quite obvious that by increasing the number of users in the system some performance degradation is created. The interference brought by the additional users, usually treated as additive Gaussian noise, will have different effects whether we have a DS-CDMA or a CS-CDMA system. In the case of DS-CDMA, the capacity of reducing the effect of interference is based on the fact that the spreading sequence makes every interferer appear noise like. For a large number of users, the interference dominates the total noise because the sequences do not reduce the energy of the interference. The result significantly reduces the capacity of interference cancellation and consequently increases the bit error rate. Alternatively, CS-CDMA systems that rely on the powerful code's capacity of recover from errors do not depend of the spreading sequences ability to isolate the users. Additionally, CS-CDMA systems benefit from the possibility of coding to achieve diversity, which in most cases represents a significant improvement in performance. Therefore, when the number of users increases, it is expected that CS-CDMA systems perform better than DS-CDMA systems.

Until this point, all of the analysis that we have made assumes a particular number of users. This means all the considerations about performance are valid for a given number of users. In this section we analyze performance for a different number of users. We investigate the factors that make performance change, by changing the number of users, given that the values of ACG and the distance spectrum remain the same.

Figure 5 presents the performance analysis of different codes as a function of the system's normalized load in a fading environment. Despite the general degradation in performance with the increased number of users, which is due to the effect of the reducing capacity of interference rejection, it can be observed that each code has its own way to response to the bad increasing. Code rates  $R=1/60$  to  $1/120$  have less (proportional) degradation in performance in heavy-load situations. The variation of the average effective SNIR per coded bit as a function of the load explains this fact. The average effective SNIR per coded bit, defined in Equation (3.5), decreases more rapidly with the load for



higher code rates. This can be confirmed in Figure 8. In the cases of codes with approximately the same rate of change of an average effective SNR per channel path, the variation in performance with the load will be proportional. This means that the curves in the plots of probability of bit error versus  $E_b/N_0$  for the different number of users will be parallel.

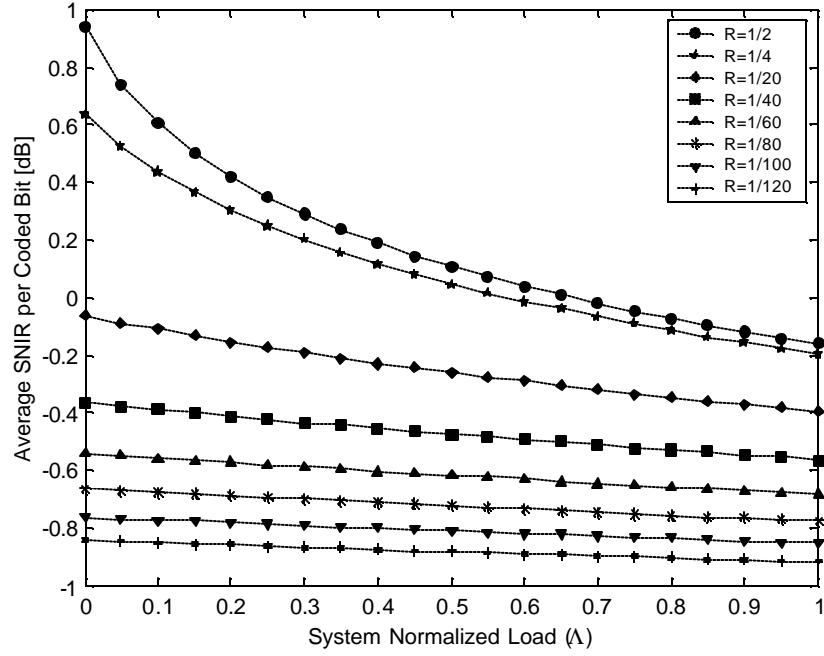


Figure 8. Average SNIR per coded bit for a  $E_b/N_0$  of 12 dB, as a function of the system's normalized load.

## E. SUMMARY

In this chapter we investigated the performance of different combinations of DS-CDMA and CS-CDMA in a Rayleigh fading environment. It was verified that the usage of very low-rate codes does not always guarantee the best results in terms of performance and complexity and that the most important feature is the capacity of correcting errors. Eventually, the analysis of the asymptotic gain provided a good initial approach in the search for the best code and spreading factor; however, it cannot be considered conclusive, especially in the cases of similar asymptotic coding gain. The comparison of the rate

of the increase in the error weight of the codes is a good way to predict the performance, but since the probability of bit error of a system is also a function of the free distance, the analysis is more accurate in the cases of codes with approximately the same asymptotic coding gain. Finally, we analyzed the different codes for a different number of users. It was evident that the lower rate codes had the advantage over the higher rate for heavy loaded systems. The incapacity of the spreading sequences to reduce the energy of the interferences causes, after a certain point, the interference to overwhelm the total noise. Consequently the interference cancellation capacity is drastically reduced. This, in turn, increases the bit error rate. On the other hand, lower rate codes have less dependency on the spreading sequence's ability to isolate the users and more dependency on its own capacity of recover from errors. This makes those codes more appropriate to deal with the increasing interference. Additionally, lower rate codes benefit from the possibility of coding to achieve diversity. This can represent a significant advantage in environments of higher probability of error.

In spite of the usage of a specific family of low-rate codes, for the coding-spreading analysis, the criteria can be applied to any code. The procedures to determine the code that will provide the best performance are generic even though the results for different codes might be different.

In the next chapter, we address the randomness introduced by a non-ideal channel and investigate how it influences the performance of the different combinations of coding-spreading.

## IV. RANDOM TRADEOFF FACTORS

The random behavior of the channel characterizes wireless communications and consequently characterizes the uncertainty about the amplitudes and phases at the receiver. In this chapter, we address the randomness introduced by a non-ideal channel and investigate how it influences the performance of the different combinations of coding-spreading once again. The point of departure for the entire analysis is the IS-95 standard. The benchmark is the performance of a system that uses a total bandwidth expansion,  $N=128$ , an encoder with a code rate,  $R=1/2$  and a constraint length,  $K=9$ . This system is compared to systems of different combinations of coding and spreading with the same processing gain. This is done for a different number of users, channel fading and shadowing and using different techniques for interference reduction.

Therefore, Section A analyses the different coding and spreading combinations in fading-shadowing channels. The statistical model chosen to emulate the fading channel conditions is defined. Because fading is not the only random phenomena that affects wireless communications, we also incorporated the factor that considers the surrounding environment clutter changes, namely the shadowing. Two cases are studied, a worst-case scenario in which the mobile is located in any corner of the hexagon cell in a seven cell cluster and a more realistic scenario in which the mobile can be located in any position on the cell, described by a uniform probability density function.

Section B analyses the performance of the different combinations in the same fading-shadowing environment using two different techniques for interference reduction, sectoring and power control.

### A. PERFORMANCE IN FADING-SHADOWING CHANNELS

Performance analysis in non-ideal channels requires statistical models that can emulate the characteristics of the communications' environment with enough flexibility to adjust the different parameters. Based on this, the Nakagami- $m$  distribution was chosen

to model the fading in the channel for the considered systems. The main reason for this choice was Nakagami- $m$  distribution's ability to match the observed signal statistics in fading environments [11] and Nakagami- $m$  distribution's flexibility to vary the statistical channel representation, simply by changing the value of the parameter  $m$ . The Nakagami- $m$  distribution allows the emulation of fading conditions as different as when line-of-sight (LOS) is not available and numerous multipath components arrive at the receiver ( $m \leq 1$ ). This includes the special case in which the channel is modeled as a Rayleigh fading channel ( $m=1$ ). Additionally, modeling the case where LOS exists but the multipath phenomena is still present is possible, with another special case when  $m=2$ , which corresponds to the Ricean fading. Because fading is not the only random phenomena that affects wireless communications, we also incorporate a factor that considers whether the surrounding environmental clutter may be vastly different at two different locations having the same distance to the transmitter. The slow variation of the mean signal level due to shadowing from terrain, buildings, trees, etc, is usually modeled by a log-normal distribution [25].

In our analysis we considered a BPSK system with forward error correction coding, whose probability of bit error is upper bounded by the Equation (3.1) and the first event error probability, described in Chapter III, can be generically defined by [26]

$$P_2(d) \Big|_{z_d} = Q \left( \sqrt{\frac{z_d}{\mathbf{a}}} \right) \quad (4.1)$$

where the  $Q$  function denotes the Gaussian integral function,  $\mathbf{a}$  considers the received SNR, interference, path loss, spreading, etc, and  $z_d$  is the value assumed by the random variable  $Z_d$ , defined as the sum of  $d$  Nakagami- $m$  square-lognormal random variables as follows:

$$Z_d = \sum_{l=1}^d R_l^2 \widetilde{X}_l \quad (4.2)$$

where  $R_l^2$  is the Nakagami square random variable,  $d$  is the distance from the all zero path in the code's Trellis diagram and  $\widetilde{X}_l$  is a lognormal random variable with a zero mean and variance of  $\mathbf{I} \mathbf{s}_{dB}$ , with  $\mathbf{I}$  defined as  $\ln(10)/10$  and  $\mathbf{s}_{dB}$  as the variance of the

Gaussian random variable that considers the difference between the path losses at a given distance from the median path loss, defined in [26]. The index  $l$  in (4.2) runs over the set of  $d$  bits in which the two paths differ.

To obtain the probability of bit error for the different codes, we must compute the first-event error probability and apply it to (3.1), which means solving

$$\begin{aligned} P_2(d) &= \int_{-\infty}^{\infty} P_2(d) \Big|_{z_d} p_{Z_d}(z_d) dz_d \\ &= \int_{-\infty}^{\infty} Q\left(\sqrt{\frac{z_d}{a}}\right) p_{Z_d}(z_d) dz_d. \end{aligned} \quad (4.3)$$

Due to the complexity of the channel model, no analytical solutions can be reasonably developed. So we use statistical modeling of solutions and probability distributions in substitution of the convolution of  $d$  probability density functions. Through Monte Carlo simulation, one can calculate the integral of (4.3) by generating one realization for the  $Z_d$  random variable and can then use this value in (4.1) to obtain one realization  $\tilde{P}_{2_i}(d)$ . This process is then repeated 100,000 times and averaged down to obtain the estimation,  $\hat{P}_2(d)$  of  $P_2(d)$  as follows:

$$\hat{P}_2(d) = \frac{1}{100,000} \sum_{i=1}^{100,000} \tilde{P}_{2_i}(d). \quad (4.4)$$

The drawbacks of this approach are the costs in computation time and the fact that accuracy depends on the random variables generator. In our case, we used MATLAB<sup>®</sup> as the programming tool and its built-in functions to generate random numbers. Therefore, the Nakagami- $m$  random variables were obtained through the generation of Gamma random variables and then through the following transformation,

$$\mathbf{k} = \sqrt{\frac{G}{m}} \quad (4.5)$$

where  $G$  represents a Gamma random variable,  $m$  is the Nakagami parameter and  $\mathbf{k}$  is the Nakagami random variable.

## 1. Worst-case

In this sub-section we discuss the tradeoff problem in which the mobile is located in any corner of a hexagon cell in a seven cell cluster, as described in Figure 9. This situation corresponds to the worst-case position in which the mobile receives the signal of three base stations, with approximately the same energy each.

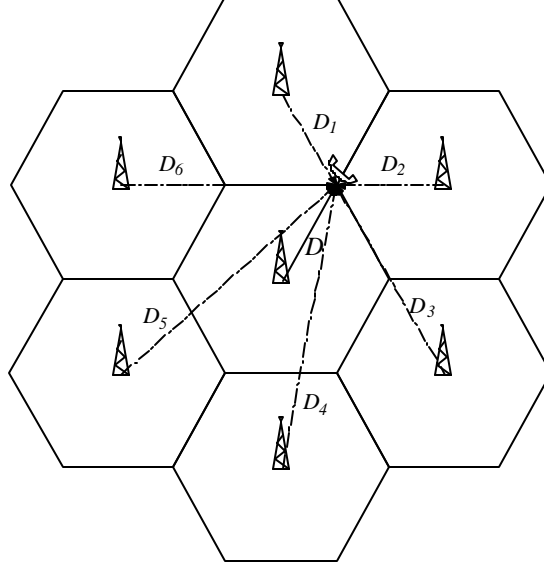


Figure 9. Mobile in the worst-case position on a seven (hexagon) cell cluster.

The distances from the adjacent cell base stations,  $D_i$ , to the mobile user in the worst-case position is given by

$$D_i = \begin{cases} D, & i=1,2 \\ 2D, & i=3,6 \\ \sqrt{7}D, & i=4,5 \end{cases} \quad (4.6)$$

where  $D$  is the length of each side of the hexagon.

The direct consequence of this position is the high amount of interference, which is received by the mobile user. As a result, the SNIR, derived in [26], corresponds to a value of  $\mathbf{a}$ , in equation (4.1), defined by

$$\mathbf{a} = \frac{\exp\left(\frac{I^2 \mathbf{s}_{dB}^2}{2}\right)}{3N_c} \sum_{i=1}^6 \sum_{j=0}^{K_i-1} \frac{L_H(D)}{L_H(D_i)} + \frac{N_o}{2RE_b} \quad (4.7)$$

where  $R$  is the code rate,  $N_c$  is the processing gain,  $K_i$  is the number of users in the adjacent cell,  $L_H(D)$  is the Hata median path loss of information carrying a signal from the center cell's base station to the mobile user at distance  $D$  and  $L_H(D_i)$  are the Hata median path loss for signals transmitted from the respective base stations. This contributes to the co-channel interference in the received signal as described in [23].

The Hata Model is the analytical expression of the Okumara empirical model, which is one of the most accurate empirical models in cellular communications. This model allows one to analyze the median path loss in an urban environment and supplies correction equations applicable to other situations. In cases of carrier frequencies from 1.5 GHz to 2 GHz, an extension should be used for the Hata model. Therefore, the values of  $L_H(D)$  and  $L_H(D_i)$  can be calculated from the following expressions:

$$L_H[dB] = 46.3 + 33.9 \log f_c - 13.82 \log h_{base} - a(h_{mobile}) + (44.9 - 6.55 \log h_{base}) \log D + C_M \quad (4.8)$$

$$a(h_{mobile}) = (1.1 \log f_c - 0.7) h_{mobile} - (1.56 \log f_c - 0.8) \text{ (dB)} \quad (4.9)$$

$$C_M = \begin{cases} 0 \text{ dB, for medium sized city and suburban areas} \\ 3 \text{ dB, for metropolitan centers} \end{cases} \quad (4.10)$$

where  $h_{base}$  and  $h_{mobile}$  are the heights of the base station and mobile antennas, considered as 30 m and 1 m respectively,  $f_c$  the carrier frequency in MHz (which in our case is 2000),  $D$  is the distance between the base station and the mobile, possessing the value of 1 km for our purposes and finally,  $C_M$  is an operating area correction factor, which we considered as 3 dB.

Hence, using equations (3.1), (4.1) and the values of  $\mathbf{a}$  defined in (4.7), evaluating the probability of bit error through Monte Carlo simulations for different values of fading and shadowing is possible.

### *a. Fading Variations*

The multipath fading is a characteristic phenomenon of wireless communications, resulting in fluctuations of amplitude and phase of the received signal over time. In the case of coherent modulation schemes, the fading effects on the phase can severely degrade the performance, unless the receiver has some features to compensate for it. Thus it is often assumed that phase effects due to fading are completely corrected at the receiver. This means the coherent demodulation is perfect. In our analysis, we also make this assumption.

In this sub-section, we investigate the performance of the different codes in a Nakagami- $m$  fading environment with shadowing. The parameter  $m$  can assume any value from 0.5 to infinity, but in our case we only compare the performances for three values of  $m$  that cover the most common situations:  $m=0.5$  represents the one-sided Gaussian distribution,  $m=1$  corresponds to the Rayleigh distribution and finally  $m=2$  covers the Ricean distribution. For the sake of comparing performance with the changes in fading, we use fixed values for shadowing, assigning  $\mathbf{s}_{dB}=4$ .

Figure 10 presents the probability of bit error, as a function of the  $E_b/N_0$ , for different combinations of coding-spreading,  $m=0.5$ ,  $\mathbf{s}_{dB}=4$  and 10 users per adjacent cell. This case represents the one-sided Gaussian fading, which corresponds to the worst-case fading, typical of very congested downtown areas with slow-moving pedestrians and vehicles. No LOS is available, so even the first arriving path exhibits high amounts of fading, due to the decrease in power with the delay.

Figure 11 presents the probability of bit error, as a function of the  $E_b/N_0$  for different combinations of coding-spreading,  $m=1$ ,  $\mathbf{s}_{dB}=4$  and 10 users per adjacent cell. This represents the Rayleigh fading situation, frequently used to model multipath fading with no direct LOS path. Again, the first arriving path exhibits high amounts of fading. Finally, Figure 12 presents the case of  $m=2$ ,  $\mathbf{s}_{dB}=4$  and the same number of users per adjacent cell as the previous figures. This situation is used to model propagation paths con-



sisting of one strong direct LOS component and many random weaker components, known as Ricean fading.

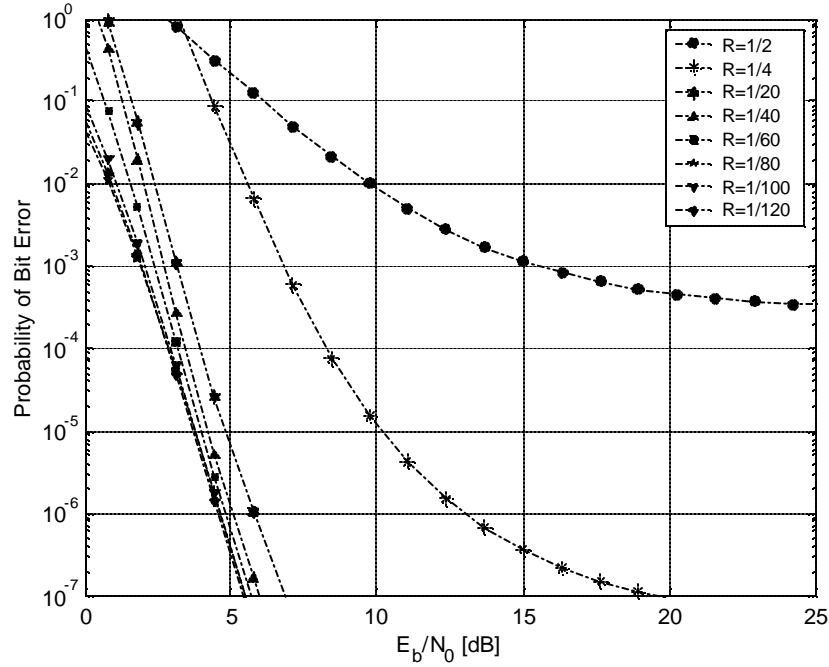


Figure 10. Probability of bit error for different code rates with the total bandwidth expansion  $N=128$  in a Nakagami Fading ( $m=0.5$ ) and Lognormal Shadowing ( $S_{dB}=4$ ) channel, for 10 users per cell – Worst-case.

The systems in which the bandwidth expansion is mainly provided by the coding obviously present better performances. In fact, for a fixed value of shadowing and number of users in the adjacent cells, the performances of  $R=1/20$  to  $R=1/120$  are barely independent of the amount of fading in the channel. The  $E_b/N_0$  required to achieve a probability of bit error of  $10^{-5}$  for  $R=1/20$  to  $1/120$  is around 6 dB, no matter how deep the fading environment is. The reason for this relies on the fact that coding can benefit from the possibility of achieving diversity, which is well known to be very effective in fading environments. On the other hand, in the systems in which bandwidth expansion is mainly due to the spreading sequences, the degradation in performance with the fading is quite evident. The code rate  $1/4$  has a difference of 3 dB, for a probability of bit error of  $10^{-5}$ , when the fading increases ( $m=2$  to  $m=0.5$ ), while  $R=1/2$  has a required  $E_b/N_0$  of 11 dB to reach the same probability of bit error in Ricean fading ( $m=2$ ) and cannot reach  $10^{-5}$  at all for  $m=0.5$ .

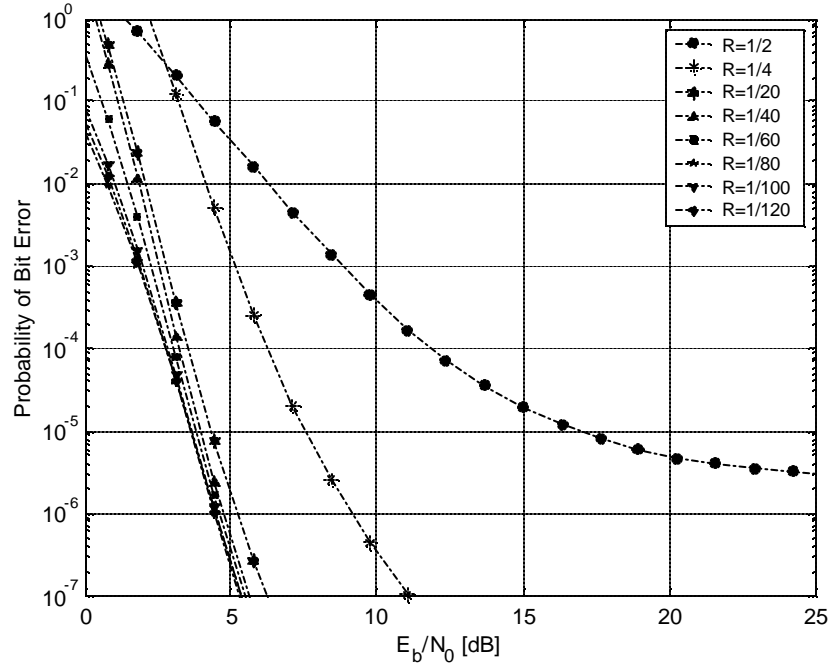


Figure 11. Probability of bit error for different code rates with the total bandwidth expansion  $N=128$  in a Nakagami Fading ( $m=1$ ) and Lognormal Shadowing ( $s_{dB}=4$ ) channel, for 10 users per cell – Worst-case.

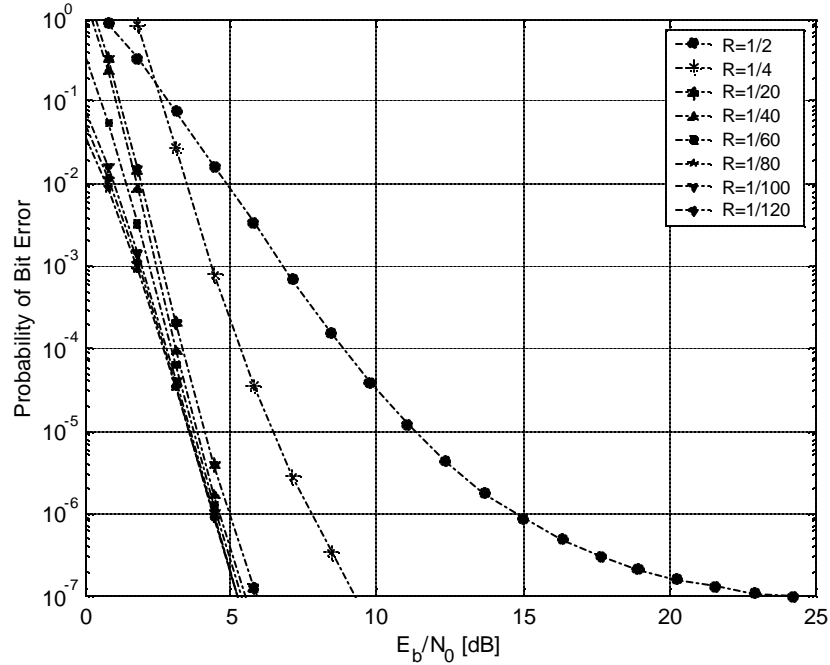


Figure 12. Probability of bit error for different code rates with the total bandwidth expansion  $N=128$  in a Nakagami Fading ( $m=2$ ) and Lognormal Shadowing ( $s_{dB}=4$ ) channel, for 10 users per cell – Worst-case.

Additionally, it can be observed that the best coding-spreading tradeoff is a combination of both direct sequence and code-spreading with a larger fraction of bandwidth provided by the coding. The best performance is exhibited by the  $R=1/80$ , which corresponds to a contribution of coding to the total bandwidth expansion of 62.5%. This is a very interesting result since theoretical expressions for Rayleigh fading in equations (3.2) to (3.5) indicated that the best performance is achieved by the lowest rate code, as presented in Figure 4.

#### ***b. Shadowing Variations***

In an environment in which the multipath is superimposed on log-normal shadowing, the receiver does not average out the envelope fading due to multipath, but rather reacts to the instantaneous composite multipath/shadowing signal [27]. When the shadowing increases, the actual path loss at a given distance will differ significantly from the predicted average path loss.

Figures 13 to 15 represent the probability of bit error for different combinations of coding-spreading for  $m=0.5, 1$  and  $2$  and  $S_{dB} = 7$  for 10 users per adjacent cell. A significant degradation in performance is seen in systems in which the bandwidth expansion is mainly due to the spreading sequences. The code rate of  $1/4$  has experienced an increase of 6 dB in the  $E_b/N_0$ , required to achieve a probability of bit error of  $10^{-5}$ , just due to the increase in shadowing, while in the case of  $R=1/2$  the increase in shadowing make  $10^{-5}$  inaccessible. The code rates of  $1/20$  to  $1/120$  have a degradation of less than 1 dB for the same probability of bit error, but the best performance is now achieved by the lowest code rate. Again, this is explained by the fact that coding can benefit from the possibility to achieve diversity, which assumes a special importance when the received signal can vary significantly.

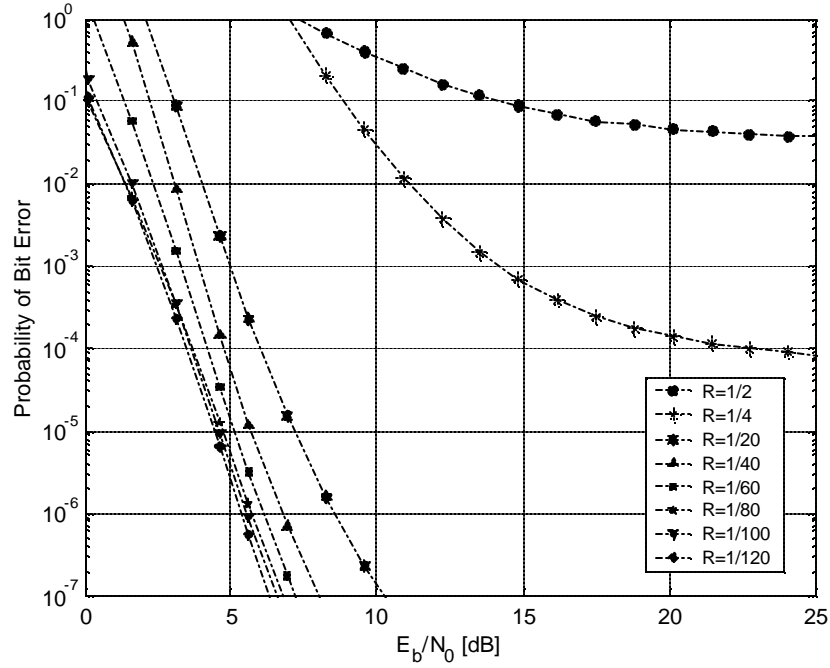


Figure 13. Probability of bit error for different code rates with the total bandwidth expansion  $N=128$  in a Nakagami Fading ( $m=0.5$ ) and Lognormal Shadowing ( $s_{dB}=7$ ) channel, for 10 users per cell – Worst-case.

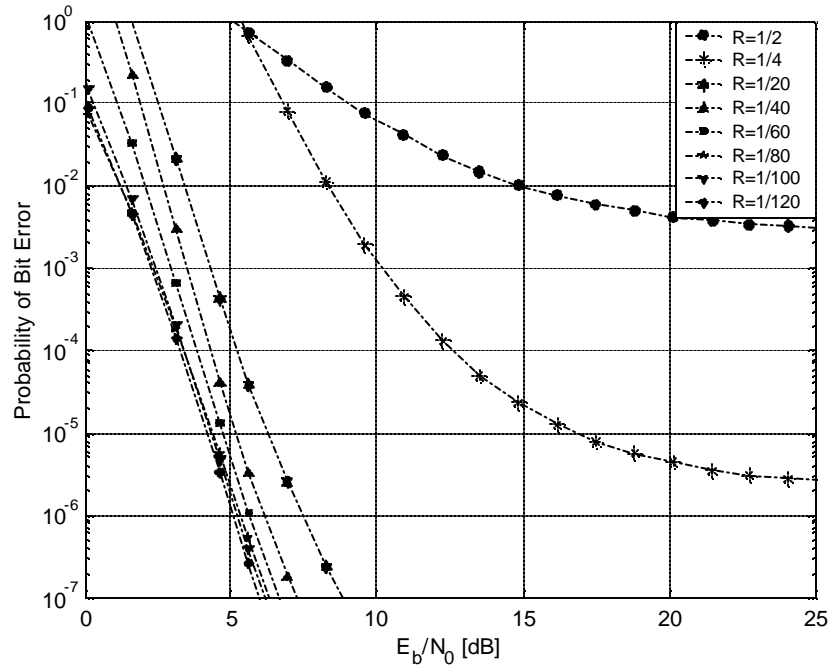


Figure 14. Probability of bit error for different code rates with the total bandwidth expansion  $N=128$  in a Nakagami Fading ( $m=1$ ) and Lognormal Shadowing ( $s_{dB}=7$ ) channel, for 10 users per cell – Worst-case.

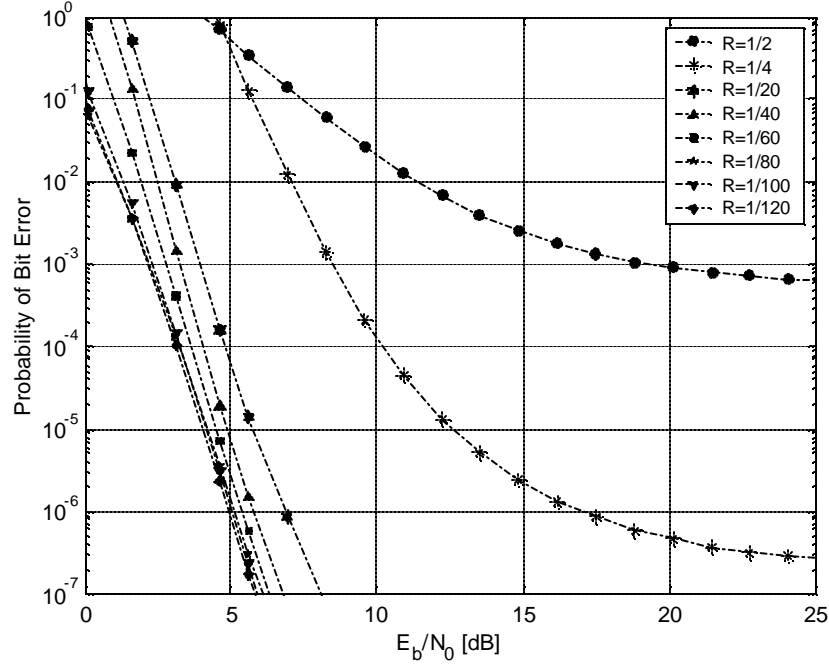


Figure 15. Probability of bit error for different code rates with the total bandwidth expansion  $N=128$  in a Nakagami Fading ( $m=2$ ) and Lognormal Shadowing ( $s_{dB}=7$ ) channel, for 10 users per cell – Worst-case.

### c. Variations in the Number of Users

We have seen the behavior of the different codes under different types of fading and shadowing intensity for a given number of users (10) in the adjacent cells. In this sub-section, we investigate the codes' performance when the number of users changes. As the number of users per cell increases, the amount of intercell interference received by a mobile user increases as well and so does the probability of a bit error. Depending on the characteristics of the channel and the minimum probability of bit error specifications, defining the typical number of users allowed in a particular system is possible. Figures 16 and 17 show the performance of the different combinations of coding-spreading in Nakagami- $m$  fading and lognormal shadowing for the cases of 20 and 40 users per adjacent cell. As expected (see Section III. C) the various combinations of coding-spreading react differently to the increasing of number of users. CS-CDMA systems are less sensitive to load changes than DS-CDMA systems. Code rate 1/80, which pre-

sented the best performance for 10 users per adjacent cell, in Figure 10, is overcome by the lower rate codes when the number of users increases to 20 or 40. This is a consequence of the incapacity of larger spreading sequence component, in the combination of  $R=1/80$ , to discard the energy of the new users. The result is the dominance of interference energy over the total noise. Coding can deal with interference in a more efficient way so that, the higher the coding component, the better the performance. Similar results are obtained for different values of fading, as shown in Figures 18 to 21, even though the results are not as obvious as in the case of  $m=0.5$ .

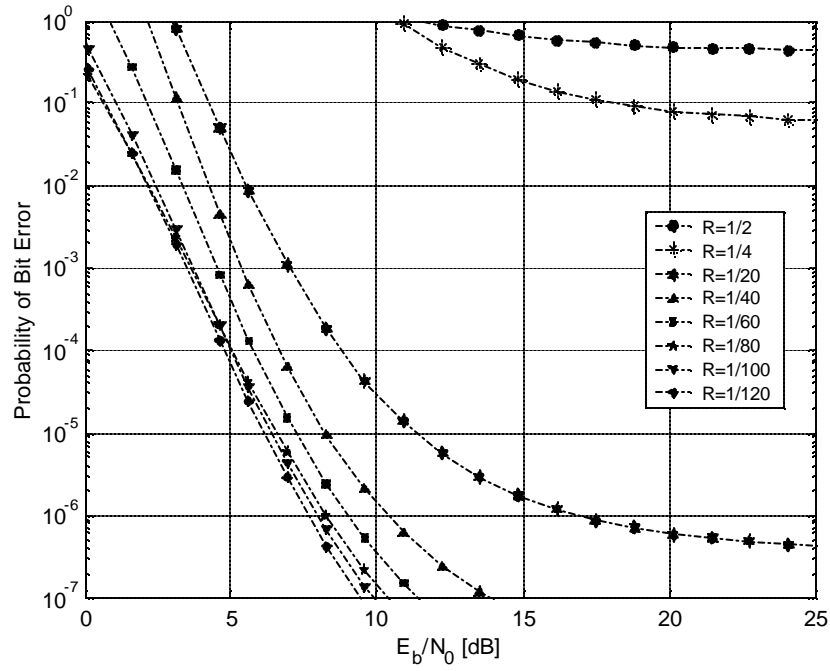


Figure 16. Probability of bit error for different code rates with the total bandwidth expansion  $N=128$  in a Nakagami Fading ( $m=0.5$ ) and Lognormal Shadowing ( $s_{dB}=7$ ) channel, for 20 users per cell – Worst-case.

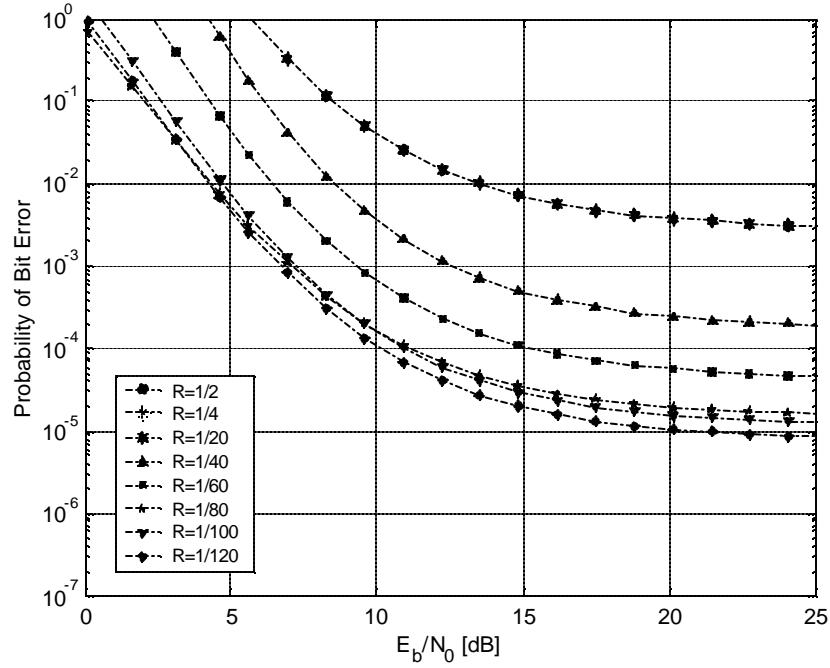


Figure 17. Probability of bit error for different code rates with the total bandwidth expansion  $N=128$  in a Nakagami Fading ( $m=0.5$ ) and Lognormal Shadowing ( $s_{dB}=7$ ) channel, for 40 users per cell – Worst-case.

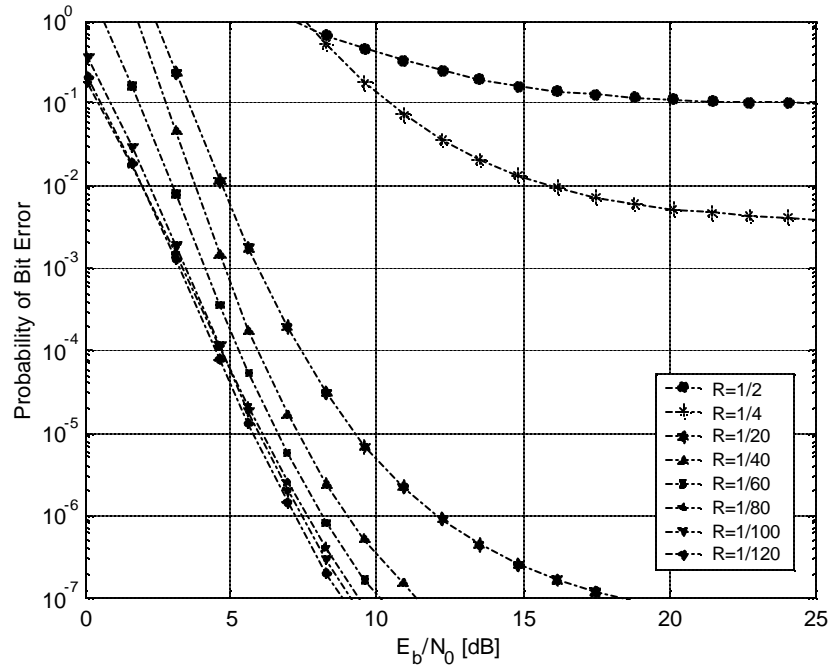


Figure 18. Probability of bit error for different code rates with the total bandwidth expansion  $N=128$  in a Nakagami Fading ( $m=1$ ) and Lognormal Shadowing ( $s_{dB}=7$ ) channel, for 20 users per cell – Worst-case.

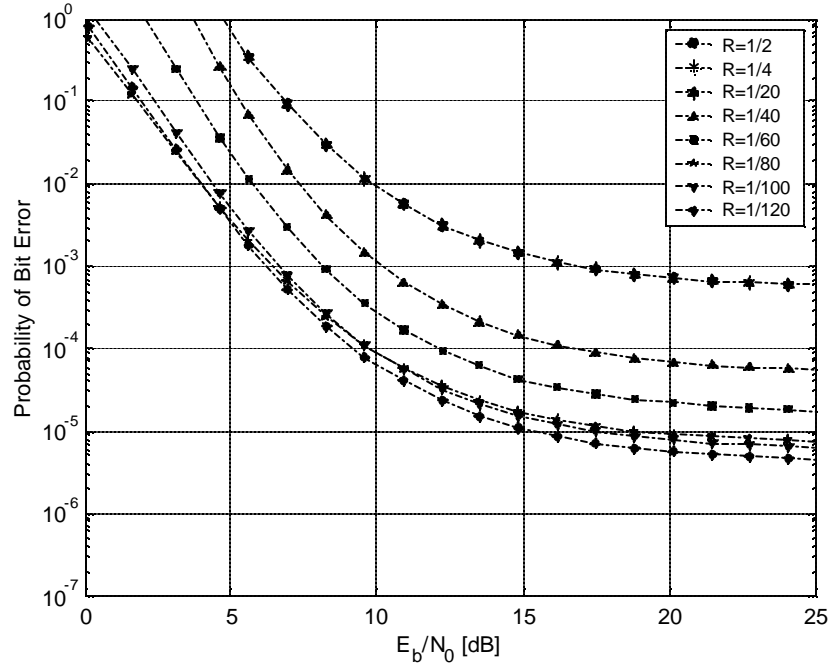


Figure 19. Probability of bit error for different code rates with the total bandwidth expansion  $N=128$  in a Nakagami Fading ( $m=1$ ) and Lognormal Shadowing ( $S_{dB}=7$ ) channel, for 40 users per cell – Worst-case.

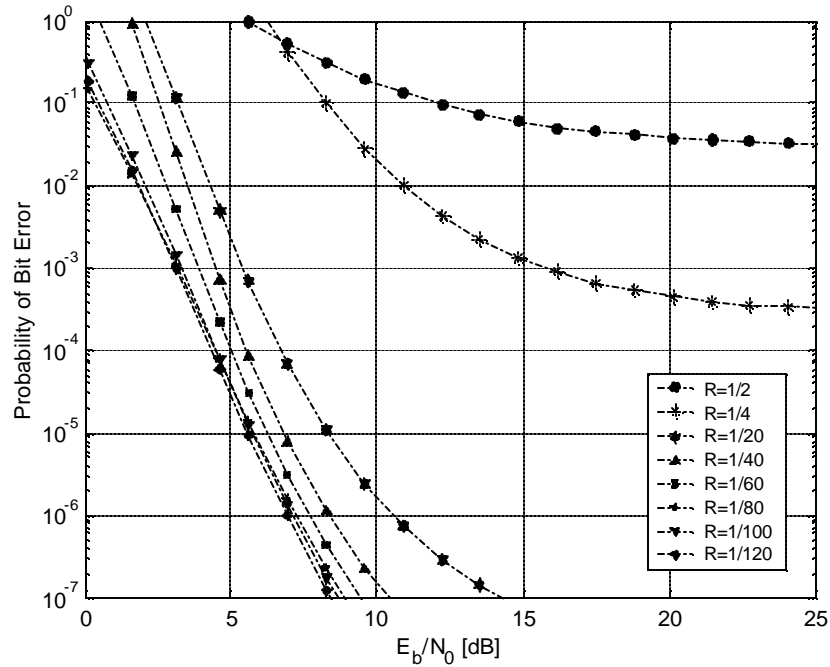


Figure 20. Probability of bit error for different code rates with the total bandwidth expansion  $N=128$  in a Nakagami Fading ( $m=2$ ) and Lognormal Shadowing ( $S_{dB}=7$ ) channel, for 20 users per cell – Worst-case.



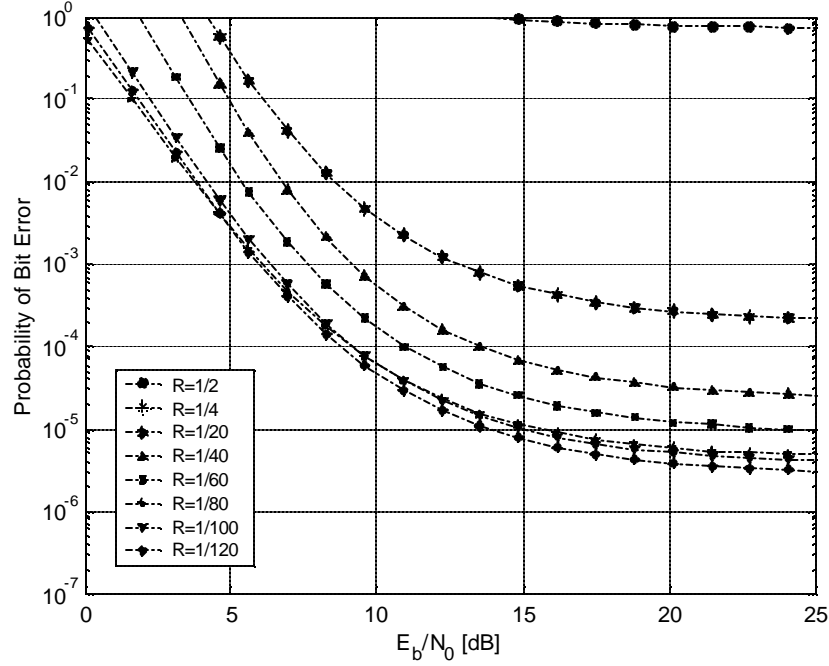


Figure 21. Probability of bit error for different code rates with the total bandwidth expansion  $N=128$  in a Nakagami Fading ( $m=2$ ) and Lognormal Shadowing ( $S_{dB}=7$ ) channel, for 40 users per cell – Worst-case.

## 2. Uniform User Distribution

This section analyzes the different combinations of coding and spreading in a more realistic scenario. It is assumed that the user can be physically located anywhere in the cell, following a uniform probability distribution function. In the real world, not all of the user position distribution in the cells follows a uniform behavior, but in most cases the approach will be good. Based on this, the angular positions of a user can be described by a uniform random variable and the radial positions by a beta random variable, in which the intended mobile user's position in the center cell is defined by  $(r, \theta)$  where  $0 < r < 1$  and  $-\pi < \theta \leq \pi$ . Therefore, for simplicity sake, the hexagonal cells will be replaced by overlapping circular cells as represented in Figure 22

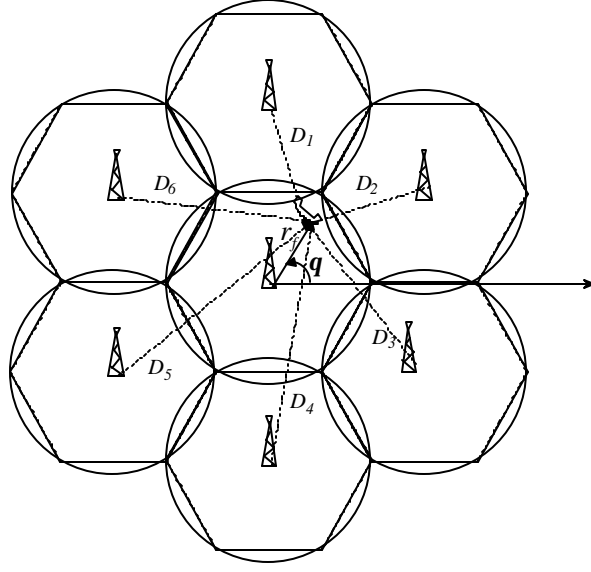


Figure 22. Mobile in a Seven (Circular) Cell Cluster.

where the distance  $D_i$  from each adjacent base station to the mobile user in the center cell is a function of  $r$  and  $\mathbf{q}$  and is given by

$$D_i = \begin{cases} \sqrt{r^2 - 2\sqrt{3}r \cos \mathbf{q} + 3}, & i=1 \\ \sqrt{r^2 - \sqrt{3}r \cos \mathbf{q} - 3r \sin \mathbf{q} + 3}, & i=2 \\ \sqrt{r^2 + \sqrt{3}r \cos \mathbf{q} - 3r \sin \mathbf{q} + 3}, & i=3 \\ \sqrt{r^2 + 2\sqrt{3}r \cos \mathbf{q} + 3}, & i=4 \\ \sqrt{r^2 + \sqrt{3}r \cos \mathbf{q} + 3r \sin \mathbf{q} + 3}, & i=5 \\ \sqrt{r^2 - \sqrt{3}r \cos \mathbf{q} + 3r \sin \mathbf{q} + 3}, & i=6. \end{cases} \quad (4.11)$$

Since these distances  $D_i$  are randomized, using the Hata model in order to predict the path loss is too difficult. So we use a simpler expression presented in [23] and when properly set, it gives the same results as the Hata model. The path loss can be calculated by

$$\bar{L}_n(D) \propto \left( \frac{D}{d_0} \right)^n \quad (4.12)$$

where  $n$  is the path loss exponent (indicating the increasing rate of path loss with the distance) and  $d_0$  is the close-in reference distance, which is determined from measurements close to the transmitter. It turns out that, for  $n=4$  (this corresponds to shadowed urban cellular radio environment), the results obtained for the path loss are the same as in the case of using the Hata model for a frequency of 2 GHz and a base station antenna height of 30 m and a mobile antenna height of 1 m [26].

Therefore, in the case of uniform user distribution through the cells, assuming that the intended mobile user's position is fixed and exactly defined using the parameters  $r$  and  $\mathbf{q}$  as  $r_f$  and  $\mathbf{q}_f$ , the SNIR was derived in [26] and corresponds to a value of  $\mathbf{a}$  defined by

$$\begin{aligned} \mathbf{a} &= -\frac{\exp\left(\frac{\mathbf{I}^2 \mathbf{S}_{dB}^2}{2}\right)}{3N_c} \sum_{i=1}^6 \sum_{j=0}^{k_i-1} \frac{\bar{L}_n(r_f)}{\bar{L}_n(D_i)} + \frac{N_o}{2RE_b} \\ &= -\frac{\exp\left(\frac{\mathbf{I}^2 \mathbf{S}_{dB}^2}{2}\right)}{3N_c} \sum_{i=1}^6 \sum_{j=0}^{k_i-1} \frac{r_f^n}{D_i^n} + \frac{N_o}{2RE_b} \end{aligned} \quad (4.13)$$

where  $n$  is the path loss exponent.

To obtain the BER for the different codes, one need to compute the first-event error probability and apply it to (3.1), which means solving

$$\tilde{P}_{2_i}(d) = \int_{-p}^p \int_0^1 \int_{-\infty}^{\infty} \frac{r}{p} Q \left[ \sqrt{\frac{z_d}{\frac{\exp\left(\frac{\mathbf{I}^2 \mathbf{S}_{dB}^2}{2}\right)}{3N_c} \sum_{i=1}^6 \sum_{j=0}^{k_i-1} \frac{r_f^n}{D_i^n} + \frac{N_o r^n}{2RE_b r_f^n}}} \right] p_{z_d}(z_d) dz_d dr d\mathbf{q}. \quad (4.14)$$

Again, using equations (3.1), (4.1) and the value of  $\mathbf{a}$  defined in (4.13), one can evaluate the probability of bit error through Monte Carlo simulations for different values of fading and shadowing.

### *a. Fading Variations*

The approach used to study the performance of the various combinations of coding-spreading in the case of uniform user distribution is the same as the one presented in Section IV.A.1, for the worst case. It is considered a fixed shadowing and number of users per adjacent cell and three types of fading.

Figures 23 to 25 present the probability of bit error for  $m=0.5, 1$  and  $2$ . The results obtained follow the general behavior of the ones presented in Section A.2. The considerations regarding the best coding-spreading tradeoff, as a function of the fading, presented in Section A.1.a, are essentially valid for this section, with exception of  $R=1/80$ . For a uniform user distribution along the cell, the performances obtained are obviously better than in the worst-case scenario. The less demanding conditions of a uniform distributed user position, as opposed to worst-case position, allow the  $R=1/80$  to become the code rate with the better performance. The higher rate codes in particular, present a smaller difference in performance with relation to the lower rate codes. The  $E_b/N_0$  required to achieve a probability of bit error of  $10^{-5}$ , which in the present case is around 2 dB smaller than in the worst-case. For  $R=1/4$  to  $1/120$  and 6 dB for  $R=1/2$ , considering a probability of bit error of  $10^{-3}$ .

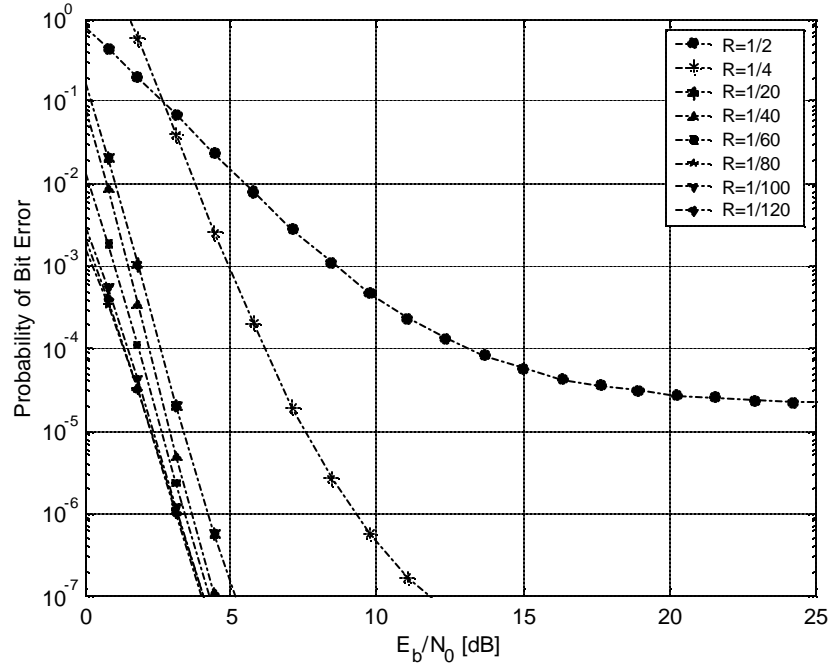


Figure 23. Probability of bit error for different code rates with the total bandwidth expansion  $N=128$  in a Nakagami Fading ( $m=0.5$ ) and Lognormal Shadowing ( $s_{dB}=4$ ) channel, for 10 users per adjacent cell – Uniform User Distribution.

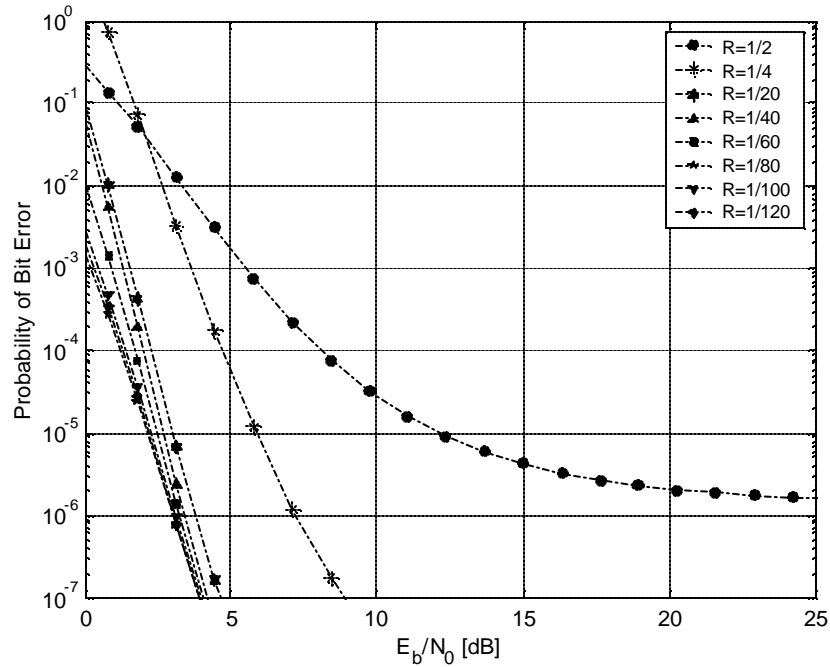


Figure 24. Probability of bit error for different code rates with the total bandwidth expansion  $N=128$  in a Nakagami Fading ( $m=1$ ) and Lognormal Shadowing ( $s_{dB}=4$ ) channel, for 10 users per adjacent cell – Uniform User Distribution.

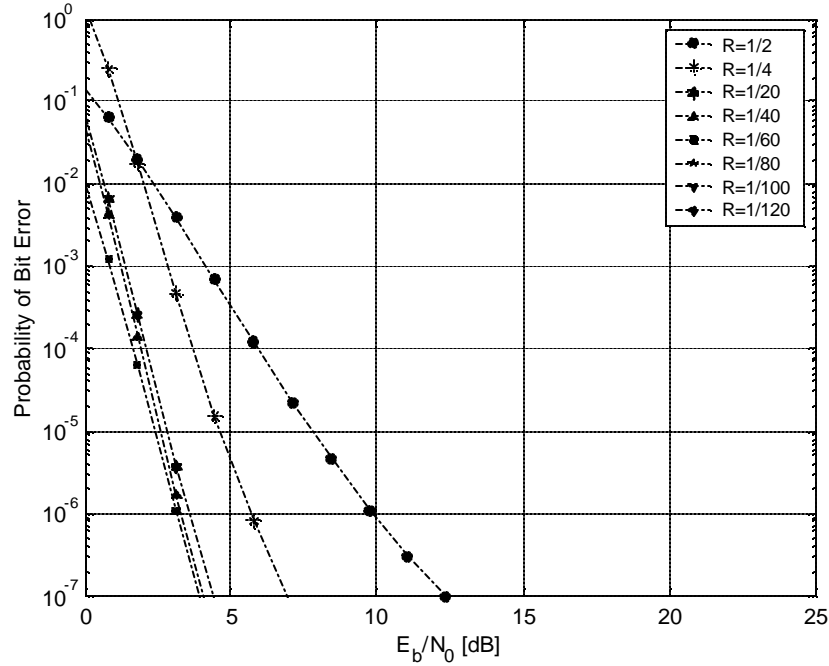


Figure 25. Probability of bit error for different code rates with the total bandwidth expansion  $N=128$  in a Nakagami Fading ( $m=2$ ) and Lognormal Shadowing ( $S_{dB}=4$ ) channel, for 10 users per adjacent cell – Uniform User Distribution.

### *b. Shadowing Variations*

The qualitative results obtained for shadowing variations in the case of uniform user distribution in the cell are similar to the worst-case. Just as in the case of fading variations, the performances of all the combinations of coding-spreading are obviously better than in the worst-case scenario, particularly for higher rate codes, as presented in Figures 26 to 28. The main difference between the uniform user distribution along the cell and the worst-case scenario is in the  $E_b/N_0$ , required to achieve a given probability of bit error. For  $R=1/2$  the required  $E_b/N_0$  to achieve the same probability of bit error is roughly 8 dB smaller than in the worst-case scenario, while  $R=1/4$  to  $1/120$  require an  $E_b/N_0$  that is 3 dB smaller than in the worst-case scenario.

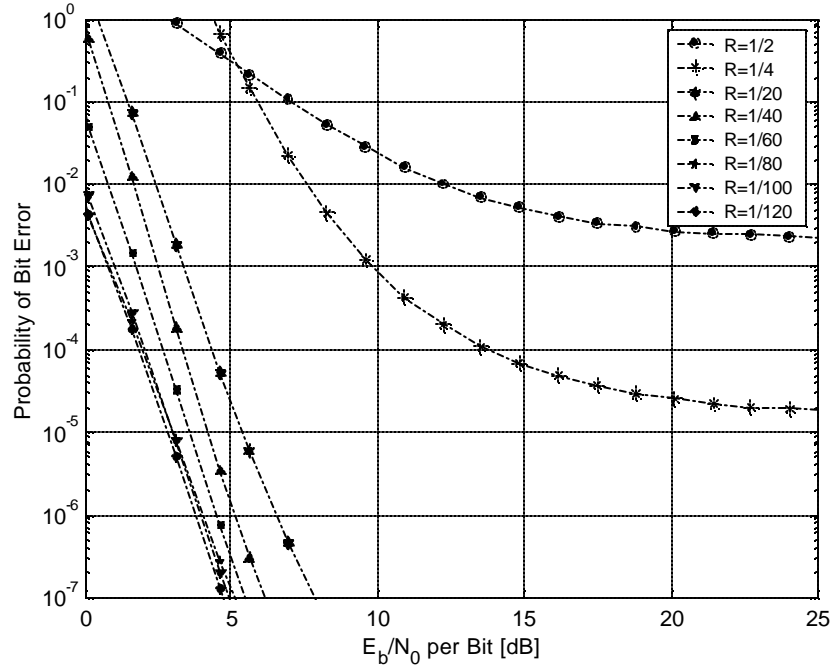


Figure 26. Probability of bit error for different code rates with the total bandwidth expansion  $N=128$  in a Nakagami Fading ( $m=0.5$ ) and Lognormal Shadowing ( $S_{dB}=7$ ) channel, for 10 users per adjacent cell – Uniform User Distribution.

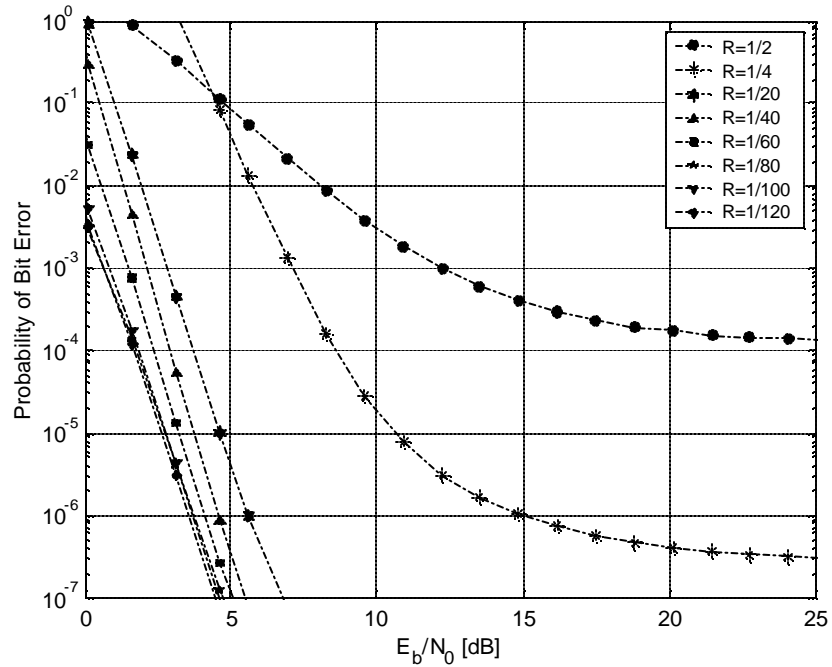


Figure 27. Probability of bit error for different code rates with the total bandwidth expansion  $N=128$  in a Nakagami Fading ( $m = 1$ ) and Lognormal Shadowing ( $S_{dB}=7$ ) channel, for 10 users per adjacent cell – Uniform User Distribution.

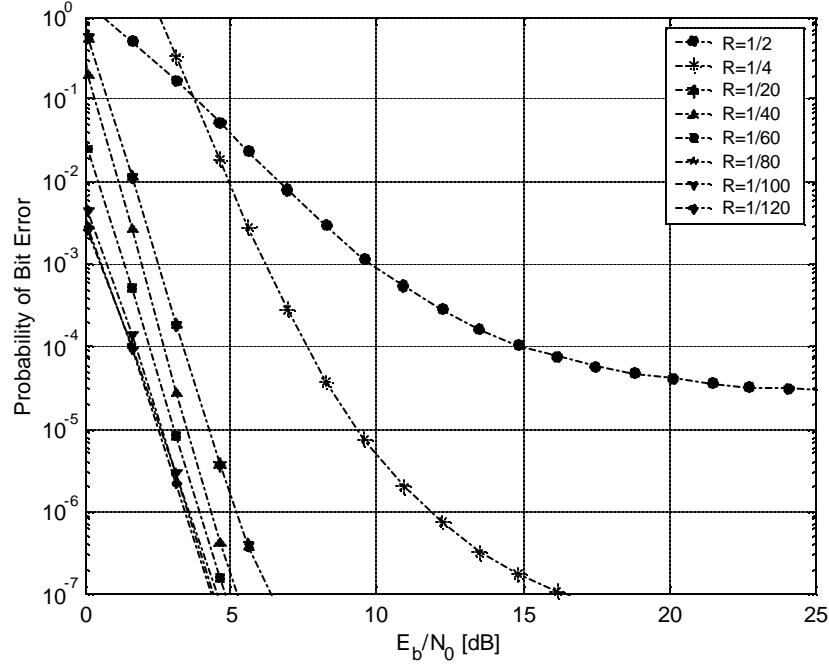


Figure 28. Probability of bit error for different code rates with the total bandwidth expansion  $N=128$  in a Nakagami Fading ( $m=2$ ) and Lognormal Shadowing ( $S_{dB}=7$ ) channel, for 10 users per adjacent cell – Uniform User Distribution.

#### *d. Variations in the Number of Users*

Once again, the general behavior of the results obtained for the uniform user distribution in the cell is similar to the worst-case scenario. However, for  $R=1/80$  the degradation in performance, with the increasing number of users, is smoother than in the worst-case scenario. For a uniform user distribution, the rank of best performances is roughly maintained when the number of users goes from 10 to 40, while in the worst-case scenario, the lower rate codes overcame the performance of the higher rate codes. In other words,  $R=1/80$  roughly maintains the best performance of the different combinations of coding and spreading for 10, 20 and 40 users, for a uniform user distribution. In a worst-case scenario,  $R=1/80$  presents the best performance for 10 users, but when the number of users increases, the lower rate codes provide better results.



This observation does not mean that in a uniform user distribution the relative performances are independent of the number of users. The point (number of users) in which the lower rate codes overcame the performance of  $R=1/80$  will be higher. This means a larger number of users is required to achieve these results.

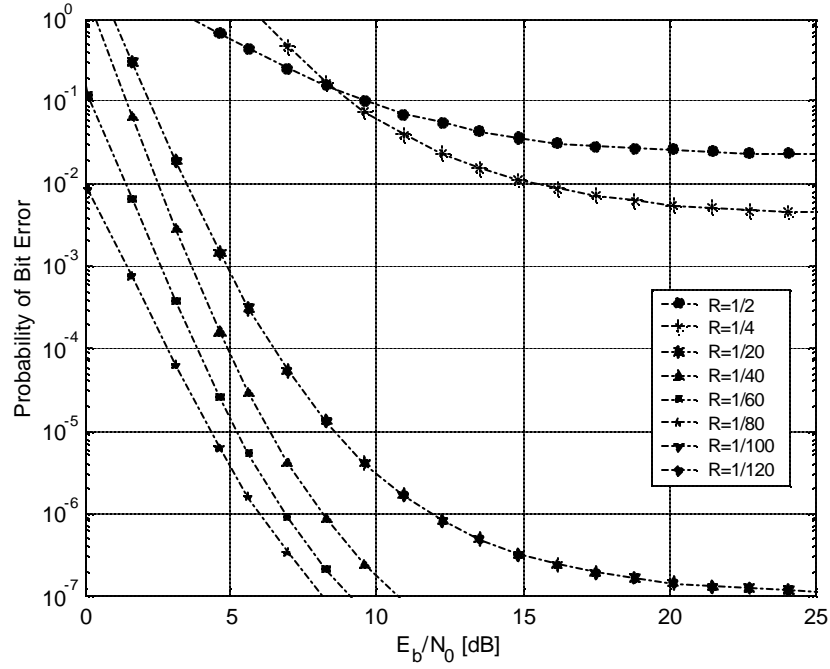


Figure 29. Probability of bit error for different code rates with the total bandwidth expansion  $N=128$  in a Nakagami Fading ( $m = 0.5$ ) and Lognormal Shadowing ( $s_{dB}=7$ ) channel, for 20 users per adjacent cell – Uniform User Distribution.

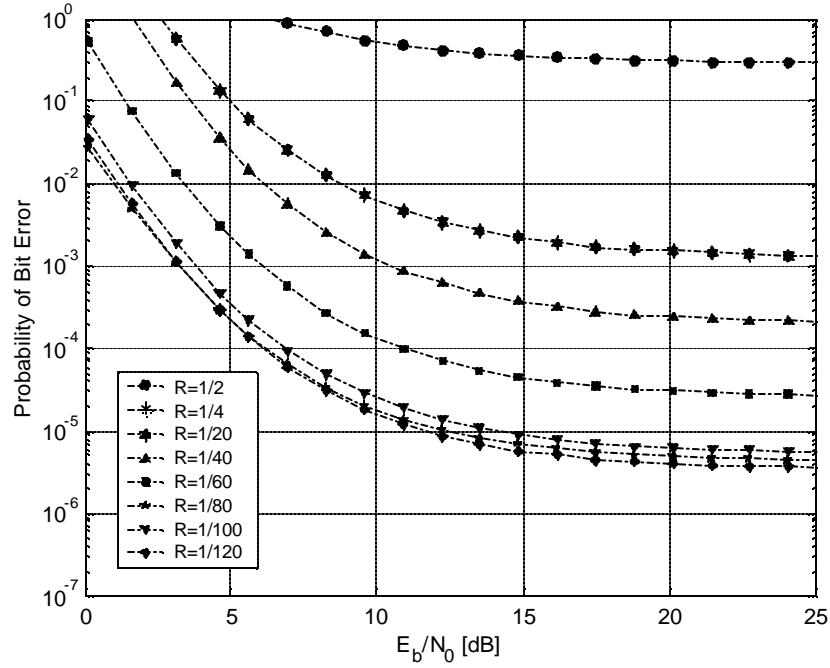


Figure 30. Probability of bit error for different code rates with the total bandwidth expansion  $N=128$  in a Nakagami Fading ( $m=0.5$ ) and Lognormal Shadowing ( $s_{dB}=7$ ) channel, for 40 users per adjacent cell – Uniform User Distribution.

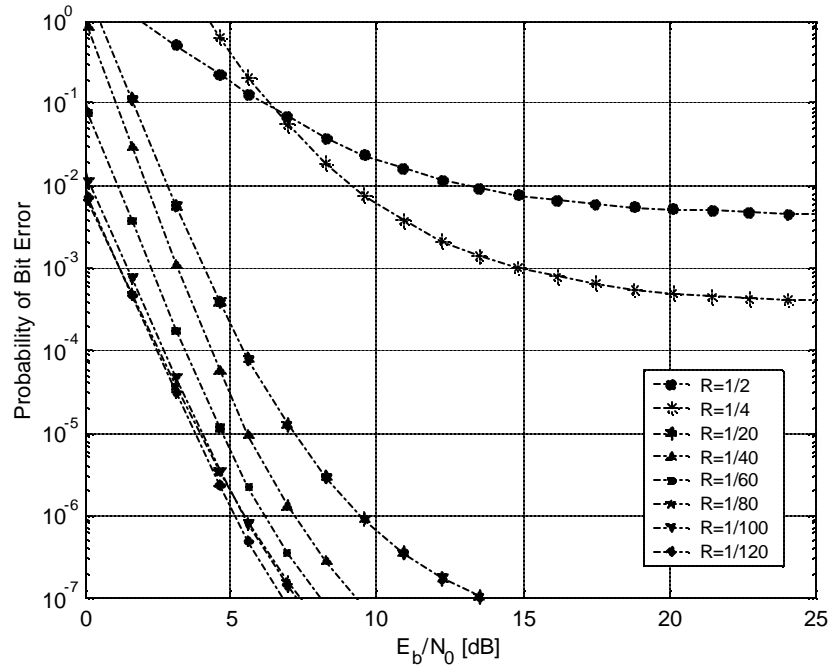


Figure 31. Probability of bit error for different code rates with the total bandwidth expansion  $N=128$  in a Nakagami Fading ( $m=1$ ) and Lognormal Shadowing ( $s_{dB}=7$ ) channel, for 20 users per adjacent cell – Uniform User Distribution.

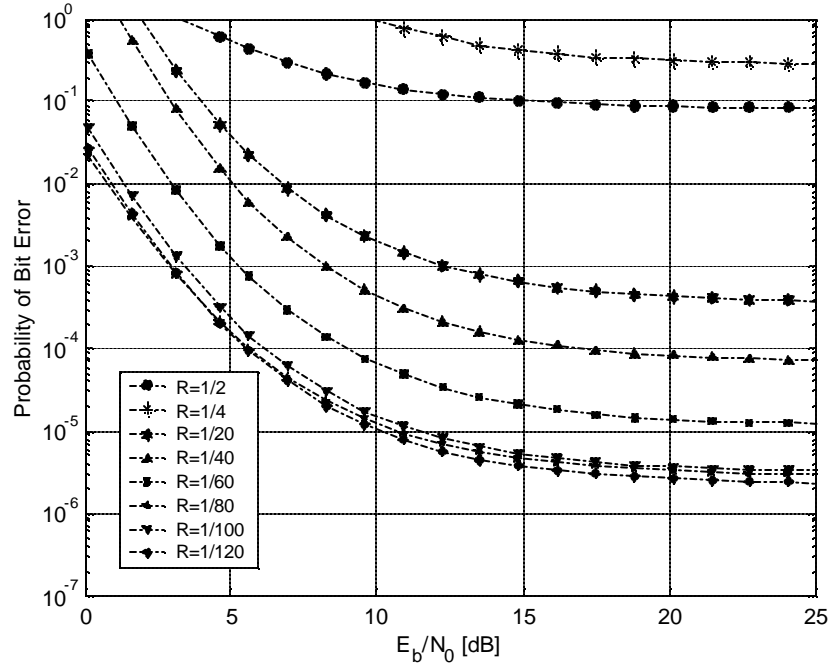


Figure 32. Probability of bit error for different code rates with the total bandwidth expansion  $N=128$  in a Nakagami Fading ( $m=1$ ) and Lognormal Shadowing ( $s_{dB}=7$ ) channel, for 40 users per adjacent cell – Uniform User Distribution.

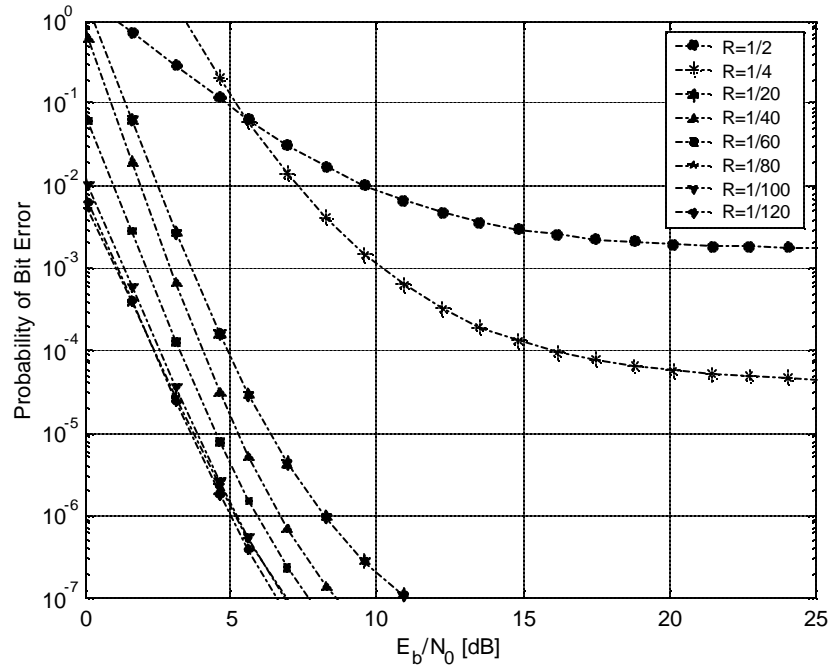


Figure 33. Probability of bit error for different code rates with the total bandwidth expansion  $N=128$  in a Nakagami Fading ( $m=2$ ) and Lognormal Shadowing ( $s_{dB}=7$ ) channel, for 20 users per adjacent cell – Uniform User Distribution.

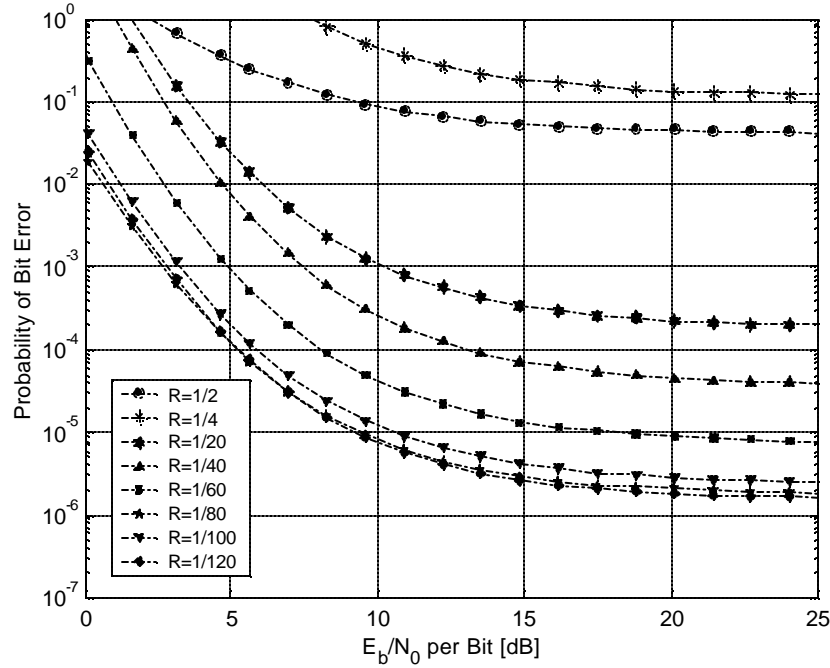


Figure 34. Probability of bit error for different code rates with the total bandwidth expansion  $N=128$  in a Nakagami Fading ( $m=2$ ) and Lognormal Shadowing ( $S_{dB}=7$ ) channel, for 40 users per adjacent cell – Uniform User Distribution.

## B. PERFORMANCE WITH INTERFERENCE REDUCTION TECHNIQUES

This section is dedicated to analyzing the performance of the different coding and spreading combinations in fading-shadowing channels by using interference reduction techniques. One technique that one can use to reduce the interference and increase the capacity of CDMA systems is “sectoring.” In this approach, the cells are split in different sectors, usually three ( $120^\circ$ ) or six ( $60^\circ$ ) and a single omni-directional antenna at the base station is replaced by several directional antennas, each radiating within its specified sector. The co-channel interference reduction depends on the number of sectors and is basically due to the fact that each antenna in a cell will receive interference from only a fraction of the co-channel cells [23]. The main drawbacks of sectoring are the increasing number of antennas at the base station, the relative decreasing in efficiency for the higher number of sectors and the increase in the number of handoffs across the cell. The other interference technique considered is “power control.” In this case the base station dy-

namically adjusts its transmitted power in each channel in order to maintain the received power of every user equal, constant and independent of the relative position in the cell. Reducing the transmitted power in the user channels to the minimum required to maintain acceptable communications eliminates the effect of shadowing and enhances the system's overall performance by reducing the co-channel interference.

The communications channel model used in this analysis is the same as in the previous Section but the different systems now have a better capacity to deal with the co-channel interference. Sub-section B.1 investigates the performance of the different codes, when six sectors are used in each cell and compares them to the case of no sectoring, presented in Section A.2. Section B.2 contains the analysis of the codes in the power controlled systems, for the case of sectoring. The results are compared with the cases of section B.1.

## **1.      Sectoring**

When sectoring is applied to CDMA systems, the interference received in each antenna of a cell is only a fraction of the co-channel interference. This allows an increase in the system's capacity that is proportional to the number of sectors. This section discusses the tradeoff problem in the case of uniform user distribution in which the cells are split in six sectors of  $60^\circ$ . As a consequence, the amount of co-channel interference received by each mobile user is reduced to roughly 1/6. The same type of analysis used in the previous section is applied to the case of sectoring.

### ***a.      Fading Variations***

Since sectoring only affects the amount of co-channel interference received by each user, the analysis of performance for fading variations can provide a fairly good indication of the weight of co-channel interference in the overall noise-plus-interference. Performance comparisons between Figures 23 and 35, 24 and 36, and 25

and 37 confirm what one should expect. The amount of co-channel interference affects the codes exponentially as the code rate increases. In other words, the lowest rate code (1/20) is less affected by the co-channel interference while the highest code rate is highly affected. Reducing the co-channel interference reconfirms the  $R=1/80$  as the best code rate which creates the best performance.

Similar to the case of no sectoring, the performance results obtained for lower rate codes indicate that their error correction capacity can make the performance of CS-CDMA systems fairly independent of the fading. On the other hand, higher code rates, like 1/2 and 1/4, present a “quasi” independence. If we compare the results of the systems with and without sectoring, we realize that the difference, for  $m=0.5$ , 1 and 2, in the case of sectoring is less than 2 dB for a probability of bit error of  $10^{-5}$ , while the same difference is greater than 20 dB for the case of no sectoring.

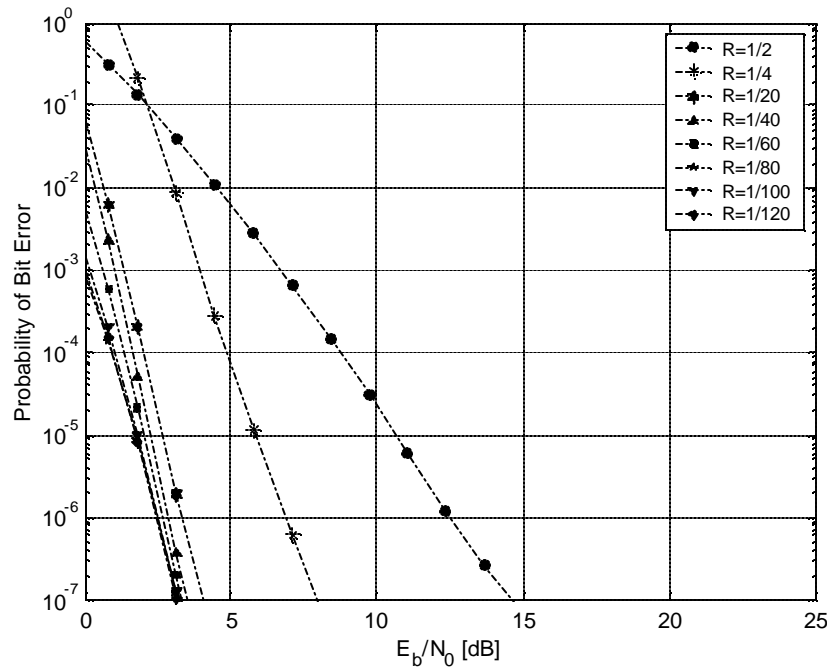


Figure 35. Probability of bit error for different code rates with the total bandwidth expansion  $N=128$  in a Nakagami Fading ( $m=0.5$ ) and Lognormal Shadowing ( $S_{dB}=4$ ) for 10 users per adjacent cell – Uniform User Distribution with Six Sectors.

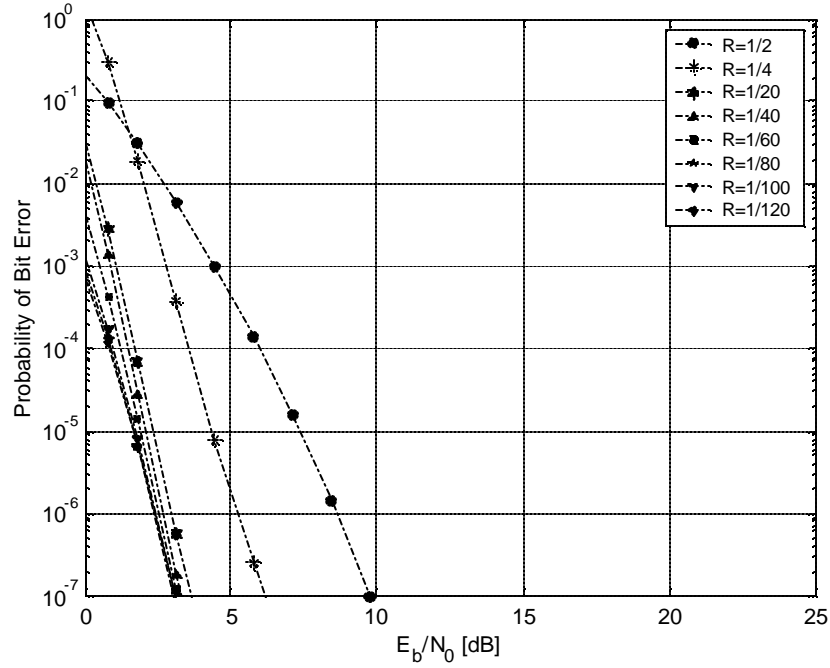


Figure 36. Probability of bit error for different code rates with the total bandwidth expansion  $N=128$  in a Nakagami Fading ( $m=1$ ) and Lognormal Shadowing ( $s_{dB}=4$ ) for 10 users per adjacent cell – Uniform User Distribution with Six Sectors.

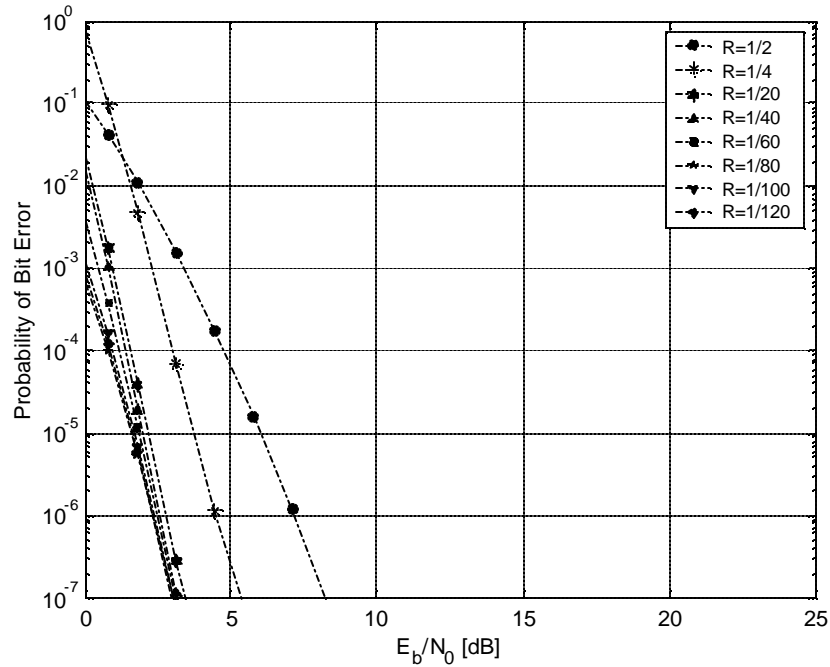


Figure 37. Probability of bit error for different code rates with the total bandwidth expansion  $N=128$  in a Nakagami Fading ( $m=2$ ) and Lognormal Shadowing ( $s_{dB}=4$ ) for 10 users per adjacent cell – Uniform User Distribution with Six Sectors.

### b. Shadowing Variations

Figures 38 to 40 present performances for different code rates for  $m=0.5$ , 1 and 2 and for  $s_{dB}=7$ . The results obtained lead to the same conclusions as in the case of the fading variations analysis, which is the dependence of higher code rates on co-channel interference. Increasing the shadowing effect, which degraded the performance of  $R=1/80$  in Figures 13 to 15 and 26 to 28, is now compensated for by a decrease in the co-channel interference. The result reassigned to  $R=1/80$  the best performance of all.

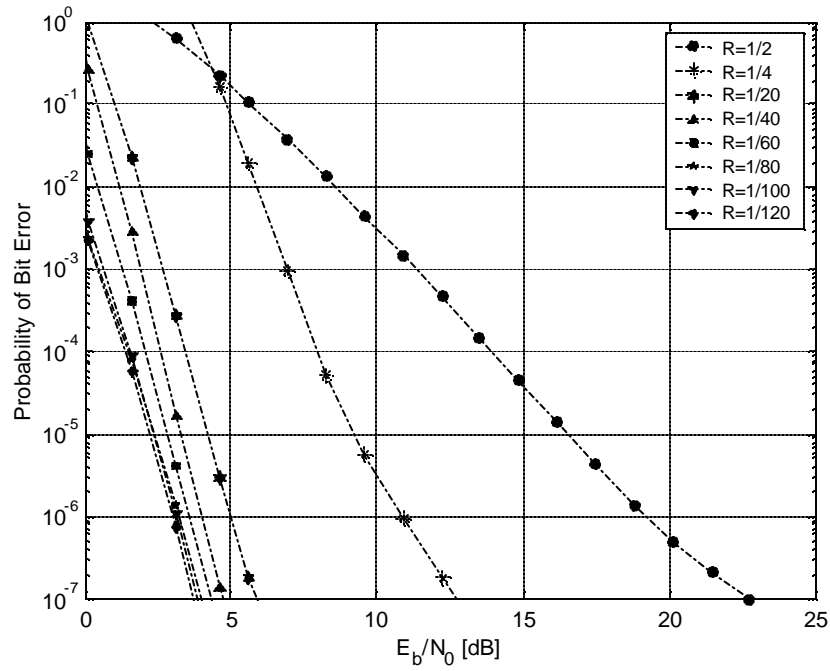


Figure 38. Probability of bit error for different code rates with the total bandwidth expansion  $N=128$  in a Nakagami Fading ( $m=0.5$ ) and Lognormal Shadowing ( $s_{dB}=7$ ) channel, for 10 users per adjacent cell – Uniform User Distribution with Six Sectors.



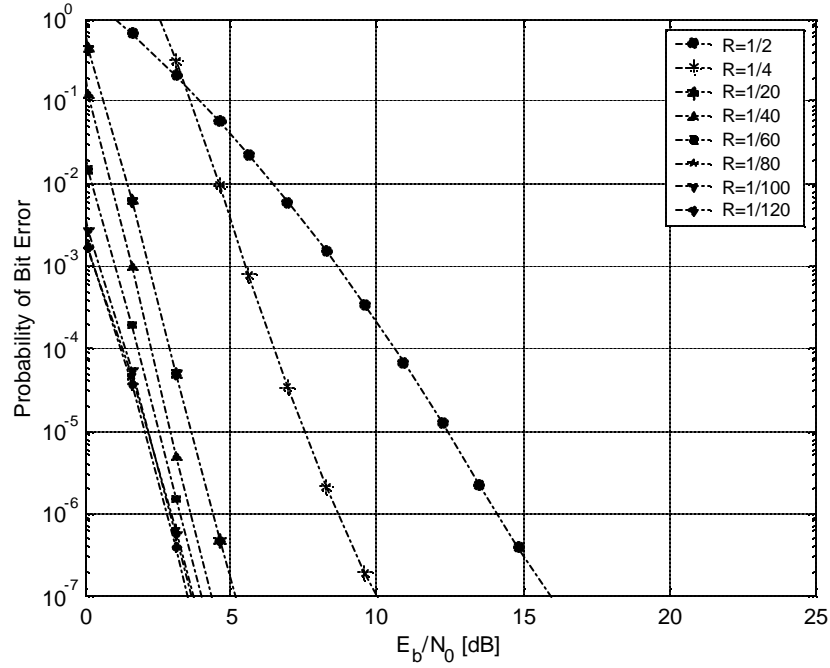


Figure 39. Probability of bit error for different code rates with the total bandwidth expansion  $N=128$  in a Nakagami Fading ( $m=1$ ) and Lognormal Shadowing ( $s_{dB}=7$ ) channel, for 10 users per adjacent cell – Uniform User Distribution with Six Sectors.

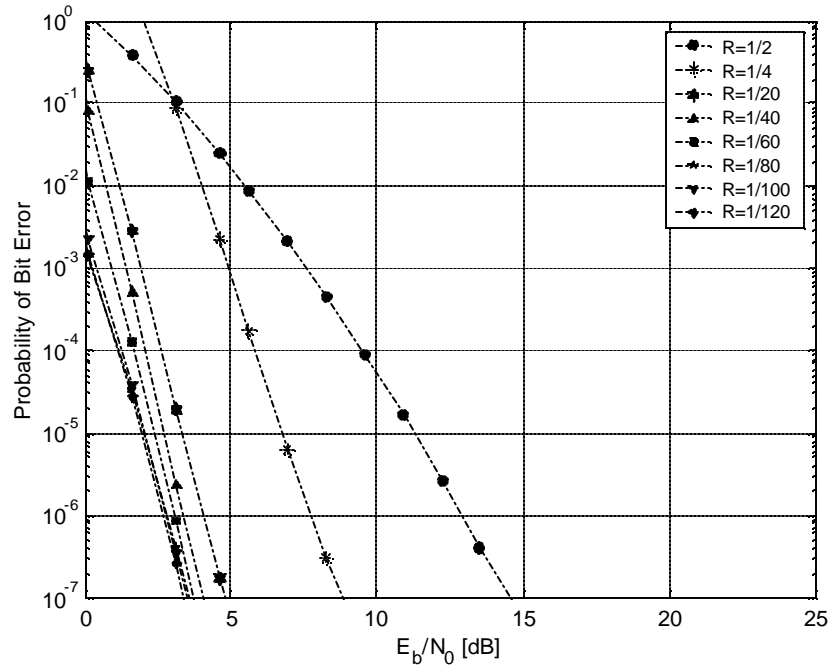


Figure 40. Probability of bit error for different code rates with the total bandwidth expansion  $N=128$  in a Nakagami Fading ( $m=2$ ) and Lognormal Shadowing ( $s_{dB}=7$ ) channel, for 10 users per adjacent cell – Uniform User Distribution with Six Sectors.

### c. Variations in the Number of Users

Since the main goal of sectoring is to reduce the effects of co-channel interference, the best way to observe the improved performance is by increasing the number of users. Comparing Figures 28, 31 and 32 and Figures 41 to 43 reveals the discrepancy of results when sectoring is used. Without sectoring, even a relatively insignificant amount of users (20) make implementing  $R=1/2$  inappropriate. Sectoring limits the amount of interference added by new users in order to smooth out the degradation in performance.

The exponential effect of co-channel interference with the increase code rates is even more obvious than in the case of 10 users when comparing the aforementioned figures.

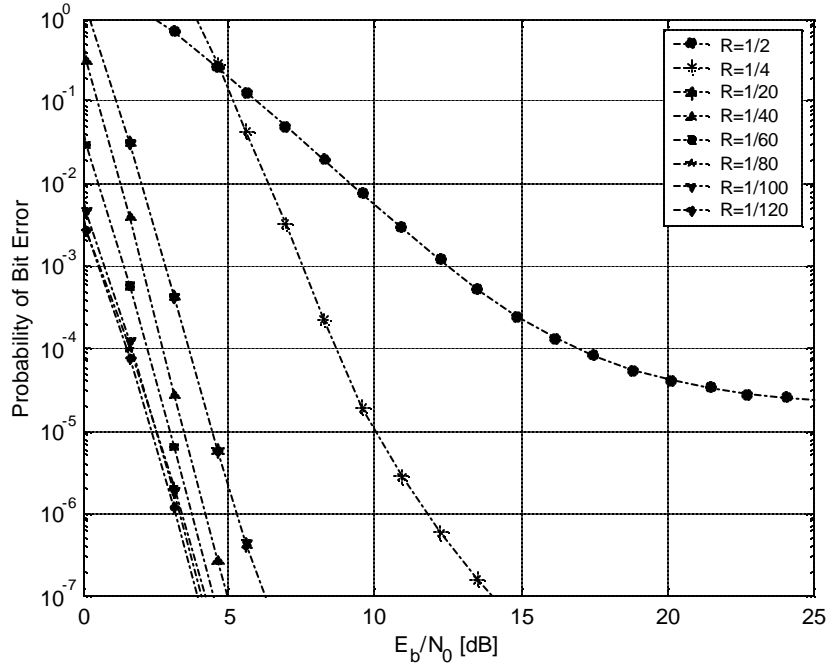


Figure 41. Probability of bit error for different code rates with the total bandwidth expansion  $N=128$  in a Nakagami Fading ( $m=0.5$ ) and Lognormal Shadowing ( $S_{dB}=7$ ) channel, for 20 users per adjacent cell – Uniform User Distribution with Six Sectors.

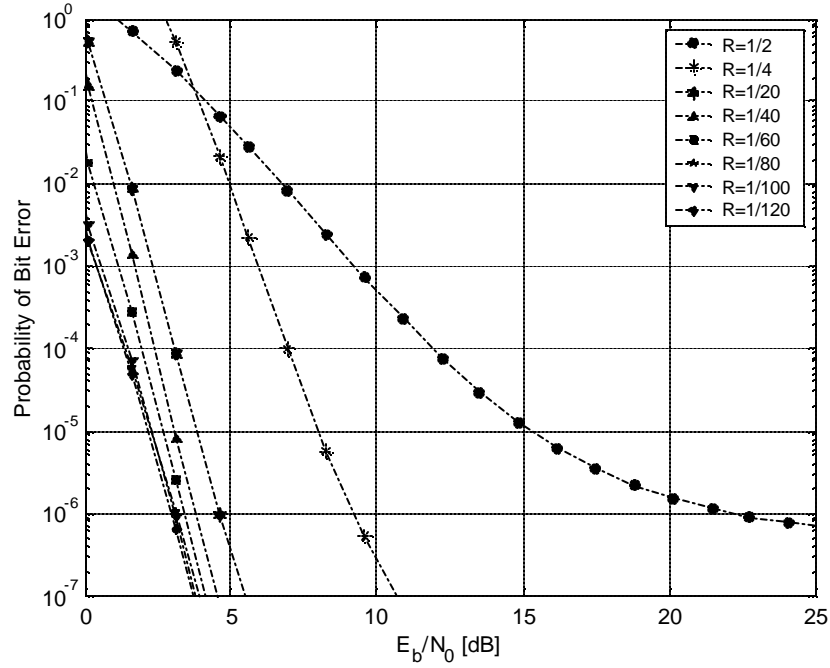


Figure 42. Probability of bit error for different code rates with the total bandwidth expansion  $N=128$  in a Nakagami Fading ( $m=1$ ) and Lognormal Shadowing ( $S_{dB}=7$ ) channel, for 20 users per adjacent cell – Uniform User Distribution with Six Sectors.

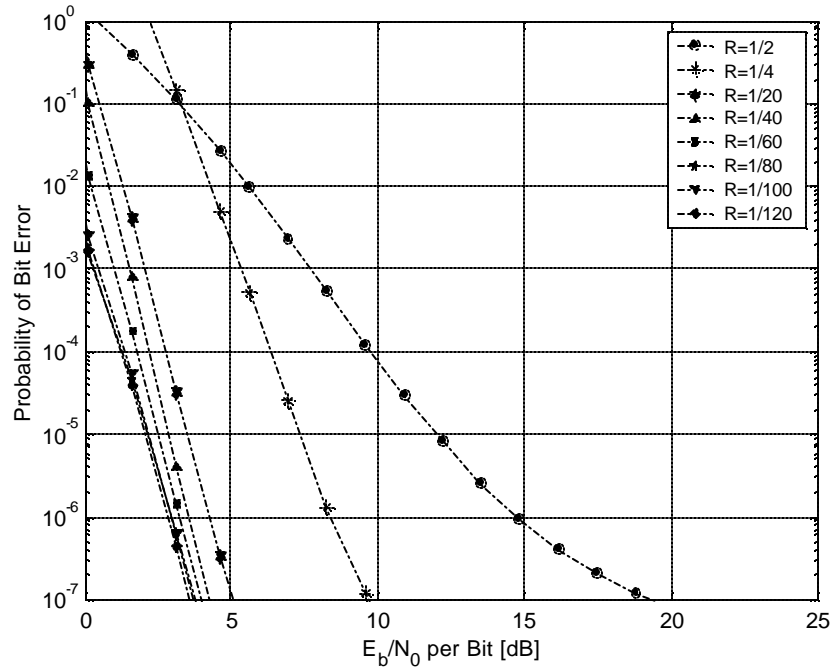


Figure 43. Probability of bit error for different code rates with the total bandwidth expansion  $N=128$  in a Nakagami Fading ( $m=2$ ) and Lognormal Shadowing ( $S_{dB}=7$ ) channel, for 20 users per adjacent cell – Uniform User Distribution with Six Sectors.

## 2. Power Control

The system performance can be enhanced if the base station's transmitted power is adjusted in a way that each user receives the same power independently of its position in the cell. Since CDMA is a interference-limited system, the performance can be greatly improved due to the reduced transmitting power to non-intended users, which reduces the co-channel interference from users located in other cells. Each mobile user, when receiving the information signal, measures the actual power received and reports it back to the base station, making the received power for each mobile user a deterministic variable.

Therefore, in the case of uniform user distribution through the cells and power control system, the SNIR was derived in [26] and corresponds to a value of  $\mathbf{a}$  defined by

$$\mathbf{a} = \frac{\exp(\mathbf{I}^2 \mathbf{s}_{dB}^2)}{3N} \sum_{i=1}^6 \sum_{j=0}^{k_i-1} \frac{\mathbb{E}[r_{ij}^n]}{D_i^n} + \frac{N_o}{2RE_b}. \quad (4.15)$$

Adjusting the power factor to achieve the target power level for all users overcomes the lognormal shadowing effect on the information signal. So the probability of bit error for the different codes is obtained by computing the first-event error probability and applying it to (3.1), which means solving the following integral for the case where  $Z_d$  is a sum of  $d$  independent Nakagami- $m$ -square random variables and  $\mathbf{a}$  generating by various realizations for  $r$  and  $\mathbf{q}$  random variables.

$$\tilde{P}_{2_i}(d) = \int_{-\infty}^{\infty} \int_{-p}^p \int_o^1 \mathcal{Q} \left[ \sqrt{\frac{z_d}{\frac{\exp(\mathbf{I}^2 \mathbf{s}_{dB}^2)}{3N} \sum_{i=1}^6 \sum_{j=0}^{k_i-1} \frac{\mathbb{E}[r_{ij}^n]}{D_i^n} + \frac{N_o}{2RE_b}}} \right] p_{Z_d}(z_d) p_{R,\mathbf{q}}(r, \mathbf{q}) dr d\mathbf{q} dz_d. \quad (4.16)$$

Again, using equations (3.1), (4.1) and the value of  $\mathbf{a}$  defined in (4.15), it is possible to evaluate the probability of bit error, through Monte Carlo simulations, for different values of fading and shadowing.

### a. Fading Variations

Using sectoring and power control reduces the co-channel interference and eliminates the effect of shadowing. So when we compare Figures 23 to 25 and 26 to 28 with Figures 44 to 46, the differences are evident. Besides the huge reduction in the  $E_b/N_0$  required to reach a probability of bit error below  $10^{-5}$  for  $R=1/2$ , the equalization of performances for code rates below  $1/20$  is also an interesting result. Code rate  $1/80$  performed identically to the lowest code rate independently of the type of fading. This presented the best performance of all.

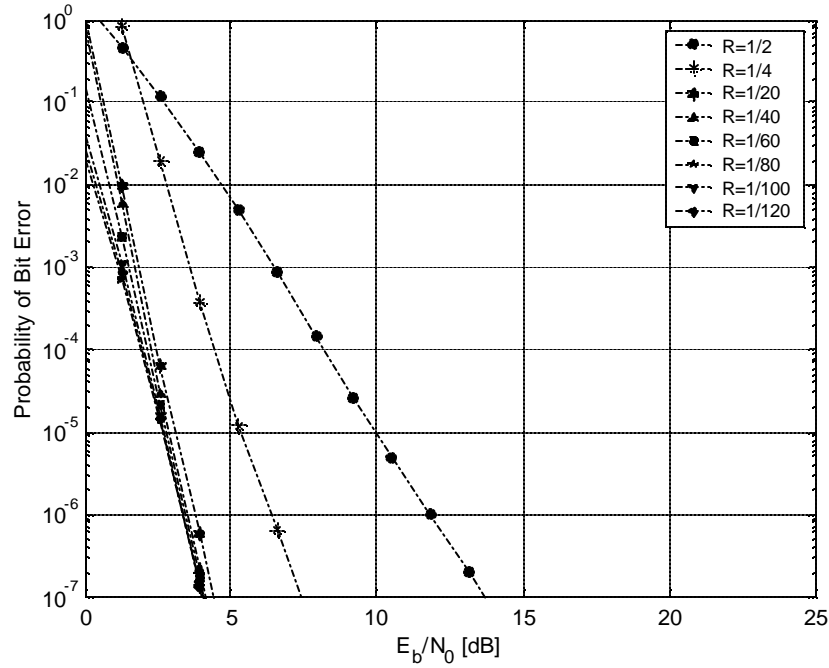


Figure 44. Probability of bit error for different code rates with the total bandwidth expansion  $N=128$  in a Nakagami Fading ( $m=0.5$ ) for 10 users per adjacent cell – Uniform User Distribution with Six Sectors and Power Control.

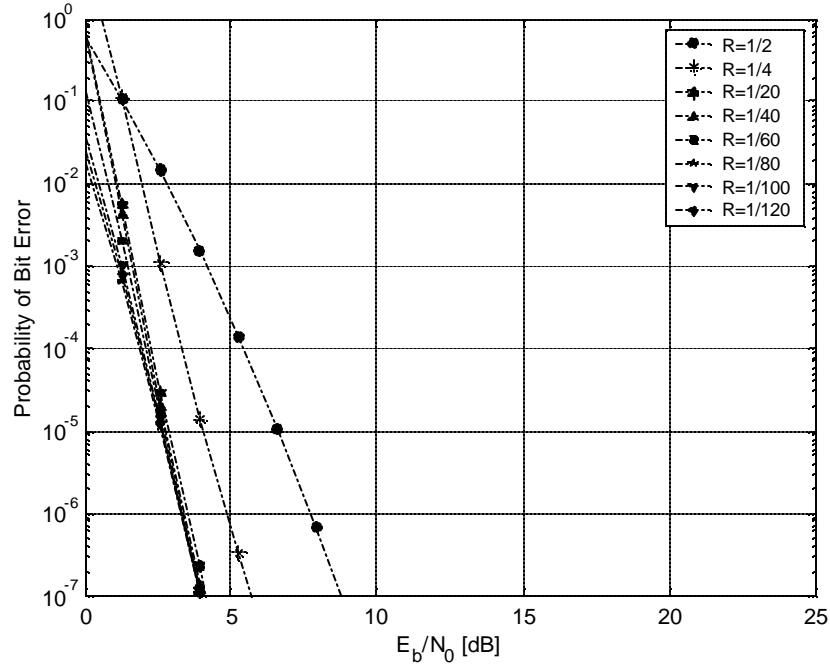


Figure 45. Probability of bit error for different code rates with the total bandwidth expansion  $N=128$  in a Nakagami Fading ( $m=1$ ) channel, for 10 users per adjacent cell – Uniform User Distribution with Six Sectors and Power Control.

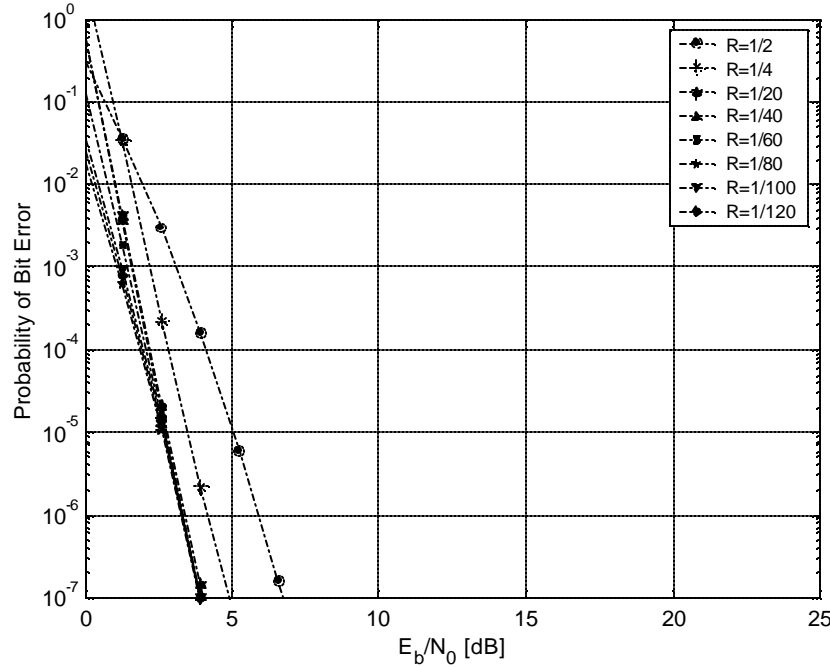


Figure 46. Probability of bit error for different code rates with the total bandwidth expansion  $N=128$  in a Nakagami Fading ( $m=2$ ) channel, for 10 users per adjacent cell – Uniform User Distribution with Six Sectors and Power Control.

### *b. Variations in the Number of Users*

The most important feature of interference reduction techniques is definitely the increase in the system's capacity. The differences between Figures 30, 32 and 34 and Figures 47, 52 and 57 are so dramatic that a simple comparison of results reveals why real CDMA cellular systems cannot be implemented without interference reduction techniques. Figures 47 to 61 represent the best approximation to real world systems presented in this thesis and provide information to infer about the best coding-spreading tradeoff to use. In fact, all the discussion made for the different cases and scenarios presented until this point basically served to interpret the results of Figures 47 to 61.

This section presents the performance analysis of the different code rates in three fading environments and for a different number of users. Figures 47 to 51 represent the performance in one-sided Gaussian fading for 40, 80, 120, 160 and 200 users respectively. Figures 52 to 56 represent the performance in Rayleigh fading for the same number of users. Finally, Figures 57 to 61 represent the performance for Ricean fading for the same number of users. The results obtained are qualitatively similar and can be summarized as follows: When the number of users is smaller than the total bandwidth expansion value, the differences in performance for code rates lower than  $1/20$ , which represent a percentage of bandwidth expansion due to coding greater than 15%, are roughly the same. This is equivalent to saying that a system with 85% of the bandwidth expansion due to spreading sequence (and consequently relatively easy to implement and synchronize), would have roughly the same performance as systems that are much more difficult to implement because of the difficulty of synchronizing all code-spreading systems.

On the other hand, when the number of users exceeds the total bandwidth expansion value, the capacity of CS-CDMA systems to increase the system's capacity generally determines the performances of the different codes. The exception is  $R=1/80$ . Code rate  $1/80$  corresponds to 62.5% of the bandwidth expansion provided by the coding and the remainder of 37.5% is provided by the spreading sequences. This seems to be the

optimal proportions of coding and spreading that can use the best features of each technique. The optimal point is not exactly half way between coding and spreading, but it is a point that corresponds to the code rate with the maximum asymptotic coding gain available and is close to the “fifty-fifty” point.

The results obtained have extraordinary advantages. Not only does code rate 1/80 provide the best performance of the studied combinations of coding and spreading, but it also can be implemented with a significant amount of bandwidth expansion to be provided by spreading sequences, simplifying the implementation and synchronization.

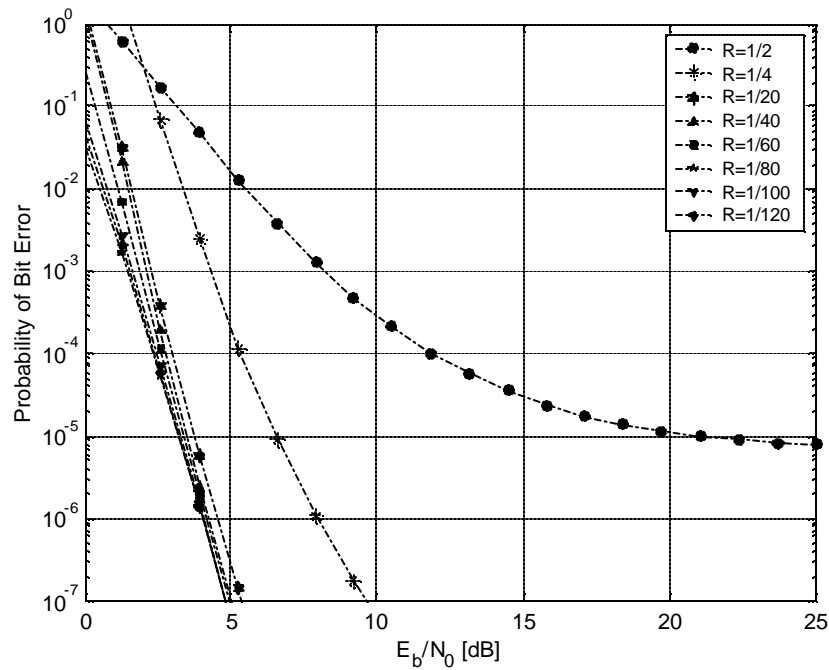


Figure 47. Probability of bit error for different code rates with the total bandwidth expansion  $N=128$  in a Nakagami Fading ( $m=0.5$ ) for 40 users per adjacent cell – Uniform User Distribution with Six Sectors and Power Control.



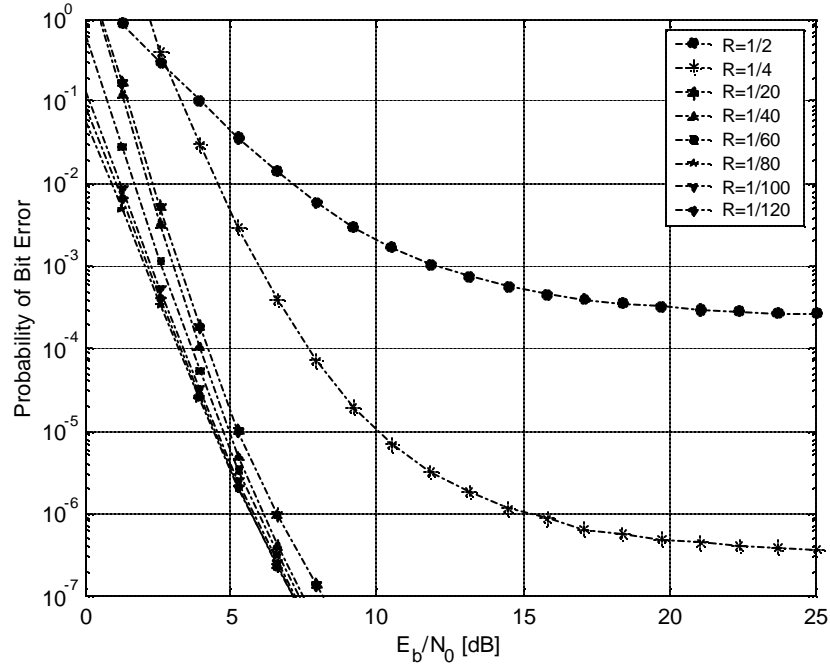


Figure 48. Probability of bit error for different code rates with the total bandwidth expansion  $N=128$  in a Nakagami Fading ( $m=0.5$ ) for 80 users per adjacent cell – Uniform User Distribution with Six Sectors and Power Control.

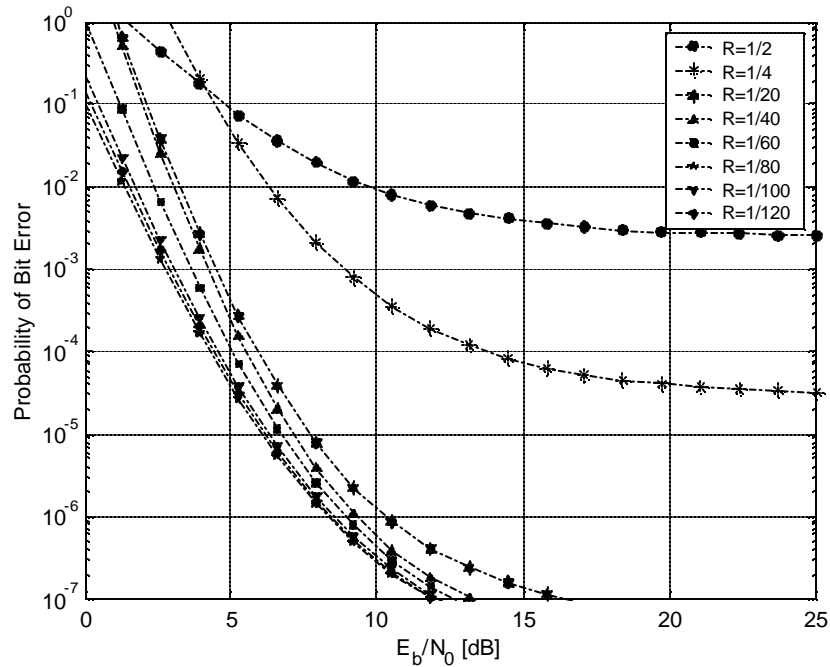


Figure 49. Probability of bit error for different code rates with the total bandwidth expansion  $N=128$  in a Nakagami Fading ( $m=0.5$ ) for 120 users per adjacent cell – Uniform User Distribution with Six Sectors and Power Control.

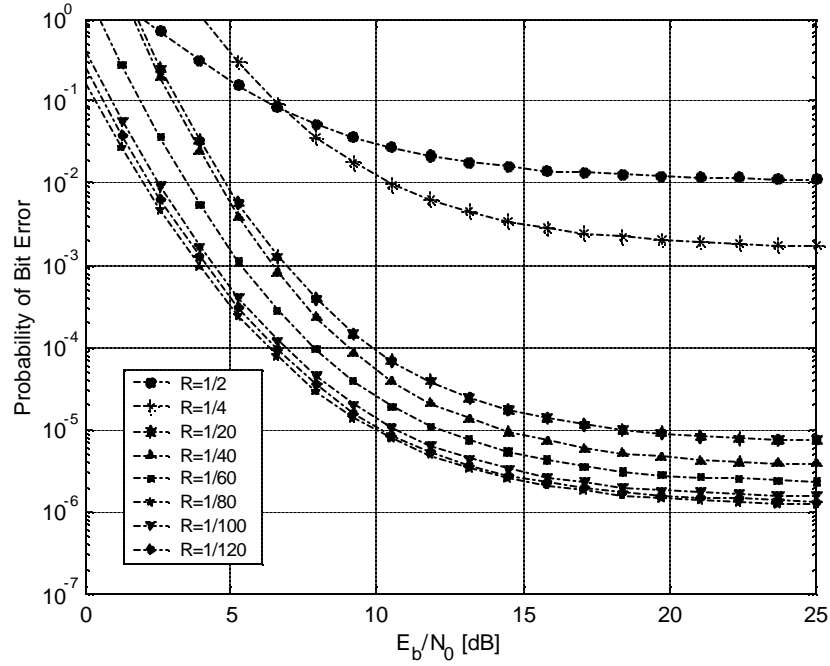


Figure 50. Probability of bit error for different code rates with the total bandwidth expansion  $N=128$  in a Nakagami Fading ( $m=0.5$ ) for 160 users per adjacent cell – Uniform User Distribution with Six Sectors and Power Control.

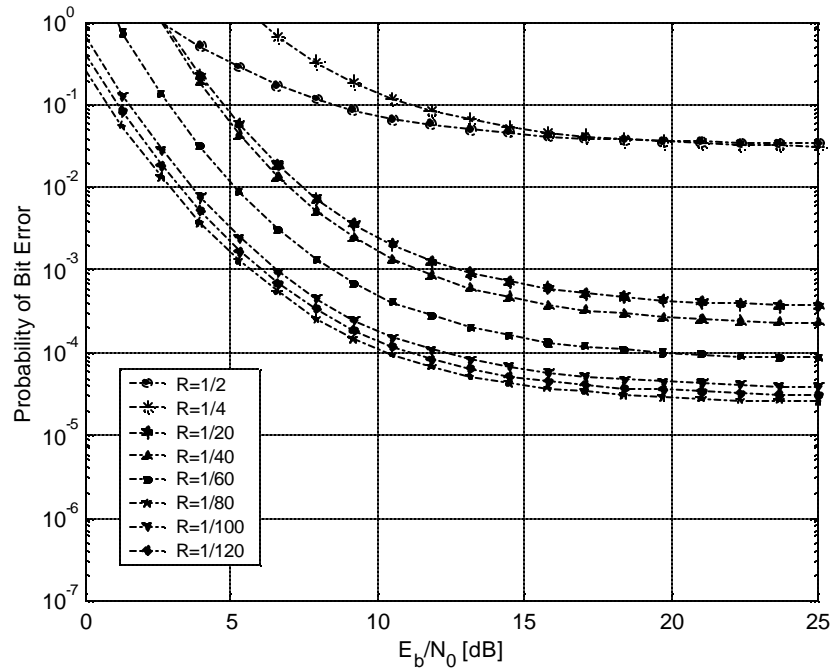


Figure 51. Probability of bit error for different code rates with the total bandwidth expansion  $N=128$  in a Nakagami Fading ( $m=0.5$ ) for 200 users per adjacent cell – Uniform User Distribution with Six Sectors and Power Control.

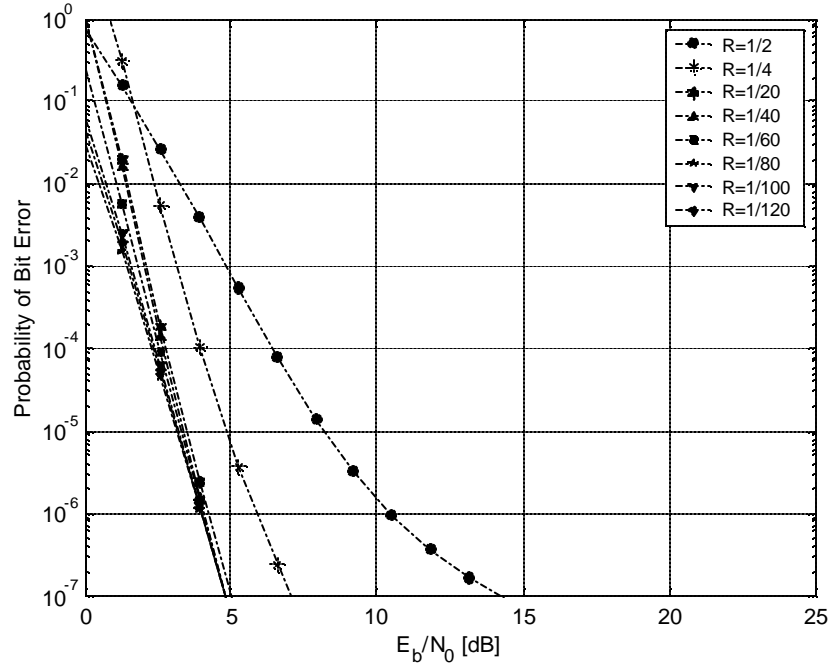


Figure 52. Probability of bit error for different code rates with the total bandwidth expansion  $N=128$  in a Nakagami Fading ( $m=1$ ) for 40 users per adjacent cell – Uniform User Distribution with Six Sectors and Power Control.

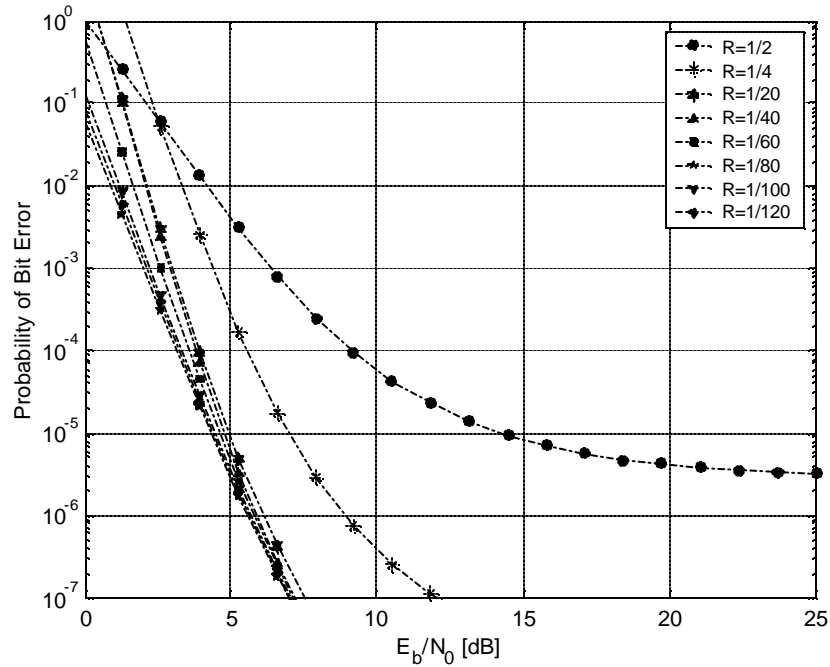


Figure 53. Probability of bit error for different code rates with the total bandwidth expansion  $N=128$  in a Nakagami Fading ( $m=1$ ) for 80 users per adjacent cell – Uniform User Distribution with Six Sectors and Power Control.

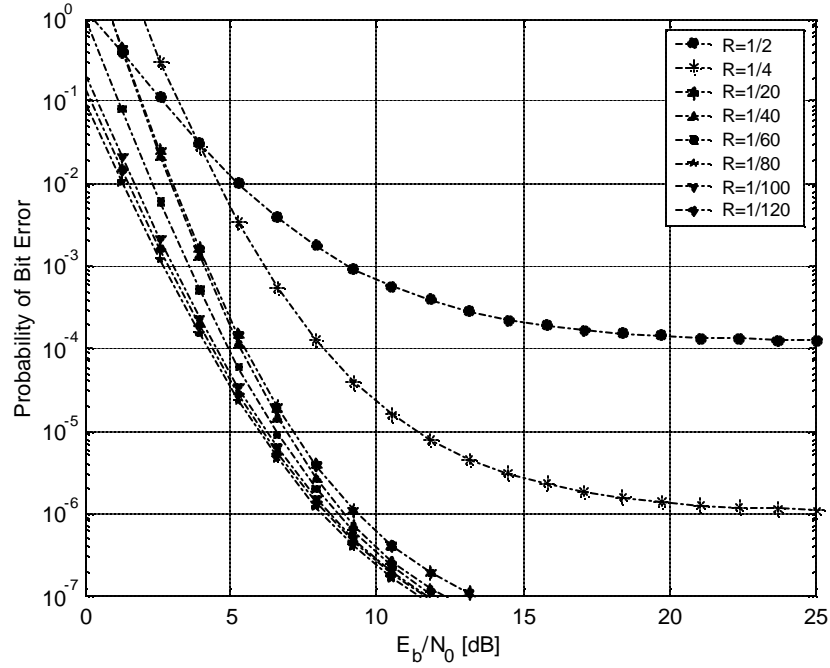


Figure 54. Probability of bit error for different code rates with the total bandwidth expansion  $N=128$  in a Nakagami Fading ( $m=1$ ) for 120 users per adjacent cell – Uniform User Distribution with Six Sectors and Power Control.

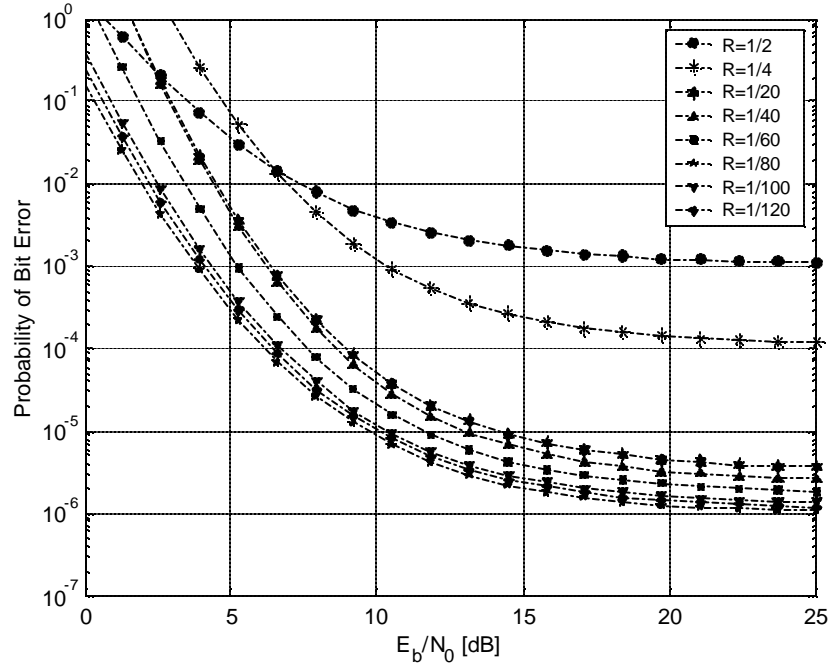


Figure 55. Probability of bit error for different code rates with the total bandwidth expansion  $N=128$  in a Nakagami Fading ( $m=1$ ) for 160 users per adjacent cell – Uniform User Distribution with Six Sectors and Power Control.

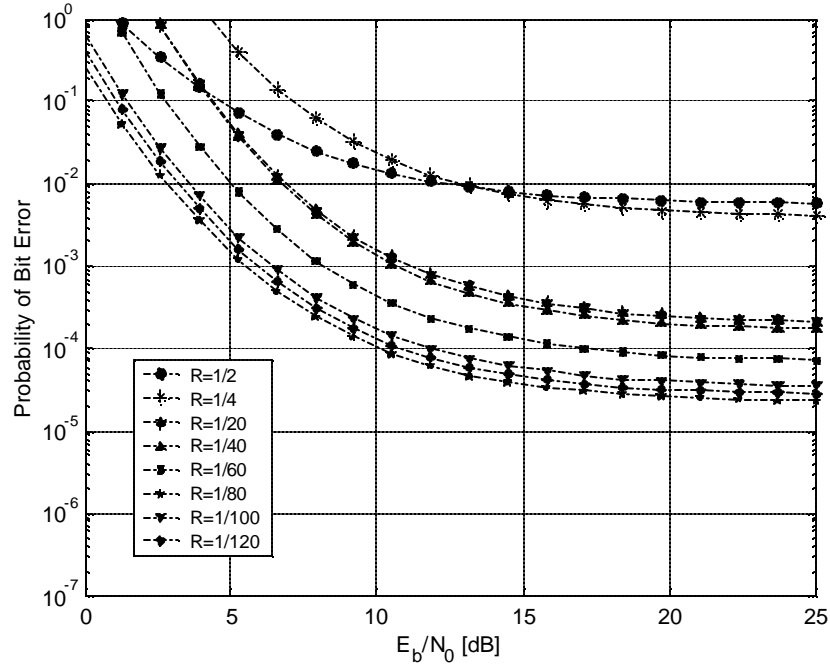


Figure 56. Probability of bit error for different code rates with the total bandwidth expansion  $N=128$  in a Nakagami Fading ( $m=1$ ) for 200 users per adjacent cell – Uniform User Distribution with Six Sectors and Power Control.

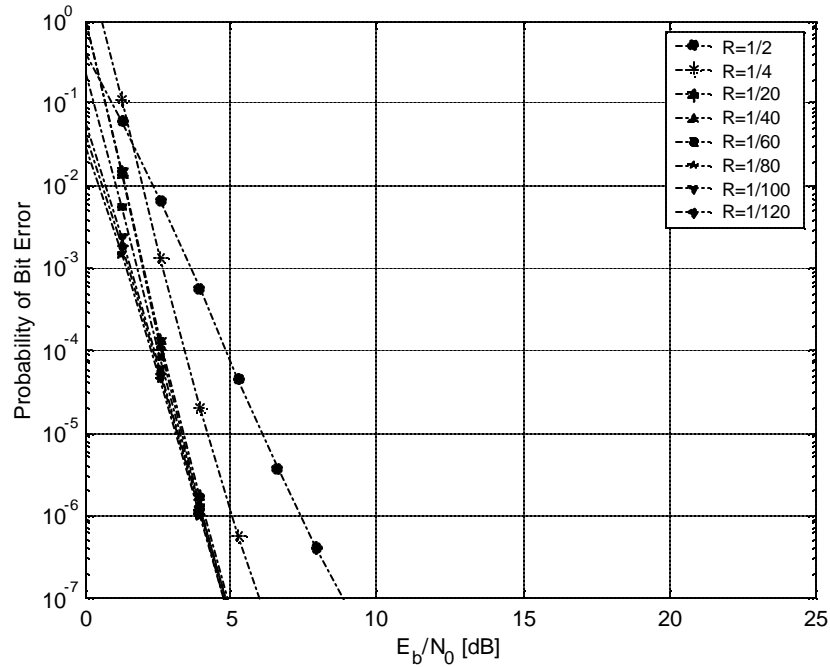


Figure 57. Probability of bit error for different code rates with the total bandwidth expansion  $N=128$  in a Nakagami Fading ( $m=2$ ) for 40 users per adjacent cell – Uniform User Distribution with Six Sectors and Power Control.

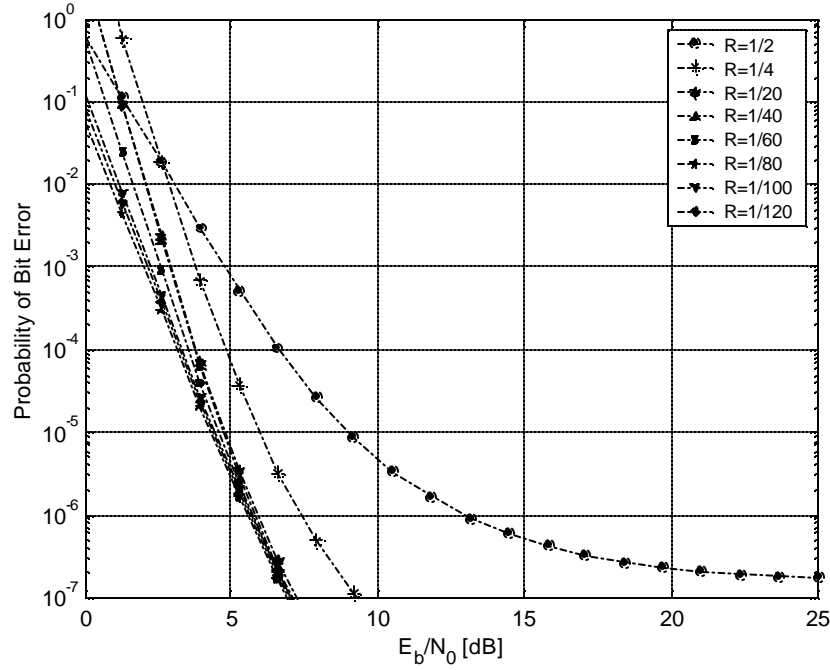


Figure 58. Probability of bit error for different code rates with the total bandwidth expansion  $N=128$  in a Nakagami Fading ( $m=2$ ) channel, for 80 users per adjacent cell – Uniform User Distribution with Six Sectors and Power Control.

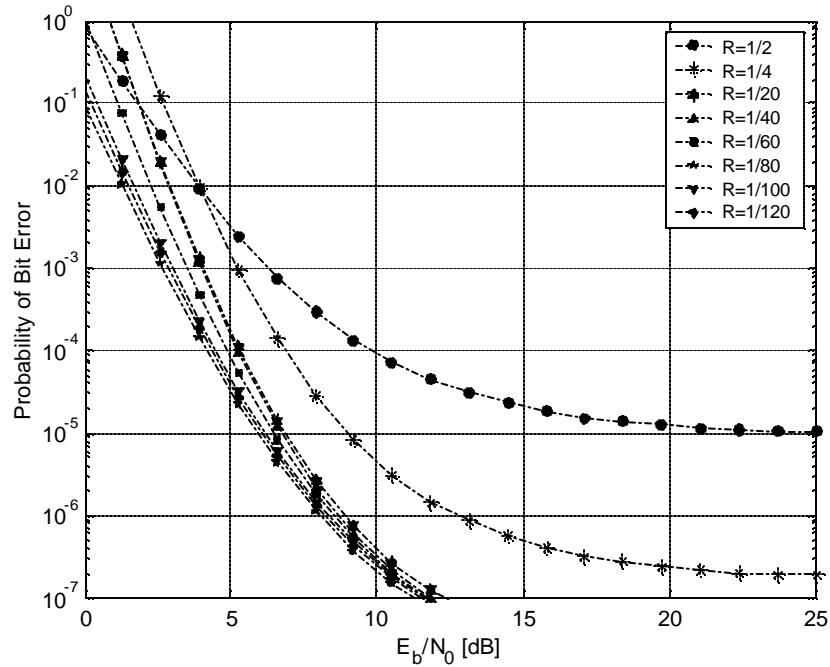


Figure 59. Probability of bit error for different code rates with the total bandwidth expansion  $N=128$  in a Nakagami Fading ( $m=2$ ) channel, for 120 users per adjacent cell – Uniform User Distribution with Six Sectors and Power Control.

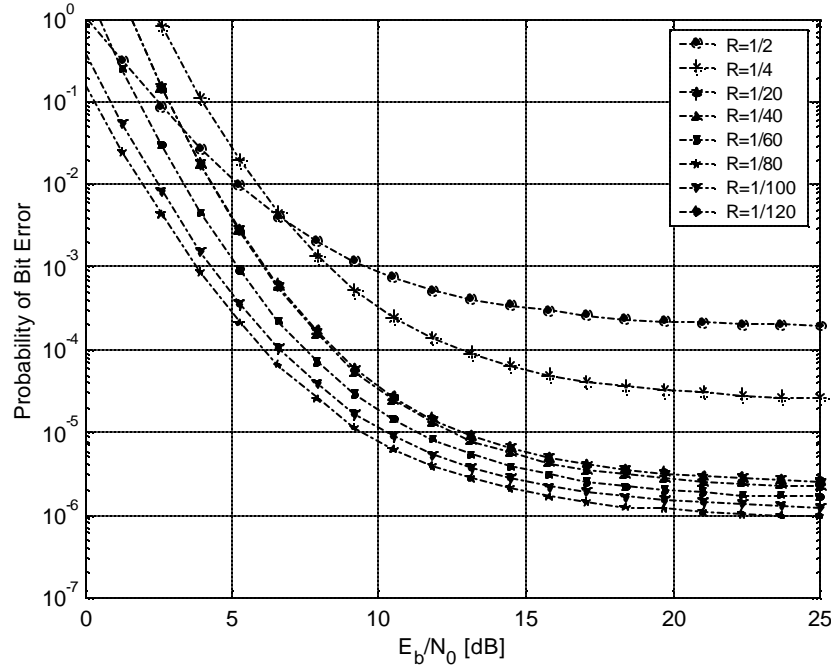


Figure 60. Probability of bit error for different code rates with the total bandwidth expansion  $N=128$  in a Nakagami Fading ( $m=2$ ) channel, for 160 users per adjacent cell – Uniform User Distribution with Six Sectors and Power Control.

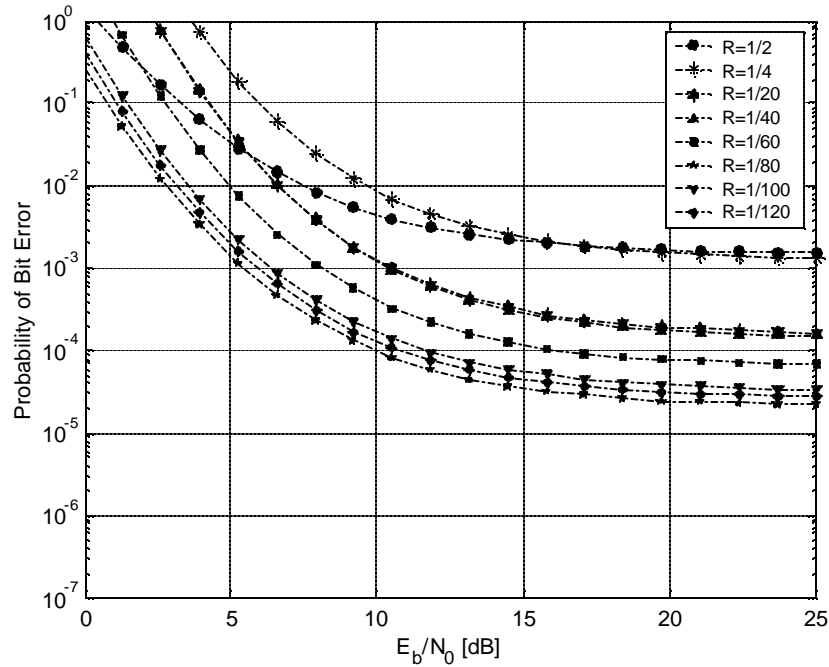


Figure 61. Probability of bit error for different code rates with the total bandwidth expansion  $N=128$  in a Nakagami Fading ( $m=2$ ) channel, for 200 users per adjacent cell – Uniform User Distribution with Six Sectors and Power Control.

## C. SUMMARY

This chapter analyzed the random tradeoff factors that affect the performance of DS-CDMA and CS-CDMA systems. The randomness introduced by a non-ideal channel was addressed and its influence in the performance of the different combinations of coding-spreading was investigated.

Two situations were studied. The first one in which the user position was analyzed for a worst-case scenario and a uniform user distribution through the cell was dedicated to evaluating the system's performance in a Nakagami- $m$  fading with log-normal shadowing. The results demonstrated that lower rate codes are less susceptible to fading and shadowing variations than the higher rate codes. The best performance was achieved by  $R=1/80$  and  $R=1/120$  with slightly different variations in shadowing and in the number of users.

The second situation studied interference reduction techniques. The same channel model and user distribution was then used in the cases of sectoring and power control. The results revealed that reducing the co-channel interference and eliminating the shadowing effects made the performances of code rates lower than  $1/20$  very similar for a number of users smaller than the total bandwidth expansion value. The differences in performance for code rates lower than  $1/20$ , which represent a percentage of bandwidth expansion due to coding greater than 15%, is roughly the same. This is equivalent to saying that a system with 85% of the bandwidth expansion due to spreading sequence—and consequently relatively easy to implement and synchronize—would have roughly the same performance as systems that are much more difficult to implement owing to the complexity of synchronizing all code-spreading systems.

When the number of users exceeds the total bandwidth expansion value, the better performance is exhibited by  $R=1/80$ . This code rate provides 62.5% of the total bandwidth expansion, which means that the remaining 37.5% must be provided by the spreading sequences. This significant amount of bandwidth expansion provided by the spreading sequences tremendously simplifies the implementation and synchronization, when



compared to systems in which all the bandwidth expansion is due to coding. In the next chapter we summarize the conclusions and suggest areas for further research.

THIS PAGE INTENTIONALLY LEFT BLANK

## **V. CONCLUSIONS AND FUTURE WORK**

In the study of the coding spreading presented in this thesis, we investigated the usage of maximum free-distance low-rate convolutional codes mainly to provide the bandwidth expansion that CDMA systems require to combat fading and to facilitate the multiple access. The performance of those CS-CDMA systems was compared with the performance of DS-CDMA as defined in the IS-95 standard, for different scenarios and for channel models. The results allowed us to establish the criteria for defining the combination of coding and spreading that can potentially provide the best performance for specific operation conditions. The results are summarized in the following section. Furthermore, we discuss some topics for future research.

### **A. CONCLUSIONS**

Chapter III analyzed the coding-spreading tradeoff problem and the factors the system's designer can employ to control such problems. This can potentially affect the tradeoff and, consequently the performance of the systems. In our study, we investigated the coding characteristics, namely the asymptotic coding gain, the code distance spectrum and the number of users and their effect in the system's performance. Based on this analysis, we defined the criteria to select the codes that can potentially provide the best performances.

It was verified that using very low-rate codes does not always guarantee the best results in terms of performance and complexity. It was also verified that the capacity of correcting errors is a very important feature. The analysis of the asymptotic gain showed that it can provide a good initial approach in the search for the best code and for the best spreading factor; however, the results cannot be conclusive, especially in the cases of similar asymptotic coding gain. Comparing the rate of the increase in the error weight of the codes is a good method for predicting the performance, but since the probability of bit error of a system is also a function of the free distance, the analysis is more accurate in the cases of codes with approximately the same asymptotic coding gain. Finally, we ana-

lyzed the different codes for a different number of users. Using a simple channel model that employed BPSK systems in Rayleigh fading, we concluded that the performance is inversely proportional to the code rate. In other words, the lowest code rate provides the best performance.

In Chapter IV, we addressed the randomness introduced by a non-ideal channel and its effect on the coding-spreading tradeoff. Two scenarios were analyzed, a worst-case scenario in which the mobile is located in any corner of the hexagon cell in a seven cell cluster and a more realistic scenario in which the mobile can be located in any position on the cell, described by a uniform probability density function. The study analyzed fading, shadowing and the number of user's variations for both scenarios. Additionally, we introduced sectoring and power control to the models and investigated the differences in performances and the effect on the tradeoff.

The results obtained in the study of the random tradeoff factors were very interesting. It was observed that analyzing the deterministic tradeoff factors cannot accurately predict what combination of coding and spreading can provide the best performance. It was also observed that there are compromises due to implementation issues that can only be properly evaluated by analyzing the performance with accurate models of the systems.

Chapter IV.B demonstrated that the idea of “the lower the better,” suggested in [3], [4] and [8], is at least questionable. A code rate of  $1/80$  performed as well as the lowest rate code and in some cases better, such as in heavily loaded systems and has “only” 62.5% of the bandwidth expansion due to coding. Also,  $R=1/80$  always performed better than  $R=1/100$ . Lowering the code rate does not always provide the best performance, especially if the shadowing and the amount of co-channel interference can be controlled.

The best combination of coding and spreading proved to be an actual tradeoff. Unfortunately, in a system's design, the best performance is not the only goal. There are other practical factors, sometimes more important than the performance, that can determine the final requirements of the system. For instance, budget issues or practical constraints, such as decoding complexity or synchronization, can justify using a significant fraction of the bandwidth expansion due to spreading sequences. Therefore, optimizing the coding-spreading tradeoff may not maximize the performance.

According to the previous considerations, the results obtained became even more relevant. In fact, the code rate of  $1/80$  provided the best performance of the studied combinations of coding and spreading and could also be implemented with a significant amount of bandwidth expansion to be provided by the spreading sequences. This represents the best of two worlds, simplified implementation and synchronization and the best performance for high capacity systems.

Additionally, if the required number of users in the system is smaller than the total bandwidth expansion value, the performance of code rates lower than  $1/20$  are roughly the same. The code rate of  $1/20$  corresponds to a system in which the percentage of bandwidth expansion due to coding is 15%. This is equivalent to saying that a system with 85% of the bandwidth expansion due to the spreading sequence would have roughly the same performance as an all code-spreading system. In this case, the results obtained were even more surprising. Systems relatively easy to implement and synchronize revealed performances similar to systems that were more complex and difficult to synchronize.

## **B. FUTURE WORK**

As we have seen, the coding-spreading tradeoff is highly dependent on the requirements of the systems and its operating conditions. The transition to the third generation of mobile communications will demand new configurations and specifications, so to introduce other interference reduction techniques, such as Smart Antennas, in the modeled system will require further research.

The optimum coding-spreading operating point is also a strong function of the type of receiver used. We used a matched filter, which is more robust, to channel estimation errors and to model our receiver, but there are different types of receivers that can be used. For example, the Least Minimum Mean Square Error (LMMSE) receiver is known to be more robust to imperfect power control.

Finally, the usage of a strong component of coding raises the problem of synchronization. Possible ways to overcome the difficulty of synchronization require further research.

## APPENDIX A. NESTED MAXIMUM FREE DISTANCE CODES

Table A.1 contains the nested maximum free distance codes presented in [8] from code rate  $1/4$  to  $1/259$  for constraint lengths 7 through 11.

<i>Code Group</i>	<i>Code Rate (R)</i>	$d_{free}$ (K=7)	$d_{free}$ (K=8)	$d_{free}$ (K=9)	$d_{free}$ (K=10)	$d_{free}$ (K=11)
A	$\frac{1}{4} \dots \frac{1}{19}$	20	22	24	27	29
B	$\frac{1}{20} \dots \frac{1}{39}$	102	114	125	136	148
C	$\frac{1}{40} \dots \frac{1}{59}$	205	228	251	274	296
D	$\frac{1}{60} \dots \frac{1}{79}$	308	342	376	411	445
E	$\frac{1}{80} \dots \frac{1}{99}$	411	456	502	548	594
F	$\frac{1}{100} \dots \frac{1}{119}$	514	571	628	685	742
G	$\frac{1}{120} \dots \frac{1}{139}$	616	685	754	822	891
H	$\frac{1}{140} \dots \frac{1}{159}$	720	800	880	960	1040
I	$\frac{1}{160} \dots \frac{1}{179}$	822	914	1005	1096	1188
J	$\frac{1}{180} \dots \frac{1}{199}$	925	1028	1131	1234	1336
K	$\frac{1}{200} \dots \frac{1}{219}$	1028	1142	1256	1371	1485
L	$\frac{1}{220} \dots \frac{1}{239}$	1131	1256	1382	1508	1634
M	$\frac{1}{240} \dots \frac{1}{259}$	1234	1371	1508	1645	1782
N	$\frac{1}{260} \dots \frac{1}{279}$	1336	1485	1634	1782	1931
O	$\frac{1}{260} \dots \frac{1}{279}$	1440	1600	1760	1920	2080
P	$\frac{1}{260} \dots \frac{1}{279}$	1542	1714	1885	2056	2228
Q	$\frac{1}{260} \dots \frac{1}{279}$	1645	1828	2011	2194	2376
R	$\frac{1}{260} \dots \frac{1}{279}$	1748	1942	2136	2331	2525
S	$\frac{1}{260} \dots \frac{1}{279}$	1851	2056	2262	2468	2674
T	$\frac{1}{260} \dots \frac{1}{279}$	1954	2171	2388	2605	2822
U	$\frac{1}{260} \dots \frac{1}{279}$	2056	2285	2514	2742	2971
V	$\frac{1}{260} \dots \frac{1}{279}$	2160	2400	2640	2880	3120
W	$\frac{1}{260} \dots \frac{1}{279}$	2262	2514	2765	3016	3268
X	$\frac{1}{260} \dots \frac{1}{279}$	2365	2628	2891	3154	3416
Y	$\frac{1}{260} \dots \frac{1}{279}$	2468	2742	3016	3291	3565
Z	$\frac{1}{240} \dots \frac{1}{259}$	2571	2856	3142	3428	3714

Table A.1 Convolutional codes with maximum free distance (MFD) presented in [8].

THIS PAGE INTENTIONALLY LEFT BLANK



## LIST OF REFERENCES

- [1] “Mobile Station-Base Station Compatibility Standard for Dual-Mode Wideband Spread Spectrum Cellular System,” TIA/EIA Interim Standard 95 (IS-95), Washington, D.C.: Telecommunications Industry Association, July 1993 (amended as IS-95-A in May 1995).
- [2] William C.Y. Lee, *Lee’s Essentials of Wireless Communications*, McGraw-Hill, 2001.
- [3] A. J. Viterbi, “Very Low Rate Convolutional Codes for Maximum Theoretical Performance of Spread-Spectrum Multiple Access Channels,” *IEEE J. Select. Areas Communications*, vol. 8, pp. 641-649, May 1990.
- [4] J. Y. N. Hui, “Throughput Analysis for Code Division Multiple Accessing of the Spread Spectrum Channel,” *IEEE J. Select. Areas Communications*, vol. SAC-2, pp. 482-486, July 1984.
- [5] R. F. Ormondroyd and J. J. Maxey, “Performance of Low Rate Orthogonal Convolutional Codes in DS-CDMA Applications,” *IEEE Trans. Veh. Technol.*, vol. 46, pp. 320-328, May 1997.
- [6] K. Rikkinen, “Comparison of Very Low Rate Coding Methods for CDMA Radio Communications System,” *Proc. IEEE Int. Symp. Spread Spectrum Techniques and Applications*, Oulu, Finland, 1994, pp. 268-272.
- [7] Y. M. Kim and B. D. Woerner, “Comparison of Trellis Coding and Low Rate Convolutional Coding for CDMA,” *Proc. IEEE Military Communications Conf.*, Fort Monmouth, NJ, 1994, pp. 765-769.
- [8] Pal Frenger, Pal Orten and Tony Ottoson, “Code-Spread CDMA Using Maximum Free Distance Low-Rate Convolutional Code,” *IEEE Trans. Commun.*, vol. 48, pp. 135-144, January 2000.
- [9] Lian Zhao and Jon W. Mark and Young C. Yoon, “Coding-Spreading Tradeoff Analysis for DS-CDMA Systems,” *IEEE J. Select. Areas Communications*, vol. 8, pp. 641-649, May 1990.
- [10] Venugopal V. Veeravalli and Ashok Mantravadi, “The Coding Spreading Tradeoff in CDMA Systems,” *IEEE J. Select. Areas Communications*, vol. 20 no. 2, pp. 396-408, February 2002.
- [11] J. G. Proakis, *Digital Communications*, Fourth Edition, New York: McGraw-Hill, 2001.

- [12] Jhong Sam Lee and Leonard E. Miller, *CDMA Systems Engineering Handbook*, Boston, Massachusetts: Artech House Publishers, 1998.
- [13] G. C. Clark Jr. and J. B. Cain, *Error Correction Coding for Digital Communications*, New York: Plenum Press, 1981.
- [14] Rolf Johannesson, Kamil Sh. Zigangirov, *Fundamentals of Convolutional Coding*, Piscataway, New Jersey: IEEE Press, 1999.
- [15] Shu Lin and Daniel J. Costello, Jr., *Error Control Coding: Fundamentals and Applications*, Eaglewood Cliffs, New Jersey: Prentice Hall PTR, 1983.
- [16] Stephen B. Wicker, *Error Control Systems for Digital Communication and Storage*, Upper Saddle River, New Jersey: Prentice Hall PTR, 1995.
- [17] P. J. Lee, "New Short Constraint Length Rate  $1/n$  Convolutional Codes which Minimize the Required SNR for Given Desired Bit Error Rates", *IEEE Trans. Commun*, vol. COM-33, no. 2, pp. 171-177, February 1985.
- [18] S. Lefrancois and D. Haccoun, "Search Procedures for Very Low-rate Quasi-Optimal Convolutional Codes", *Proc. IEEE International Symposium on Information Theory*, Trondheim, Norway, 1994, pp. 278.
- [19] S. Lefrancois and D. Haccoun, "Search Procedures for Very Low-rate Quasi-Optimal Convolutional Codes", *Proc. Canadian Conference on Electrical and Computer Engineering*, Halifax Canada, 1994, pp. 210-213.
- [20] Vijay K. Garg, *Wireless Network Evolution: 2G to 3G*, Upper Saddle River, New Jersey: Prentice Hall PTR, 2002.
- [21] E. Biglieri, G. Caire and G. Taricco, "CDMA System Design Through Asymptotic Analysis", *IEEE Trans. Commun*, vol. 48 no. 11, pp. 1882-1896, November 2000.
- [22] M. Bickel, W. Granzow and P. Schramm, "Optimization of Code Rate and Spreading Factor for Direct-Sequence CDMA Systems", *Proc. Intl. Symposium on Spread Spectrum Techniques and Applications*, vol. 2, pp. 585-589, 1996.
- [23] Theodore S. Rappaport, *Wireless Communications*, Upper Saddle River: NJ: Prentice Hall, 2002.
- [24] Jean Conan, "The Weight Spectra of Some Short Low-Rate Convolutional Codes", *IEEE Trans. Commun*, vol. COM-32 no. 9, pp. 562-568, September 1984.
- [25] H. Suzuki, "A Statistical Model for Urban Multipath Propagation", *IEEE Trans. Commun*, vol. COM-22, pp.731-732, May 1974.

[26] J. E. Tighe, "Modeling and Analysis of Cellular Forward System," Ph.D. Dissertation, Naval Postgraduate School, Monterey, California, March 2001.

[27] G. L. Stuber, *Principles of Mobile Communications*, Norwell, Massachusetts: Kluwer Academic Publishers, 1996.

THIS PAGE INTENTIONALLY LEFT BLANK

## BIBLIOGRAPHY

William C.Y. Lee, *Lee's Essentials of Wireless Communications*, McGraw-Hill, 2001.

Pal Frenger, Pal Orten and Tony Ottoson, "Code-Spread CDMA Using Maximum Free Distance Low-Rate Convolutional Code," *IEEE Trans. Commun*, vol. 48, pp. 135-144, January 2000.

Lian Zhao and Jon W. Mark and Young C. Yoon, "Coding-Spreading Tradeoff Analysis for DS-CDMA Systems," *IEEE J. Select. Areas Communications*, vol. 8, pp. 641-649, May 1990.

Venugopal V. Veeravalli and Ashok Mantravadi, "The Coding Spreading Tradeoff in CDMA Systems," *IEEE J. Select. Areas Communications*, vol. 20 no. 2, pp. 396-408, February 2002.

J. G. Proakis, *Digital Communications*, Fourth Edition, New York: McGraw-Hill, 2001.

Jhong Sam Lee and Leonard E. Miller, *CDMA Systems Engineering Handbook*, Boston, Massachusetts: Artech House Publishers, 1998.

G. C. Clark Jr. and J. B. Cain, *Error Correction Coding for Digital Communications*. New York: Plenum Press, 1981.

Rolf Johannesson, Kamil Sh. Zigangirov, *Fundamentals of Convolutional Coding*, Piscataway, New Jersey: IEEE Press, 1999.

Shu Lin and Daniel J. Costello, Jr., *Error Control Coding: Fundamentals and Applications*, Eaglewood Cliffs, New Jersey: Prentice Hall PTR, 1983.

Stephen B. Wicker, *Error Control Systems for Digital Communication and Storage*, Upper Saddle River, New Jersey: Prentice Hall PTR, 1995.

Vijay K. Garg, *Wireless Network Evolution: 2G to 3G*, Upper Saddle River, New Jersey: Prentice Hall PTR, 2002.

Theodore S. Rappaport, *Wireless Communications*, Upper Saddle River: NJ: Prentice Hall, 2002.

J. E. Tighe, "Modeling and Analysis of Cellular CDMA Forward Channel," Ph.D. Dissertation, Naval Postgraduate School, Monterey, California, March 2001.

THIS PAGE INTENTIONALLY LEFT BLANK

## INITIAL DISTRIBUTION LIST

1. Defense Technical Information Center  
Ft. Belvoir, Virginia
2. Dudley Knox Library  
Naval Postgraduate School  
Monterey, California
3. Chairman, Code EC  
Electrical and Computer Engineering Department  
Naval Postgraduate School  
Monterey, California
4. Prof. Tri T. Ha, Code EC/Ha  
Naval Postgraduate School  
Monterey, California
5. CDR Jan E. Tighe  
Naval Information Warfare Activity  
Fort Meade, Maryland
6. Prof. Jovan E. Lebaric, Code EC/Lb  
Naval Postgraduate School  
Monterey, California